© THE QUEEN'S PRINTER FOR ONTARIO
2000

REPRODUCED WITH PERMISSION

L'IMPRIMEUR DE LA REINE POUR L'ONTARIO

REPRODUIT AVEC PERMISSION

micromedia
a division of IHS Canada

20 Victoria Street
Toronto, Ontario M5C 2N8
Tel.: (416) 362-5211
Toll Free: 1-800-387-2689
Fax: (416) 362-6161
Email: info@micromedia.on.ca

Ontario

Geology of the Kamiskotia Area

Ontario Geological Survey
Study 59

C.T. Barrie

2000

©Queen's Printer for Ontario, 2000

ISSN 0704-2590
ISBN 0-7778-8555-7

All publications of the Ontario Geological Survey and the Ministry of Northern Development and Mines are available for viewing and purchase at the following locations:

Mines and Minerals Information Centre
900 Bay Street, Room M2-17
Toronto, Ontario M7A 1C3
Telephone: 1-800-665-4480 (within Ontario)
(416) 314-3800
Fax: (416) 314-3797

Mines Library
933 Ramsey Lake Road, Level A3
Sudbury, Ontario P3E 6B5
Telephone: (705) 670-5615

Purchases may be made only through:

Publication Sales
933 Ramsey Lake Road, Level A3
Sudbury, Ontario P3E 6B5
Telephone: (705) 670-5691
Fax: (705) 670-5770
1-888-415-9847(toll-free)
E-mail: pubsales@ndm.gov.on.ca

Use of Visa or Mastercard ensures the fastest possible service. Cheques or money orders should be made payable to the *Minister of Finance*.

Canadian Cataloguing in Publication Data

Barrie, C.Tucker (Charles Tucker), 1956-
Geology of the Kamiskotia area

(Ontario Geological Survey study, ISSN 0704-2590; 59)
Includes bibliographical references and index.
ISBN 0-7778-8555-7

1. Geology–Ontario–Kamiskotia Lake Region. I. Ontario Geological Survey. II. Title. III. Series.

QE191.B37 2000 557.13'142 C99-964015-1

Every possible effort has been made to ensure the accuracy of the information contained in this report; however, the Ontario Ministry of Northern Development and Mines does not assume any liability for errors that may occur. Source references are included in the report and users may wish to verify critical information.

If you wish to reproduce any of the text, tables or illustrations in this report, please write for permission to the Team Leader, Publication Services, Ministry of Northern Development and Mines, 933 Ramsey Lake Road, Level B4, Sudbury, Ontario P3E 6B5.

Cette publication est disponible en anglais seulement.

Parts of this report may be quoted if credit is given. It is recommended that reference be made in the following form:

Barrie, C.T. 2000. Geology of the Kamiskotia area; Ontario Geological Survey, Study 59, 79p.

Critical Reader: P.C. Thurston
Scientific Editors: P.J. Cashin, D.M. Stephenson

100-03470/

Contents

Abstract ix

Introduction 1
- Purpose 1
- Location, Accessibility and Physiography 1
- Previous Work 1
- Acknowledgements 4
- Summary 4

Geology 5
- Regional Geological Setting 5
- General Geology of the Kamiskotia Area 5
  - Kamiskotia Gabbroic Complex 6
    - Definition 6
      - Name, Historical Background 6
      - Choice of Lithodemic Unit Rank 7
      - Physical Boundaries 7
    - Geology 7
      - Contacts 7
      - Alteration 11
    - Petrography 11
      - Lower Zone 11
      - Middle Zone 12
      - Mixed Magma Outcrops 12
      - Upper Zone 12
      - Granophyre 12
  - Kamiskotia Volcanic Complex 12
    - Definition 12
      - Physical Boundaries 12
      - Geology 14
      - Petrography 14
  - Lower Volcanic Suite 14
  - Metasedimentary Rocks 16
  - Granitoid Rocks 16
  - Bristol Township Lamprophyre Suite 16

Structure 18
- Bedding and Layering, and Regional Folding 18
- Structural Fabric Analysis 18
  - Results 19
  - Interpretation 20
  - Summary 23

Geochronology 24
- Results of U-Pb Geochronology 24
- Sm-Nd and Rb-Sr Isochron and Regression Ages 24
- Magmatic and Structural History 25

Geochemistry 27
- Alteration 27
- KGC Cumulates 27
- KGC Chilled Rocks 32
- Granophyric Rocks 33

Kamiskotia Volcanic Complex 34
Basalts, Evolved Basalts and Andesites 34
Rhyolites 35
Lower Volcanic Suite 35
Granitoid Rocks 35
Bristol Township Lamprophyre Suite 37
Geochemical Modeling of KGC Supracrustal Magmatic Processes 38
CMAS–Type Phase Diagrams 38
Mass Balance Calculations Using Rare Earth Elements 40
Assimilation-Fractional Crystallization Modeling 42
Nd Isotope Signatures 45
Petrogenesis of the KGC Gabbros and KVC Basalts 45
Petrogenesis of KVC Rhyolites 46
Petrogenesis of Bristol Township Lamprophyre Suite 48
Economic Geology 49
Volcanogenic Copper-Zinc Deposits 49
Kam–Kotia and Jameland Mines 49
Canadian Jamieson Mine 50
Genex Mine 50
Mesothermal Gold Deposits 52
Holmer Property 52
Gold-REE Occurrence: The Croxall Property 54
De Santis Property 54
Magmatic Nickel-Copper Occurrences 56
West Whitesides Township Occurrences 56
Bean Lake–Pirsson Lake Occurrences 56
Northwest Carscallen Township Occurrences 57
Potential for Mineralization 57
Volcanogenic Copper-Zinc Deposits 57
Mesothermal Gold Deposits 57
Magmatic Nickel-Copper-PGE Deposits 58
Discussion 60
Gabbroic Complex-Granitoid Relationships in the Southern Superior Province 60
Chemical Comparison of the KGC with other Synvolcanic Intrusions of the Southern Superior Province 60
Comparison with the Skaergaard Intrusion and Eastern Iceland Volcanic Fields 60
Cogenesis of the KGC and KVC and Significance with Respect to the Formation of VMS Deposits 61
Kamiskotia–Kidd Creek Relationships 62
Time-Stratigraphic Correlation of Volcanic Rocks in the Southern Abitibi Subprovince 62
Late Transpression across the Southern Superior Province 62
Timing of Late Archean Magmatism in the Southern Superior Province 63
Late Thermal Events in the Kamiskotia Area 63
Comparison to Modern Tectonic Settings: Synthesis 64
Appendix I: Sample Locations, Petrographic Descriptions and Geochemistry for U-Pb Samples 67
Appendix II: Sample Locations by Universal Transverse Mercator Grid Coordinates 69
Appendix III: Partition Coefficients and Average Modes used in Mass Balance and Assimilation–Fractional Crystallization Calculations 72
References 73
Metric Conversion Table 79

FIGURES

1. Location of the Kamiskotia area in the Superior Province 3
2. Distribution of outcrops and major esker ridges in the Kamiskotia area 3
3. Matachewan dikes in western Godfrey Township 4
4. Geology of the Kamiskotia area 6
5. Microprobe wavelength dispersive analyses for selected samples 11
6. Foliation map 19
7. Foliation trajectory map 20
8. Mineral lineation map 21
9. Map of apparent total strain fabric 21
10. U-Pb samples locations, and general geology of the Kamiskotia–Kidd Creek area 25
11. Summary of the U-Pb ages in the Kamiskotia–Kidd Creek area 26
12. Locations of samples and traverses in the Kamiskotia Gabbroic Complex 27
13. Petrographic traverse for cumulate rocks 30
14. KGC cumulates; whole rock magnesium number, normative anorthite composition, TiO_2 and P_2O_5 versus stratigraphic height 31
15. Ni and Sc versus stratigraphic height in the KGC 31
16. Incompatible trace elements and trace element ratios: La, Yb, La/Yb, Zr, Y, and Zr/Y versus stratigraphic height in the KGC 32
17. Rare earth element profiles for Kamiskotia Gabbroic Complex rocks and related basalts 33
18. REE and trace element plots for Kamiskotia and Kidd Creek rhyolites 35
19. Rare earth element profiles for selected granitoid rocks from the Kamiskotia area 38
20. X-Y plots for Bristol Township lamprophyre suite 41
21. REE profiles for Bristol Township lamprophyre suite rocks 42
22. CMAS-type tetrahedron projections for Kamiskotia Gabbroic Complex chill samples and Kamiskotia basalts and evolved basalts 42
23. Mass balance calculations using the REE 43
24. X-Y plots for liquid compositions with AFC modeling curves 43
25. Primitive mantle-normalized profiles for Kamiskotia Gabbroic Complex average chill composition 46
26. Geology of the Kam–Kotia Mine (number six level plan) 49
27. Geology of the Canadian Jamieson Mine property 51
28. Geology of the Genex Mine area 52
29. Geology of the Genex Mine, 38 m level 53
30. Cross-section of the H and A zones, Genex Mine 53
31. Cross-section of the C zone, Genex Mine 54
32. Geology of the Holmer gold property main outcrops 55
33. Geology of the Croxall gold-REE property 56
34. Geology of the De Santis gold property outcrops 58
35. Histogram of U-Pb ages for the southern Superior Province 63
36. Tectonic model for the Kamiskotia area and parts of the southwestern Abitibi Subprovince 66

PLATES

1. Textures in the Kamiskotia Gabbroic Complex 8
2. Kamiskotia Gabbroic Complex contact zone textures 9
3. Kamiskotia Gabbroic Complex mixed magma outcrop textures 10
4. Photomicrographs of Kamiskotia Gabbroic Complex rocks 13
5. Textures in Kamiskotia Volcanic Complex rocks 15
6. Croxall property ultramafic lamprophyre suite 17
7. Deformation textures 22

TABLES

1. Table of Lithologic units in the Kamiskotia area 2
2. Summary of U-Pb ages 5
3. Summary of Sm-Nd and Rb-Sr ages 25
4. Geochemistry of Kamiskotia Gabbroic Complex cumulates 28
5. Geochemistry of chilled gabbros and Kamiskotia basalts 34
6. Geochemistry of Lower volcanic suite mafic and intermediate volcanic rocks 36
7. Geochemistry of regional granitoid rocks 37
8. Geochemistry of Bristol Township lamprophyre suite and nearby rocks 39
9. S, Ni, Cu, PGE, Au and REE abundances for KGC sulphide occurrences 59

GEOLOGICAL MAP

Map P.3396 – Geology of the Kamiskotia area; scale 1:50 000 ..... back pocket

Geology of the Kamiskotia Area

C.T. Barrie[1]

[1]Geologist, C.T. Barrie and Associates, 23 Euclid Avenue, Ottawa, Ontario K1S 2W2

Manuscript approved for publication and published with the permission of A.J. Fyon, Senior Manager, Precambrian Geology Section, Ontario Geological Survey.

Abstract

This report describes the geology, geochemistry, structural history and economic geology of the Kamiskotia area, with particular emphasis on the Kamiskotia Gabbroic and Volcanic Complexes. The area is located 15 to 40 km west of Timmins, Ontario, in the western Abitibi Subprovince.

The Kamiskotia Gabbroic Complex (KGC) is centrally located in the Kamiskotia area. The KGC is a large (170 km^2) tholeiitic intrusion and is divided into four stratigraphic units. The Lower Zone is composed of adcumulus and mesocumulus peridotite, troctolite, and gabbronorite, with Mg numbers from 73 to 86. The Middle Zone is composed of mesocumulus gabbronorites, with Mg numbers from 60 to 74. The Upper Zone is composed of mesocumulus and orthocumulus gabbronorites and ferroan gabbronorites, with Mg numbers from 37 to 64. Modal layering is observed locally, in the Lower and Upper Zones. The fourth zone is a quartz-bearing granophyre of intermediate to felsic composition, and is characterized by granophyric textures and miarolitic cavities. It both overlies and is along strike with Upper Zone cumulates. The mafic cumulates have flat REE patterns (La_N/Yb_N = 0.4 to 2.6), with chondrite-normalized REE abundances (REE_N) ranging from 0.6 to 2 for olivine-bearing Lower Zone adcumulates, to 10 to 25 for Upper Zone orthocumulates. Europium anomalies are strongly positive for the Lower Zone and diminish up-section to slightly negative for the highest stratigraphic level in the Upper Zone. The granophyres have very high incompatible element contents, with most samples containing 500 to 800 ppm Zr, REE_N = 100 to 200; and have nearly flat REE patterns (La_N/Yb_N = 1.6 to2.6) with strong negative Eu anomalies. Chilled rocks have Mg numbers from 54 to 58, REE_N = 20 to 30, and La_N/Yb_N = 0.8 to 1.2.

The Kamiskotia Volcanic Complex (KVC) overlies and is intruded by the KGC. The KVC consists of a bimodal assemblage, including tholeiitic basalts and subordinate basaltic andesites and andesites, and high silica rhyolites. Basalts occur as massive and pillowed flows, and as pillow breccias, hyaloclastite and hyaloclastic tuffs, with plagioclase phenocrysts up to 15% locally. They have Mg numbers from 47 to 67, REE_N = 17 to 37, and La_N/Yb_N = 1.4 to 1.8. Rhyolites are pyroclastic tuffs, agglomerates, welded tuffs and flow lobes, and are generally quartz- and feldspar- phyric. They are classic, high silica rhyolites, with greater than 73% SiO_2, Rb/Sr greater than 1, 300 to 400 ppm Zr, REE_N = 70 to 280 and La_N/Yb_N = 2 to 3. Basaltic andesites and andesites are similar in texture to the basalts, and are notable for their discordant, dike- and sill-like masses that cut stratigraphy proximally to massive sulphide deposits. They have Mg numbers from 31 to 47, and are unusually enriched in their incompatible element contents, with 180 to 480 ppm Zr, REE_N = 25 to 84, La_N/Yb_N = 1.2 to 2.8.

Geochemical modeling of the cumulate rocks and basalts using major oxides and trace elements and radiogenic isotope signatures, indicate that the KGC was derived from a primitive parental magma that fractionated at low pressures. Rhyolitic compositions may be derived from basaltic compositions by greater than 90 percent fractionation of mafic minerals, plagioclase and iron-titanium oxide. There is no chemical or isotopic evidence for assimilation of any chemically distinct or isotopically enriched crustal material.

Field observations support the following sequence of magmatic and structural events in the Kamiskotia area: 1) formation of the Lower volcanic suite, stratigraphically below the KGC; 2) emplacement of the KGC and KVC, and coeval intrusion of granitoid A in Turnbull Township into the crystallizing KGC; 3) regional, bulk rotation about a sub-horizontal axis of this stratigraphy to form a northeast-facing monocline; possibly synchronous with 4) emplacement of three large granitoid intrusions, superimposing their respective contact strain aureoles or zones on the stratigraphy; 5) regional sub-horizontal, bulk north-south shortening that formed a non-penetrative east-trending flattening fabric; with an element of 6) late, predominantly dextral transpression, that formed high strain zones related to a splay of the western Destor–Porcupine Fault Zone (DPFZ) within the Lower volcanic suite; and 7) emplacement of the Bristol Township lamprophyre suite along the DPFZ.

U–Pb ages from related studies help substantiate this chronology and aid in the correlation of Kamiskotia rocks across the southern Abitibi Subprovince. Zircon ages for the KGC and a KVC rhyolite are 2707±2 Ma and 2705±2 Ma, respectively. The KVC rhyolite is 10 million years younger than the chemically similar, massive sulphide-bearing Kidd Creek rhyolite located 25 km to the northwest. Two of the granitoid intrusions have zircon ages of 2696±2 Ma and 2694 ±4 Ma. Two zircon fractions from the younger granitoid intrusion exhibit inheritance, with $^{207}Pb/^{206}Pb$ minimum ages up to 2926 Ma, indicating the presence of significantly older crust in this region. A minimum age for the formation of the DPFZ in this area is given by a U-Pb garnet-titanite age for a late-tectonic, garnetite dike, part of the Bristol Township lamprophyre suite within the DPFZ, at 2687±3 Ma.

Four volcanogenic copper-zinc ± silver ± gold deposits in the KVC have been mined, with greater than seven million tons of ore recovered. One significant, mesothermal gold deposit and several prospects are located along the DPFZ in the southeastern part of the Kamiskotia area, and along a splay of the DPFZ in the Lower volcanic suite. Exposed on one gold prospect are lamprophrye dikes that contain high total rare earth element (REE_t) concentrations (up to 0.43 weight percent REE_t). Several areas in the Lower Zone of the KGC have minor, low grade Ni-Cu concentrations, with very low platinum group element (PGE) contents.

Exploration efforts should focus on the potential of copper-zinc deposits in the KVC, with particular emphasis on locating and exploring near synvolcanic faults, in areas which have been affected by strong chloritic alteration, and in the vicinity of incompatible, element-enriched basaltic andesite dikes, sills and flows. Gold exploration should concentrate in areas where rocks have been subjected to late tectonic, brittle-ductile deformation, such as the splay of the DPFZ in the Lower volcanic suite, and along the Kamiskotia Highway fault north of the Canadian Jamieson Mine. The potential for significant nickel-copper-PGE mineralization in the KGC is considered low for the following reasons: 1) there is little evidence for large-scale contamination by a more siliceous or oxide-rich crust, generally the cause for sulphide immiscibility that leads to magmatic nickel-copper deposits and 2) sulphide-bearing, cumulus and pegmatitic rocks from across the intrusion have very low platinum and palladium abundances. The potential for a bulk-tonnage, low grade REE-gold deposit in the Bristol Township lamprophyre suite should be considered, given that the lamprophyre suite is much more extensive than previously recognized.

Introduction

PURPOSE

This report describes the geology, geochemistry, geochronology, structural history and economic geology of Neoarchean rocks in the Kamiskotia area, with emphasis on the Kamiskotia Gabbroic Complex (KGC) and the Kamiskotia Volcanic Complex (KVC). Included within this report are formal definitions for the KGC and the KVC, using the guidelines of the North American Commission on Stratigraphic Nomenclature (1983) (Table 1).

Large mafic-ultramafic intrusions such as the KGC are a major component of Precambrian terranes, and they represent an important source for magmatic nickel-copper-platinum group elements and chromium deposits (Windley 1976; Naldrett 1981). The majority of these intrusions are stratiform and generally coeval with greenstone belt rocks, in contrast to the Bushveld Complex, South Africa and the Great Dyke, Zimbabwe, which are significantly younger than their country rocks. A feature common to many stratiform intrusions is their geologic setting along the boundaries between regional granitoid and greenstone belt terranes. Examples are found in the Murchison and Pietersburg belts of the Kaapvaal craton, South Africa and Swaziland (e.g., Rooiwater igneous complex and other mafic-ultramafic sills of the Pietersburg Sequence, and the Usushwana complex, Pongola Group), in the Rhodesian craton of Zimbabwe (Mashaba and Shabani mafic-ultramafic complexes), and in the Pilbara block of Western Australia (e.g., Munni Munni and Millindina complexes). Numerous examples are found across the Superior Province, with particularly large occurrences in the Wabigoon Subprovince of northwestern Ontario (e.g., Mulcahy Lake and related intrusions; Bad Vermilion and Grassy Portage intrusions), and in the Abitibi Subprovince of Ontario and Quebec (e.g., KGC, Montcalm, Doré Lake, and Bell River complexes).

This report contributes to the understanding of the petrogenesis of Archean strata-bound mafic-ultramafic intrusions, particularly those found at granitoid-greenstone boundaries, in the context of greenstone belt tectonic evolution, with particular emphasis on the KGC. For this study, lithologic and structural mapping of the KGC and surrounding granitoid-greenstone rocks provides a foundation for geochemical studies. Precise chronologic constraints on magmatic and tectonic events in the Kamiskotia area are provided by U-Pb zircon, titanite and garnet geochronology. These events are placed within the well-constrained sequence of tectonic events documented across the southern Abitibi Subprovince and southern Superior Province. Supracrustal magmatic processes for the KGC are investigated using detailed geochemical traverses of the cumulate stratigraphy and geochemistry of the KVC. Primitive source characteristics are inferred for the KGC from recent trace element and neodymium isotope geochemistry studies (Barrie and Shirey 1991). Post-crystallization thermal events are also documented using internal neodymium and strontium isotope systematics.

This report also describes the KVC in terms of its physical volcanology and geochemistry, and establishes its close temporal and genetic relationship with volcanic massive sulphide deposits, and the KGC.

Finally, the largest of the copper-zinc, lode gold, rare earth element and nickel-copper-platinum group element mines, deposits and occurrences in the area are described, in light of current metallogenetic concepts. Following these descriptions, suggestions are made for future mineral exploration in the Kamiskotia area.

LOCATION, ACCESSIBILITY AND PHYSIOGRAPHY

The study area is located 15 to 40 km west of Timmins and is bounded by longitudes 81°30′ W to 82°00′ W and latitudes 48°22′30″ N to 48°37′30″ N. It includes all of Whitesides, Carscallen, Massey, Turnbull, Côté and Robb townships and parts of Enid, Fortune, Bristol, Jamieson, Frey and Godfrey townships, in the district of Cochrane (Figure 1). Principal access routes are Highway 101 in the southeastern part, the Kamiskotia Highway (Highway 576) in the northeastern part, and from a major, east-west logging road through the central part that intersects Highway 101. Many subsidiary, all-weather logging roads are present throughout the study area, and in Robb Township, numerous trails and winter roads cover the area south and southeast of Kamiskotia Lake.

Generalized outcrop locations and the locations of prominent esker ridges are given in Figure 2. Also given in Figure 2, is the location of ground coverage for this study. Much of the information for the eastern quarter of the map is compiled from previous studies listed below. In Figure 3, the density of Paleoproterozoic Matachewan dikes is shown, which is representative of their density for approximately half of the field area. Matachewan dikes are not shown on the accompanying 1:50 000 geological map (Map P.3396, back pocket).

PREVIOUS WORK

Townships in the Kamiskotia area that have been mapped at a scale of 1:15 840 by the Ontario Department of Mines are Bristol (at a scale of 1:12 000: Ferguson 1957a), Carscallen (Ferguson 1957b), Whitesides (Leahy 1968), Côté (Bright and Hunt 1973), Robb and Jamieson (presented together at 1:31 680: Middleton 1973a), Godfrey (Hogg 1954) and Turnbull and Godfrey (presented together at 1:31 680: Middleton 1976). The geology and mineral occurrences of Turnbull and Godfrey townships have been described in an open file report (Middleton 1975), and ground magnetic survey maps have been published for Robb, Jamieson, Godfrey and Turnbull townships (Middleton 1969, 1970, 1971a, 1971b). Middleton also pro-

Table 1. Table of lithologic units in the Kamiskotia area.

PHANEROZOIC

CENOZOIC

QUATERNARY

RECENT

Stream, lake and organic bog deposits

PLEISTOCENE

Eskers, drumlinoids, glacial till

UNCONFORMITY

PRECAMBRIAN

PROTEROZOIC

Matachewan Mafic Dikes (*circa* 2450 Ma)

INTRUSIVE CONTACT

ARCHEAN

Bristol Township Lamprophyre Suite (2687±3 Ma)

Clinopyroxene–biotite lamprophyre; garnetite

INTRUSIVE CONTACT

Felsic Intrusive Rocks

Quartz diorite, tonalite; quartz monzodiorite, granodiorite; quartz monzonite, granite; aplite, pegmatite; intrusive breccia

INTRUSIVE CONTACT

Côté Township Tonalite (2694± 4 Ma)

Quartz diorite, tonalite; quartz monzodiorite, granodiorite; quartz monzonite, granite; aplite, pegmatite; intrusive breccia

INTRUSIVE CONTACT

Groundhog River Tonalite (2696± 2 Ma)

Quartz diorite, tonalite; quartz monzodiorite, granodiorite; quartz monzonite, granite; aplite, pegmatite; intrusive breccia

INTRUSIVE CONTACT

Turnbull Township Tonalite (2707 Ma)

Quartz diorite, tonalite; quartz monzodiorite, granodiorite; quartz monzonite, granite; aplite, pegmatite; hybrid rocks, agmatite

Kamiskotia Volcanic Complex

Felsic Volcanic Rocks (2705± 2 Ma)

Rhyolite quartz–feldspar crystal tuffs and agglomerates; welded quartz–feldspar rhyolite and dacite flows and tuffs; spherulitic rhyolite flows; tuffaceous volcaniclastic rocks

Mafic Volcanic Rocks

Massive and pillowed basalt; basalt tuff, breccia; plagioclase–porphyritic basalt; massive and pillowed basaltic andesite

INTRUSIVE CONTACT

Kamiskotia Gabbroic Complex

Mafic Intrusive Rocks (2707±2 Ma)

Peridotite; troctolite and olivine gabbro; magnesian gabbronorite and gabbro (locally anorthositic); ferroan gabbronorite and gabbro (locally anorthositic); hornblende gabbro and hornblendite; pegmatitic gabbro; chilled or agmatitic gabbro and gabbronorite; gabbro and gabbroic anorthosite sills; amphibolite, pyroxenite

Felsic Intrusive Rocks

Granophyric diorite, quartz diorite, tonalite; granophyric quartz monzodiorite, granodiorite, quartz monzonite, granite

INTRUSIVE CONTACT

Metasedimentary Rocks

Oxide– and sulphide–bearing iron formation; metagreywacke; argillite; metachert

Lower Volcanic Suite (>2707 Ma)

Pillowed and massive basalt; massive and tuffaceous andesite; tuffaceous dacite and rhyolite; garnet amphibolite

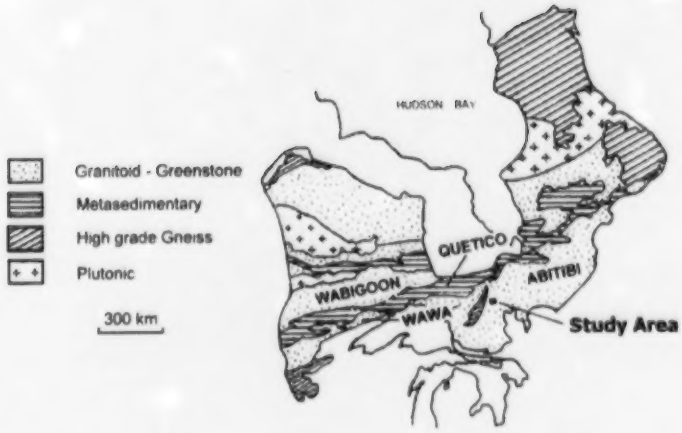

Figure 1. Location of the Kamiskotia area in the Superior Province, with major subprovinces in the southern Superior Province labeled. See Figure 2 for greater detail.

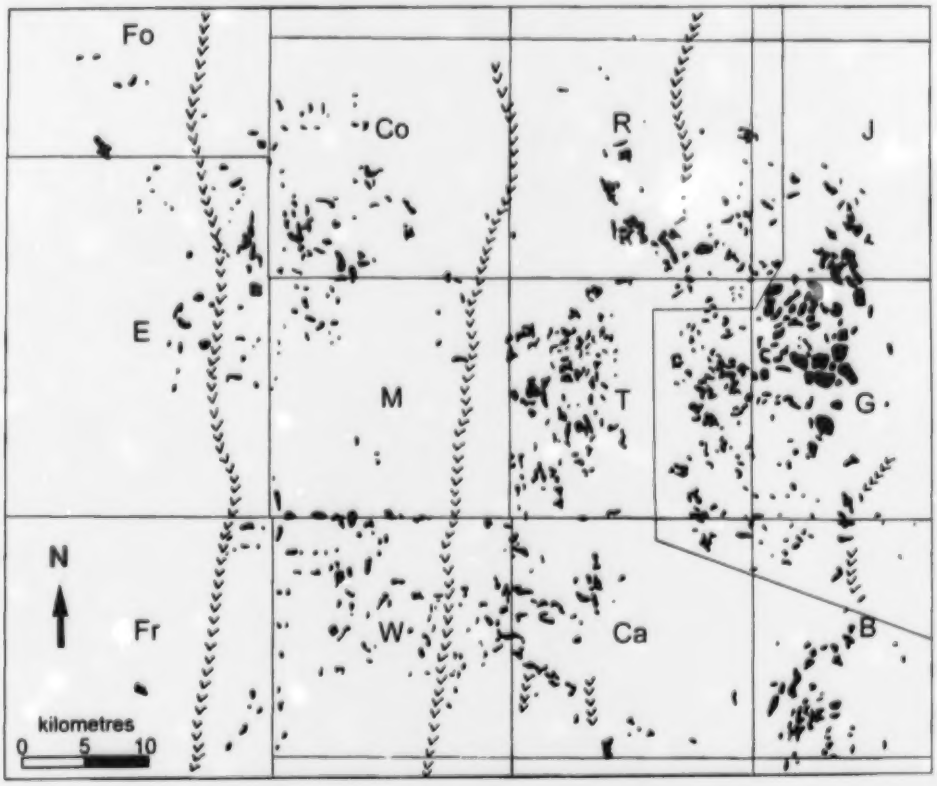

Figure 2. Distribution of outcrops (denoted in black) and major esker ridges (denoted by v-arrays) in the Kamiskotia area. Geology of Jamieson, Godfrey and northern Bristol townships (to east of irregular line) compiled from previously published maps. Township abbreviations are as follows: Fo-Fortune; Co-Côté; R-Robb; J-Jamieson; E-Enid; M-Massey; T-Turnbull; G-Godfrey; Fr-Frey; W-Whitesides; Ca-Carscallen; B-Bristol.

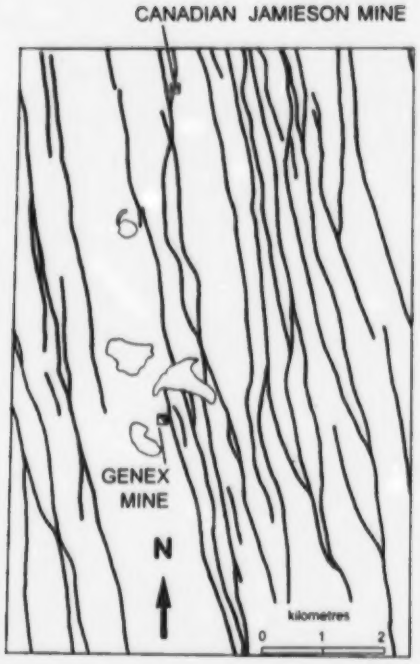

Figure 3. Matachewan dikes in western Godfrey Township (*after* Middleton 197 lb, 1973). Dike density typical for Kamiskotia area.

duced a geophysical report for Robb and Jamieson townships (Middleton 1973b) which describes the prospecting and mining activities in these townships in detail. Wolfe produced a report and an accompanying map on the geology and distribution of nickel, copper and cobalt in the Kamiskotia Gabbroic Complex (Wolfe 1970, 1971). Pyke (1982) included the geology of the Kamiskotia Volcanic Complex in his regional synthesis of the Timmins area. A series of high resolution aeromagnetic maps were produced by the Ontario Geological Survey that cover the eastern half of the area (Barlow 1988).

As part of his graduate thesis, Hart (1984) investigated the geochemistry of the Kamiskotia Volcanic Complex, and Legault (1985) studied the Genex copper deposit in Godfrey Township. This report is accompanied by a geological map at a scale of 1:50 000 (Map P. 3396, back pocket), a structural and U-Pb geochronologic study (Barrie and Davis 1990) and an Nd-Sr isotopic study (Barrie and Shirey 1989,1991) on the KGC and surrounding Archean rocks, which stem from doctoral thesis work at the University of Toronto (Barrie 1990).

ACKNOWLEDGEMENTS

There are many people who have helped during the course of this project. Those who were particularly helpful in the scientific research are Tony Naldrett and Mike Gorton of the University of Toronto, Don Davis of the Royal Ontario Museum (ROM); Steve Shirey of the Department of Terrestrial Magnetism, Carnegie Institution of Washington, D.C. (DTM); and Tony Green of Falconbridge Limited. I also thank Tom Hart and Marc Legault for permission to use geochemical data and figures from their MSc theses.

In the field, I was accompanied by a number of Falconbridge Limited employees: Mike Kerwin, Doug Hurst, Murray Jerome, Jamie Cecchetto, George MacTaggart, Paul Roos, and Kim Wyotiuk. Their assistance and good humour are greatly appreciated. Additionally, Dave Comba, Bob Stewart, Ted Barnett, Scott McLean, Paul Binney, and Phil Day all of Falconbridge Limited were helpful in providing samples or logistical support. Others were helpful by providing access to drill core or exploration properties, including Dr. Mathew Blecha of Teck Explorations Limited, Dr. Stew Fumerton of Chevron Canada Resources, Limited, and Jim Croxall, of Timmins, Ontario. I am grateful to Wil Doherty who provided high quality ICP-MS data for several challenging, REE-enriched samples.

I would like to thank the following corporations and institutions for their support: the Carnegie Institution of Washington, D.C., Falconbridge Limited, the Jack Satterley Laboratory of the ROM, the University of Toronto, and Teck Explorations Limited.

I thank the following geologists of the Ontario Geological Survey for their reviews which have improved this report: M. E. Cherry, J. A. Fyon, S. L. Jackson, and M. Sanborn-Barrie.

SUMMARY

Based on geology and fabric analysis, the sequence of major magmatic and tectonic events in the Kamiskotia area are interpreted as follows: 1) formation of the Lower volcanic suite; 2) formation of the KGC–KVC, and coeval intrusion of granitoid A into the KGC during solidification; 3) regional bulk rotation of the stratigraphy about a subhorizontal axis, to form a northeast-facing monocline; possibly accompanied by 4) diapiric intrusion of granitoids B, C and D (timing with respect to each other not established), imparting their respective contact strain aureoles or zones on mantling material; 5) regional north-south compression, probably in part synchronous with, but locally postdated by 6) ductile shear along the western Destor–Porcupine Fault Zone (DPFZ), and a related splay through the Lower volcanic suite, that exhibits a consistent sense of dextral displacement.

Geology

REGIONAL GEOLOGICAL SETTING

The Kamiskotia area is located in the westernmost part of the Abitibi Subprovince of the Superior Province (*see* Figure 1). Neoarchean metavolcanic, metasedimentary and intrusive rocks of the Ontario portion of the Abitibi Subprovince (herein termed the western Abitibi Subprovince) have been subjected to variable deformation and metamorphism. Metamorphism ranges from sub-greenschist to middle amphibolite facies, with higher metamorphic grade generally proximal to the margins of large felsic granitoid intrusions. The geology and evolution of parts of the western Abitibi Subprovince have been described and interpreted by numerous authors, most notably Dimroth et al. (1982, 1983a, 1983b), Pyke (1982), Corfu et al. (1989), Jackson and Sutcliffe (1990) and Barrie and Davis (1990).

From U-Pb geochronology, Neoarchean rocks of the western Abitibi Subprovince range in age from 2747±2 Ma for the Pacaud Group metavolcanic rocks (J.K. Mortensen, GSC, personal communication, 1989) south of Kirkland Lake, to 2673 +6/-2 Ma for an albitite dike in the McIntyre Mine of the Porcupine gold camp (Corfu et al. 1989). There is evidence for older crustal rocks in the vicinity, from xenocrystic zircons in granitic rocks and lamprophyres (Barrie and Davis 1990; Corfu 1993), from detrital zircons in the Pontiac metasedimentary rocks (Gariepy et al. 1984), and from Nd isotopic signatures (Barrie 1990). Neoarchean rocks are cut by the Paleoproterozoic Matachewan dikes, which have U-Pb zircon and baddeleyite ages of approximately 2450 Ma (Heaman 1989) (Table 2).

Table 2. Summary of U-Pb ages (*from* Barrie and Davis 1990).

SAMPLE	AGE(Ma)[1]	REMARKS
KGC Kamiskotia Gabbroic Complex	2707±2	
KR Kamiskotia Volcanic Complex Rhyolite	2705±2	
GC Granitoid C	2696±1.5 2692±5	titanite $^{207}Pb/^{206}Pb$ minimum age.
GB Granitoid B	2694±43 2698±8 2640±25	contains inheritance(?).
KCR Kidd Creek Rhyolite	2717±2	one concordant analysis along with four from sample 77-22 of Nunes and Pyke (1980).
PR Prosser Rhyolite	2716±4	
RR Reid Rhyolite	2705 +5/-3	

Samples located in Figure 10, and by Universal Transverse Mercator Grid coordinates in Appendix I. Also given in Appendix I are petrologic descriptions and whole rock geochemistry for each sample. All ages are from zircon populations unless noted otherwise.

[1] All ages for upper intercepts unless noted otherwise. All analyses of zircon populations unless noted otherwise.

GENERAL GEOLOGY OF THE KAMISKOTIA AREA

The Kamiskotia Gabbroic Complex (KGC) is a large, deformed tholeiitic intrusive complex situated centrally in the Kamiskotia area (Figure 4). It is overlain by, and in part gradational with, metavolcanic rocks of the KVC, including basalt and rhyolite, and with volumetrically minor evolved basalt and andesite, some of which occur as hypabyssal sills. The KVC hosts four volcanogenic massive sulphide deposits (*see* "Economic Geology"). The KGC footwall rocks are informally termed the Lower volcanic suite, which is capped by a 2 m thick cherty oxide-sulphide iron formation. In a general sense, this stratigraphic succession is near-vertical and faces to the north and east. Four granitoid masses composed of hornblende ± biotite

tonalite to granite, and locally rimmed with contact intrusive breccia, have intruded the stratigraphy in the Kamiskotia area. These include granitoid A (Turnbull Township tonalite), predominantly of tonalitic composition, which exhibits textures indicative of magma mixing with fine-grained KGC rocks. Granitoid A is interpreted to have intruded the base or the margin of the KGC during KGC crystallization (described below). Granitoid B (Côté Township tonalite) is predominantly tonalitic, and has a well-developed foliation parallel to its margin. Granitoids C and D, to the west and south of the KGC, are composed of several discrete plutons that range in composition from trondhjemite-tonalite to granodiorite-granite. Regional metamorphism up to the lower greenschist facies has affected the stratigraphy, except within 1 to 3 km of the granitoid-greenstone contacts that have well-developed foliations, where the metamorphic grade is up to middle amphibolite facies.

A major ductile deformation zone is present to the east and south of granitoid D, with a splay extending to the north of granitoid D through the Lower volcanic rocks. The deformation zone may represent parts of the westernmost Destor–Porcupine Fault Zone (DPFZ), a major fault boundary that extends hundreds of kilometres across the Abitibi Subprovince. Alkalic magmatic activity, represented by a lamprophyre suite with aillikitic affinities, and mesothermal lode gold mineralization, are associated with the fault zone in this region. The north-northwest-trending Matachewan mafic dike swarm cuts all stratigraphy, including deformed rocks in the DPFZ.

Kamiskotia Gabbroic Complex

DEFINITION

In this report, the Kamiskotia Gabbroic Complex (KGC) is defined in accordance with the North American Stratigraphic Code (*see* North American Commission on Stratigraphic Nomenclature 1983; *see* Table 1). The purpose for a formal definition is to provide stability in nomenclature for easy referencing, and for future studies on the KGC, and for studies concerning lithostratigraphic and time-stratigraphic correlation in the western Abitibi Subprovince. In order to define a rock unit, the Code requires a discussion of the name, historical background and unit rank; and descriptions of the rock types, physical boundaries, shape, regional correlation, age and petrogenesis. The name, historical background, unit rank, physical boundary descriptions and rock types are given below. Other aspects are discussed in detail elsewhere in this report.

Name, Historical Background

The name Kamiskotia is taken from Kamiskotia Lake and the Kamiskotia River, the most prominent bodies of water in the map area. The first reference to this area and the gabbroic rocks was in William A. Parks' survey of Niven's

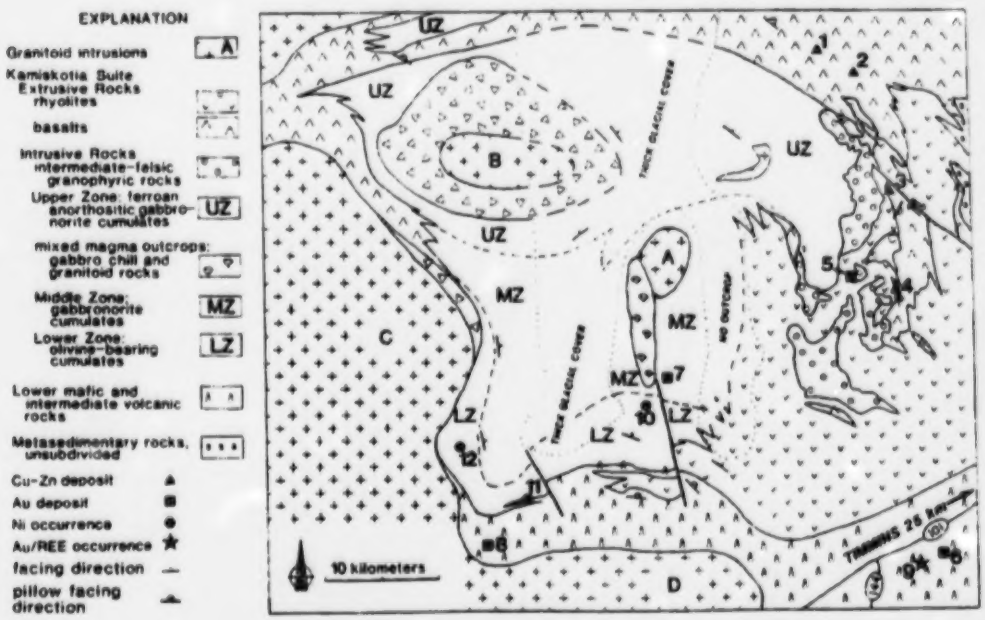

Figure 4. Geology of the Kamiskotia area. Mines (none currently producing) and mineral occurrences labelled as follows: 1. Kam–Kotia copper-zinc mine; 2. Jameland copper-zinc mine; 3. Canadian Jamieson Mines; 4. Genex Mine; 5. Lally Gold Mine; 6. Holmer gold mine; 7. De Santis gold property; 8. Union gold mine; 9. Croxall REE and gold property; 10-12. Nickel-copper occurrences.

Base Line, from Night Hawk Lake to Missanabie Lake (Parks 1900). The following excerpts are from his report:

> The Kamiskotaia-Sagaigan River enters the Mattagami on the west side, about six miles below the three sandy portages. It is about 100 feet wide at its mouth but its navigability is interrupted by rapids...On this portage occurs a peculiar hard schistose rock, striking a little south of east. It presents various shades of pink and green,and weathers out with white dots, owing to a decomposed feldspar. This rock runs up a hill of considerable height [referring to rhyolites of Kamiskotia hill in Jamieson Township]...
>
> Kamiskotia Lake is a fine body of water of from two to three miles in diameter, and containing several rocky islands. The rock at the head of the river is hard massive green to black rock, resembling diorite, but contains a large amount of quartz. Under the microscope it shows decomposed plagioclase crystals and blebs of quartz, all imbedded in a fine grained matrix, consisting largely of quartz with minute grains of a dark alteration product. It is probably an altered quartz diorite [altered KGC quartz gabbro]...

Kerr reported on his exploration in the Mattagami valley a few years later, and attempted, without success, to change the name of the Kamiskotia River (Kerr 1906):

> About four miles below Niven's second base the Mattagami receives a rather considerable tributary from the west, which I have named the Coffey [Kamiskotia River], the present Indian name, Kamiskotaia-Sagaigan, being altogether too cumbrous. We ascended this river and some of its tributaries to Lake Kamiskotia...

Choice of Lithodemic Unit Rank

The choice of "complex" as the lithodemic unit rank is based on several criteria. The North American Stratigraphic Code (*see* North American Commission on Stratigraphic Nomenclature 1983) defines "complex" as "an assemblage or mixture of rocks of two or more genetic classes, igneous, metamorphic or sedimentary, with or without highly complicated structure". The mafic cumulates and the granophyres of intermediate to felsic composition are considered to represent two separate genetic classes of igneous rocks, particularly considering the different magmatic processes that were operative during their formation (geochemical data supports their comagmatic nature; *see* "Geochemistry" section). The term "complex" has been used for this intrusion consistently in the literature (e.g., Wolfe 1970, 1971; Middleton 1969, 1970, 1973b, 1975; Pyke 1982; Campbell et al. 1981; 1982; 1984; Hart 1984; Legault 1985; Barrie 1990), although there has been variation on the rock name given and the usage of capitalization. Additionally, the Kamiskotia intrusive rocks have many similarities to well-known intrusions that are termed complexes (e.g., Bushveld Complex, South Africa; Stillwater Complex, Montana, U.S.A.; Bell River and Doré Lake Complexes, Quebec).

Physical Boundaries

The KGC occupies an area of 170 km^2, in northeastern Carscallen, northern Whitesides, eastern and central Massey, northeastern Enid, central Côté, southern Robb, western and northern Turnbull, and western Godfrey townships (*see* Map P.3396, back pocket). It is bounded to the south by the Lower volcanic suite, to the west by granitoid C, to the north and east by the KVC, and internally by granitoids A and B, in Turnbull and Côté townships, respectively. Contact relationships with adjacent rock types are described below.

GEOLOGY

Terminology for the rocks of the KGC is from Irvine (1982). The majority of KGC rocks are termed cumulates, defined as "an igneous rock characterized by a framework of touching mineral crystals and grains that evidently were concentrated through fractional crystallization of their parental magmatic liquids" (Irvine 1982). The packing of cumulus crystals is described by the terms adcumulus (<7% intercumulus minerals), mesocumulus (7 to 25% intercumulus minerals), or orthocumulus (25 to 50+% intercumulus minerals). Cumulus processes are processes related to the deposition or growth of cumulus crystals or grains, whereas postcumulus processes refer to processes that postdate cumulus processes, and may be either pre- or postsolidus (Irvine 1982).

The KGC is subdivided into four zones on the basis of field and petrographic observations and geochemistry: 1) partly layered, olivine-bearing cumulates of the Lower Zone (LZ) along the southern and western margin (*see* Figure 4); 2) gabbronorite and anorthositic gabbronorite cumulates of the Middle Zone (MZ); 3) partly layered, ferroan gabbro-norite, anorthositic gabbronorite and hornblende gabbro cumulates of the Upper Zone (UZ); and 4) granophyric rocks of intermediate and felsic composition above and along strike with the UZ cumulates. The UZ granophyre contact is irregular, with stoped blocks of partially hybridized granophyric rock within chloritized, quartz-rich UZ gabbro locally (Hart 1984).

Facing directions within the LZ and the UZ are from cumulates with cross-bedding structures, or from pyroxene-rich to plagioclase-rich gradations within individual cumulus layers (Plates 1a, b). It is possible that a synform with a north-trending axis is present in the southwestern KGC. Granitoids B, C and D represent antiformal structures, and in general facing directions are away from their margins.

Contacts

Contacts with adjacent rocks exhibit a variety of textures. The adjacent rocks display partial melt zones, and brecciated and agmatitic textures. In the KGC, textures related to the presence or migration of volatiles are found within LZ rocks, and within roof pendants and hybridized blocks of roof-rock material in the granophyre.

Along the southern boundary of the KGC, thermally metamorphosed pillow-shaped structures are present within 100 m of the contact with Lower volcanic rocks (Plate 2a). These textures are gradational with a zone 50 to 200 m wide of contorted migmatites, with local patches up to several square metres of strong epidote-chlorite-actinolite alteration in basaltic and plagioclase-porphyritic basaltic

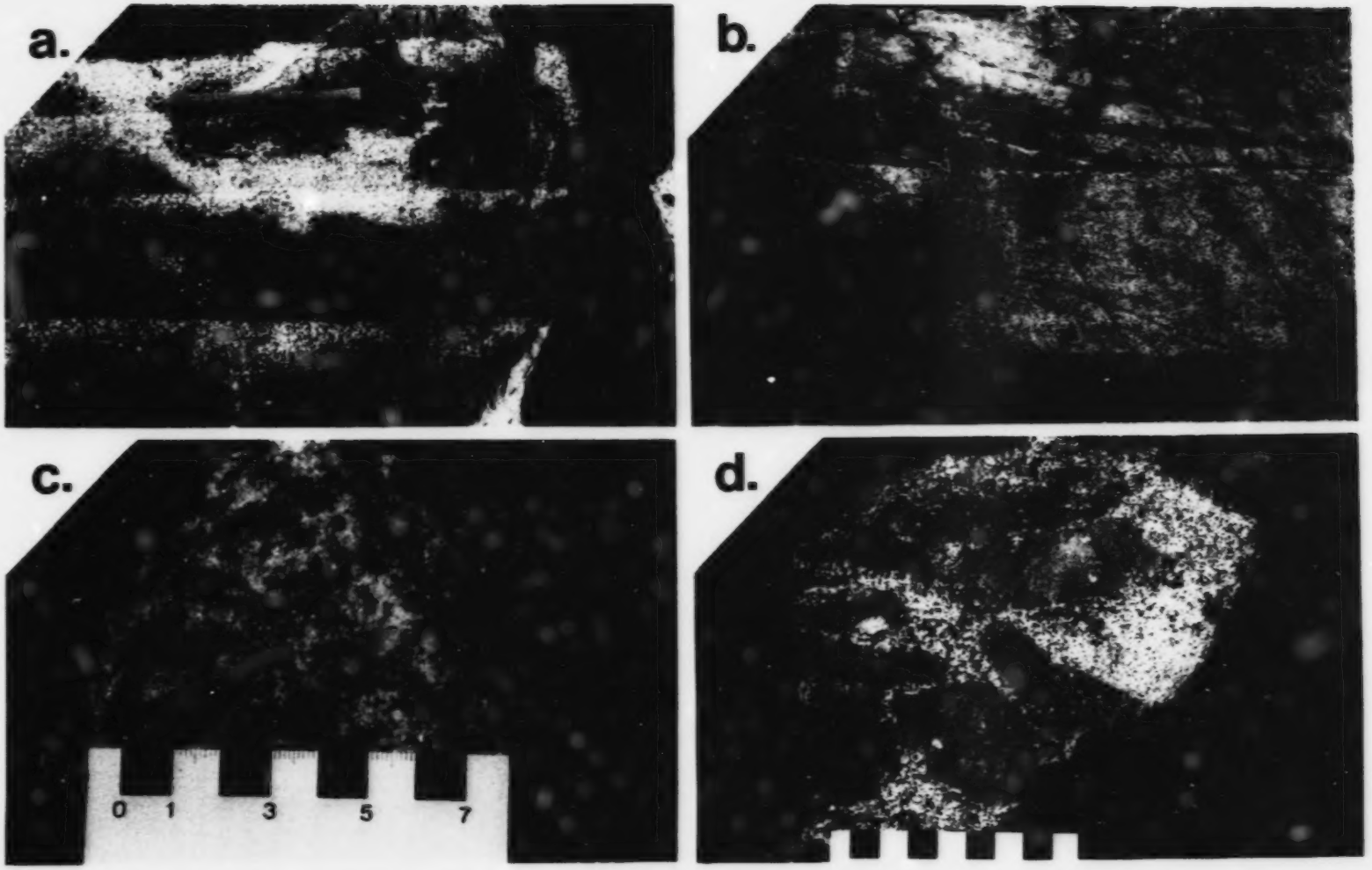

Plate 1. Textures in the KGC: a) rhythmic modal layering in Lower Zone cumulates: pyroxene-rich gabbronorite grading up into more plagioclase-rich gabbronorite; facing direction is up; b) cross-bedded layering in Lower Zone gabbronorite cumulates; facing direction is up; c) hand sample of slightly foliated gabbroic anorthosite cumulate from the Lower Zone; d) mafic enclaves in anorthositic gabbro, from the Middle Zone.

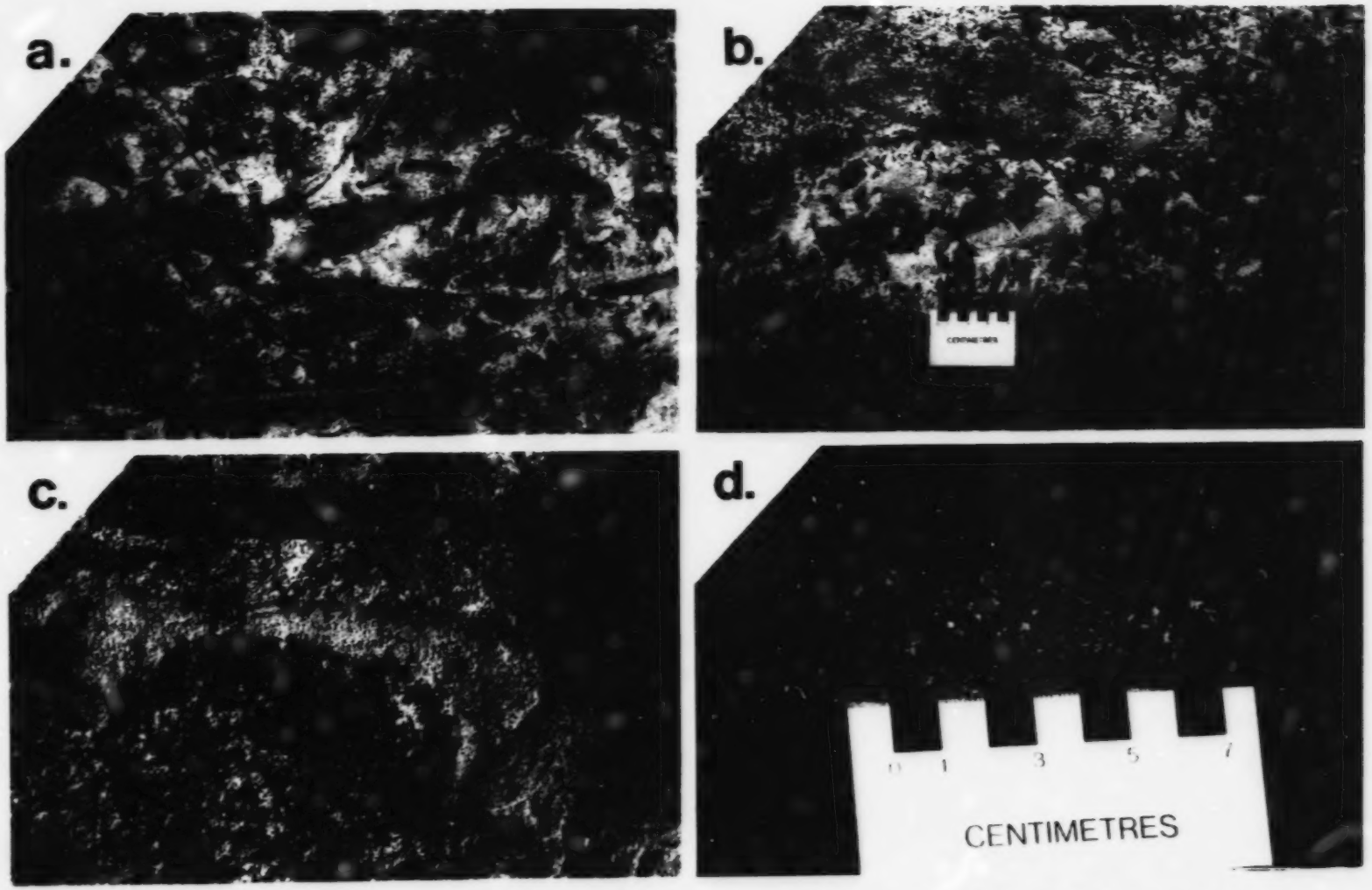

Plate 2. KGC contact zone textures: a) thermally-metamorphosed pillowed mafic metavolcanic rocks, Lower volcanic suite, northern Whitesides Township; chlorite alteration rims of pillows are now tremolite-actinolite, and pillow cores are hornfelsic with clinopyroxene porphyroblasts; b) KGC gabbro cumulate cut by mafic pegmatite dike with coxcomb texture: hornblende crystals terminate toward center of dike, northern Carscallen Township; c) hornblende-rich bud enclosed by epidote and clay, cutting KGC cumulates 50 m from basal contact, western Carscallen Township; d) "tennis ball-like" aggregates of plagioclase and altered pyroxene within subpegmatitic gabbronorite, western Whitesides Township.

material. The lower contact with KVC rhyolites has similar migmatitic textures, and also displays agmatitic textures, where partially melted rhyolite was injected into quenched gabbroic material (similar to agmatitic textures in mixed magma outcrops: Plate 3b).

Within the basal KGC, postsolidus or postcumulus textures reflect the influence of volatiles, apparently derived from partially melted wall rocks. At some localities, volatile-rich fluids have penetrated along dilatent fractures (postsolidus?: *see* Plate 2b); elsewhere fluids apparently migrated along grain boundaries, and terminated in mushroom-like structures of pegmatitic gabbro and haloes of epidote and clay minerals (postcumulus?: *see* Plate 2c). Drill core that penetrated layered LZ in western Whitesides Township exhibits another unusual texture, similar to the "tennis ball marker horizon" in the eastern Bushveld Complex. The drill core has spherical, medium-grained plagioclase aggregates up to 10 cm in diameter, within a matrix of subpegmatitic gabbronorite (*see* Plate 2d). This phenomenon is interpreted to have resulted from the aggregation of plagioclase in the presence of a "bridging liquid", which coats loose cumulate phases and bonds them into spheres with minimum surface tension at the base of the magma chamber (Lee and Sharpe 1979). The bridging liquid is apparently a siliceous partial melt of footwall rocks (in this case, cherty iron formation, and Lower volcanic suite rocks) that remains immiscible from the resident magma. Such "bridging liquids" are used in the metallurgical industry to separate particulate matter from melts (Lee and Sharpe 1979).

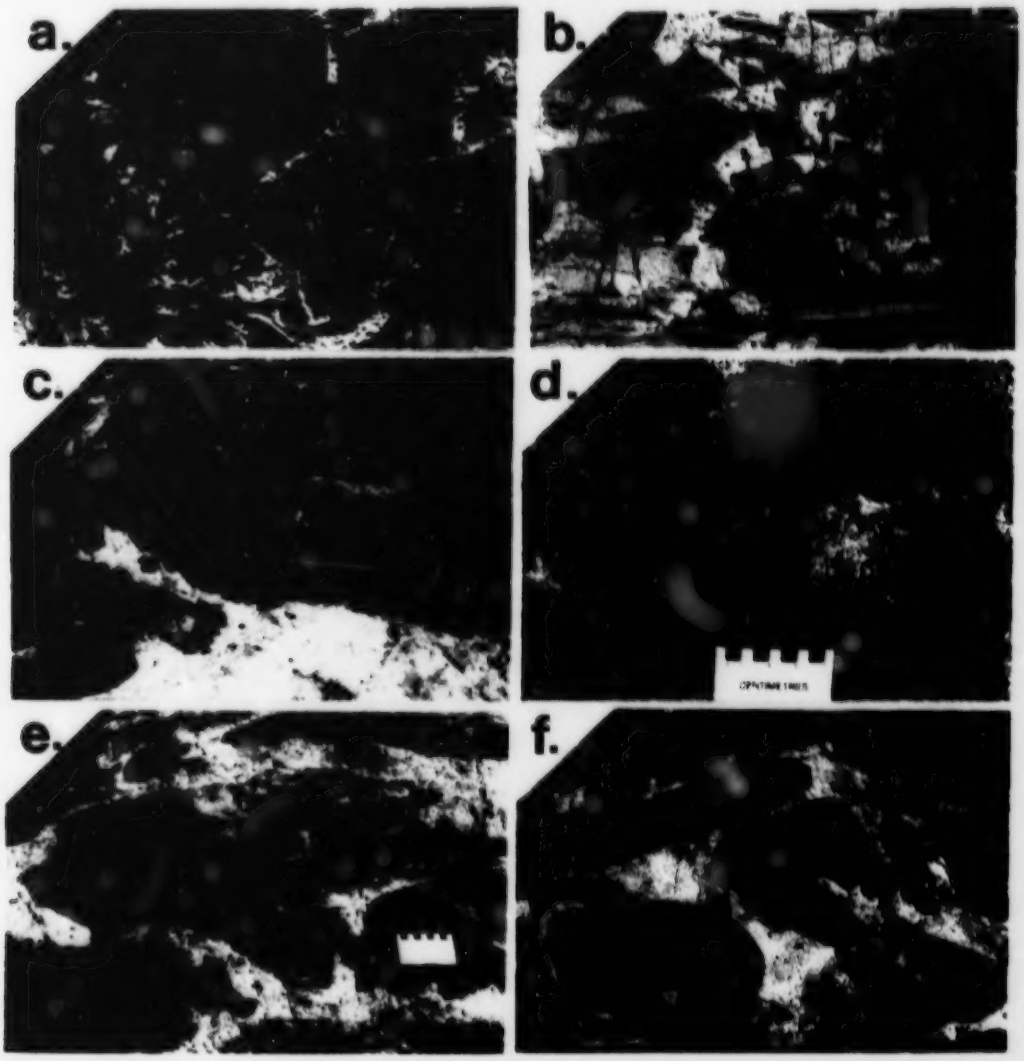

Plate 3. KGC mixed magma outcrop textures, western Turnbull Township: a) medium-grained gabbro cut by felsic dikes along brittle fractures; b) agmatitic textured fine-grained gabbro and felsic intrusion; c-f) chilled gabbro liquid forming pillow-like structures or irregular-shaped masses due to quenching in contact with cooler felsic liquid.

Blocks of felsic roof rock material have been described within the granophyre and parts of the UZ, in Godfrey and Robb townships (Hogg 1954; Middleton 1975; Hart 1984). These blocks have hybridized margins where they are in contact with more mafic intrusive rocks. Blocks of diorite within the UZ in southern Robb Township south of Kamiskotia Lake have textures similar to those found in the mixed magma outcrops in Turnbull Township, where the felsic intrusive rocks are clearly distinguished from the granophyre on the basis of trace element geochemistry. This area is reinterpreted as late injection of tonalitic liquid into the crystallizing UZ rocks (see below).

Alteration

All KGC rocks have been subjected to varying degrees of postsolidus alteration. For example, clinopyroxene is commonly partly or completely replaced by tremolite-actinolite and hornblende, and plagioclase is commonly altered to sericite, chlorite and clay. Generally the UZ cumulates are slightly altered, whereas the MZ and LZ cumulates are moderately altered. Granophyre rocks are moderately to highly altered, with abundant chlorite in the more intermediate compositions, and chlorite + epidote + sericite assemblages in felsic granophyres. Except for rare sheared outcrops, primary textures are readily discerned in outcrop and hand specimen. The following petrologic descriptions emphasize the primary cumulus and postcumulus mineralogy as determined from outcrop, hand specimen, and petrographic observations, supplemented by microprobe wavelength dispersive analyses of minerals (reported *in* Barrie 1990). Microprobe mineral analyses are presented in Figure 5.

PETROGRAPHY

Lower Zone

The LZ is distinguished from other rocks of the KGC by the sporadic presence of olivine as a cumulus phase, and by whole-rock Mg numbers that are generally greater than 75 (whole rock Mg number = mole percent MgO/(MgO + FeO), with FeO = 0.85 FeO_{total}). Modal layering and cross-bedding features are observed locally (*see* Plates 1a,b). LZ rocks include peridotite, troctolite, olivine gabbro, magnesian gabbronorite, and gabbroic anorthosite (Plate 1c) as medium-grained meso- to adcumulate, with clinopyroxene, orthopyroxene, olivine and plagioclase as cumulus phases. Chromite and sulphides occur sporadically in trace amounts in the cumulates (Plate 4a), and the LZ hosts several minor occurrences of low grade, nickel-copper sulphide mineralization. Olivine ranges in composition from Fo_{77} to Fo_{81}; clinopyroxene Mg numbers (mineral Mg number = mole percent MgO/MgO + FeO_{total}) range from 77 to 82, and plagioclase ranges from An_{79} to An_{89} (*see* Figure 5, samples A-D). Less primitive orthocumulus to mesocumulus gabbroic rocks predominate along the southern contact (*see* Figure 5, sample F). A large outcrop (300 by 300 m) of altered peridotite occurs and stands in high relief in northwest Carscallen and northeast Whitesides townships. The majority of the outcrop is composed of talc, serpentine, chlorite and magnetite; relict cumulus olivine is observed locally. The margins of the outcrop are schistose, and contact relationships with layered troctolites and olivine gabbros to the south, and gabbronorites to the north, are not discernable. The peridotite

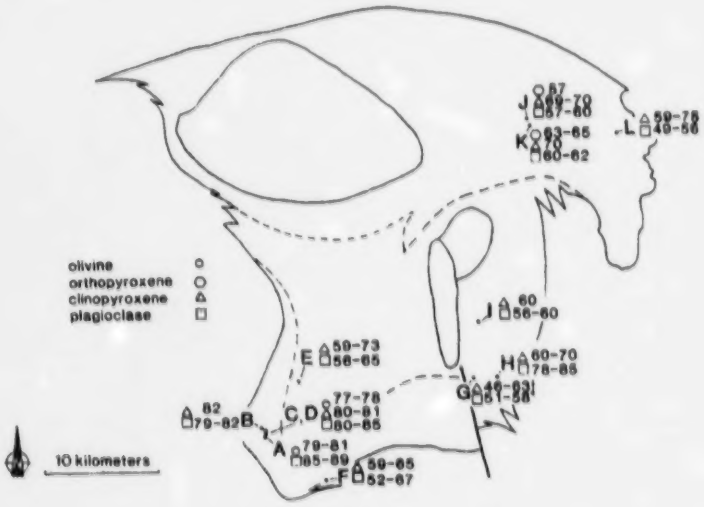

Figure 5. Microprobe wavelength dispersive analyses for selected samples. For ferromagnesian minerals, numbers are 100 x molecular MgO/MgO+FeO; for plagioclase, numbers are molecular percent anorthite content. Full chemical analyses, sample locations and description of analytical conditions given in Barrie (1990).

outcrop is believed to be concordant with surrounding KGC rocks.

Middle Zone

The MZ consists of gabbro, gabbronorite, anorthositic gabbro, and gabbroic anorthosite as massive, medium- and coarse-grained mesocumulate to adcumulate, with clinopyroxene, orthopyroxene and plagioclase as the cumulus phases. Titanomagnetite, ilmenite and sulphides occur as accessory, intercumulus phases. Subpegmatitic and pegmatitic textures are common. The majority of MZ rocks are cumulates that do not exhibit modal layering; however, mafic enclaves of basaltic or fine-grained melagabbroic material are found within anorthositic gabbro in northern Whitesides Township (Plate 1d), and mixed magma textures with granitoid A tonalite are present in western and northern Turnbull Township (described below). For cumulus MZ rocks, plagioclase ranges in composition from An_{46} to An_{70} and clinopyroxene Mg numbers range from 51 to 85 (*see* Figure 5, samples G-I).

Mixed Magma Outcrops

A wide variety of mixed magma textures between MZ and UZ gabbroic and tonalitic - granodioritic rocks occur over a 1 by 5 km area, in western Turnbull Township (*see* Figure 4). Agmatitic rocks with greater than 60% felsic intrusive material are found near and within the bounds of the granitoid A (*see* Plates 3a, b). Well-preserved mafic pillow-shaped structures up to 1 by 1 m, with quenched rims that contain fine-grained, radiating, acicular clinopyroxene and plagioclase aggregates, are found within coarse-grained, felsic intrusive rocks (*see* Plates 3c-f, 4a). The pillow-shaped structures have aphyric margins that grade into uniform, medium-grained cores. In Robb Township south of Kamiskotia Lake, tonalitic and gabbroic material is intercalated as alternating sill-like structures from 1 to 10 m thick. The gabbro becomes increasingly finer-grained toward the tonalitic sills, and exhibits a high degree of chlorite alteration. These features are similar to those found in well-documented mixed magma zones in mafic intrusions, such as the Tigalak and Newark Island layered intrusions, Labrador (Weibe and Wild 1983; Weibe 1987).

Upper Zone

The UZ consists of ferroan gabbronorite, quartz gabbro, hornblende gabbro and hornblendite, as massive and layered, medium- and coarse-grained meso- and orthocumulate. Plagioclase, clinopyroxene, orthopyroxene, pigeonite, and locally titanomagnetite are cumulus phases; apatite, and biotite occur as intercumulus phases (Plate 4b). Wolfe (1970) reported hornblende gabbro and hornblendite outcrops in the southeastern part of the UZ. Plagioclase commonly constitutes greater than 70% of the mode, and locally forms several metre-thick anorthosite layers (>90% plagioclase). Inverted pigeonite with clinopyroxene exsolution is common. Generally UZ rocks have a seriate texture and show no petrographic evidence for postcumulus overgrowths. Plagioclase compositions from petrographic determinations and microprobe analyses range from An_{46} to An_{60}; Mg numbers for clinopyroxene and orthopyroxene range from 59 to 70, and 57 to 75, respectively (*see* Figure 5, samples J-L). Cumulus magnetite contains up to 2.5 weight % V_2O_3 (Barrie 1990).

Granophyre

A wide variety of rocks are included in the granophyre zone, including diorite, quartz diorite, quartz monzodiorite, granodiorite, tonalite, quartz monzonite, quartz-feldspar porphyry and granite. These rocks are considered as one unit because the majority of them exhibit granophyric textures (Plate 4c), and because of their similar high trace element abundances (*see* "Geochemistry"). Hogg (1954) has provided the most detailed mapping and petrologic descriptions of the granophyre zone. His units "Intermediate Intrusives", "Granite", "Granophyre", and "Porphyritic Intrusives" are included in the granophyre zone of this report (*see* Figure 5). Contacts of granophyre zone rocks have irregular patterns. This is in part due to felsic granophyres that grade into KVC rocks: Hogg (1954) noted that some felsic granophyre rocks with layered spherulitic structures are gradational into rhyolites in northeastern Godfrey Township. Granophyres of intermediate composition (diorite, quartz diorite), located in northwestern Godfrey Township, are composed of acicular hornblende and actinolite, chlorite, trellis-textured leucoxene after titanomagnetite, and quartz and feldspar. Granophyres of felsic composition (quartz monzodiorite, granodiorite, tonalite, quartz monzonite, quartz-feldspar porphyry, and granite) in northwest Godfrey and southeast Jamieson townships have fine-grained margins and granophyric to locally miarolitic textures in the interior.

Kamiskotia Volcanic Complex

DEFINITION

The Kamiskotia Volcanic Complex (KVC) is defined here, in accordance with the North American Stratigraphic Code (*see* North American Commission on Stratigraphic Nomenclature 1983). The historical background, and reasons for the choice of name and lithodemic unit rank are essentially the same as those mentioned above for the KGC. Regional aspects, possible correlation with other rocks, and the age and petrogenesis of these metavolcanic rocks are discussed in detail elsewhere in this report. In this section, the descriptions of the physical boundaries and rock types are given.

Physical Boundaries

The KVC occupies an area of 210 km^2, in Carscallen, Bristol, eastern Turnbull, western Godfrey, southwestern Jamieson, southern Robb, and central Côté townships (*see* Map P.3396 back pocket and *also see* Figure 5). It is bounded to the south by the Lower volcanic suite; to the west by the KGC and granitoid A in Turnbull Township; to the north and east by a line that is parallel to stratigraphy and extends from a point 2 km north of the Kam-Kotia Mine to a point 2 km east of the Genex Mine, extending

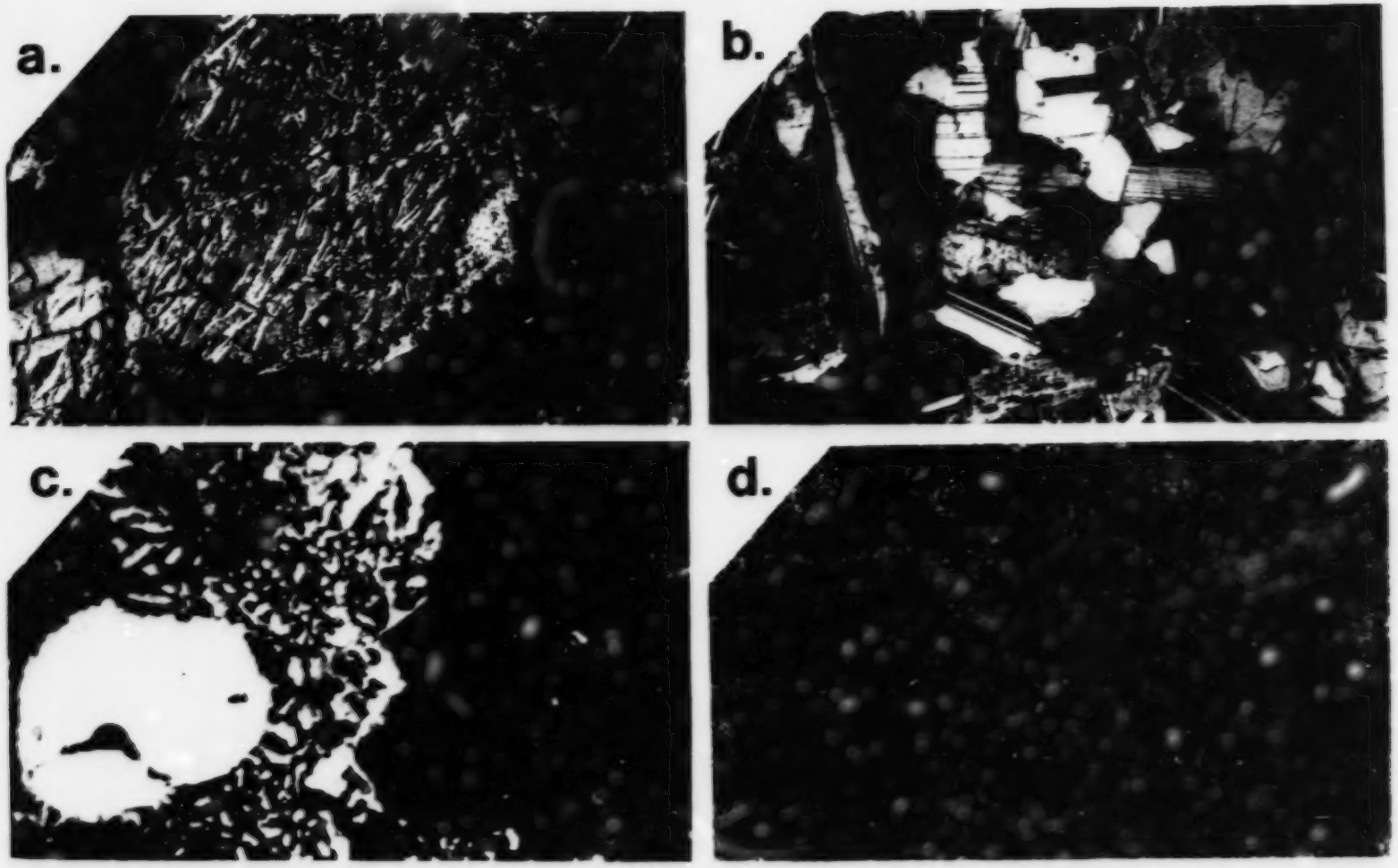

Plate 4. Photomicrographs of KGC rocks; all photomicrographs 2.2 mm across long dimension: a) cumulus olivine (center) and intercumulus plagioclase (bottom right) and sulphide (top left) in sulphide-bearing troctolite of the Lower Zone; b) ferroan gabbro of the Upper Zone, with plagioclase, pigeonite and titanium-rich magnetite; c) granophyric quartz-feldspar intergrowth surrounding partly resorbed quartz in KGC granophyre; d) quench textures in chill margin of mixed magma outcrop chilled gabbro: radiating clinopyroxene and plagioclase crystals.

into western Loveland Township to the north and toward central Bristol Township. This line represents a demarcation between metavolcanic rocks with few ground or airborne geophysical conductors to the west, and metavolcanic-metasedimentary rocks with numerous conductors to the east (Barlow 1988). The boundaries are well-defined in outcrop where they are represented by contacts with the KGC, but are less well-constrained in areas of poor exposure to the south, east and north. These boundaries are slightly more restrictive than those proposed by Middleton (1975). It is noted that the Reid Township rhyolite, with similar U-Pb age (*see* "Geochronology") and geochemistry to KVC rhyolites, may be a distal airfall deposit related to KVC magmatism.

Geology

The KVC is divided into two units: felsic volcanic rocks, consisting of massive or poorly bedded pyroclastic deposits with lesser block and ash flow material and flow-lobe complexes; and mafic volcanic rocks, consisting of massive and pillowed flows, pillow breccias and hyaloclastite tuffs and breccias. These units are observed to be intercalated on a scale of tens of metres in several locations with excellent exposure: at Mt. Jamieson in Jamieson Township, at the "Shell" outcrops 3 km to the northwest, and the Canadian Jamieson and Genex Mine properties in Godfrey Township. This implies that some mafic and felsic units are coeval.

Felsic volcanic rocks predominate in Carscallen and southern Godfrey townships. A thick sequence of pyroclastic tuffs and flows are present in Carscallen Township, with several individual units having apparent thicknesses of hundreds of metres, separated by agglomeratic units tens of metres in thickness. In northern Bristol Township, where exposures are poor, descriptions of rocks in drill core indicate a significant component of mafic metavolcanic rocks and lesser metasedimentary rocks. Some of the tuffs have fiamme-like textures that may represent primary welding. In Godfrey and eastern Turnbull townships, several layers of felsic agglomerates are present (Plate 5a) within massive, crystal-ash tuffs. A welded quartz-crystal lapilli tuff in central-southern Godfrey Township has unusual andesitic fragments with quenched rims (Comba et al. 1986), suggesting that the andesitic material quenched during a predominantly felsic pyroclastic eruption (Plate 5b). This provides additional evidence for the coeval eruption and deposition of magmas of intermediate and felsic composition. In Jamieson Township, rhyolite occurs in lobe-shaped flows (with restricted widths and thicknesses on a scale of tens to hundreds of metres). These constitute most of the outcrop ridges that extend from Mt. Jamieson, 3 km to the northeast (Comba et al. 1986). The lobe-shaped rhyolite flows are interlayered with mafic flows. They are flow banded, locally spherulitic, and occur locally as hyaloclastite, with large amygdules or lithophysae up to 3 cm in diameter. Spherulites may comprise up to 50% of a rhyolite flow on a given outcrop (Plate 5c).

Mafic volcanic rocks of the KVC predominate in Robb Township, where it forms a nearly uninterrupted, 2 km stratigraphic thickness west of the Kam-Kotia Mine. In this area, massive and pillowed basalts have relatively few amygdules (<10%). Amygdules are larger and more abundant along strike and up-section to the southeast in Godfrey Township. Thick, massive flows and sills are more common along strike to the west, whereas thinner units, including pillowed basalts and hyaloclastites, are more common toward the southeast (Middleton 1973b). Mafic metavolcanic rocks on the well-exposed Canadian Jamieson Mine property comprise massive flows, pillowed flows (Plate 4d), some with amygdules up to 0.5 mm (constituting up to 2% of the rock), and pillow breccia and hyaloclastite. Mafic rocks at the Genex Mine property are massive and pillowed flows, and pillow breccias.

Petrography

Primary mineralogy in KVC rocks is, in general, difficult to discern due to alteration. Less altered felsic tuffs and flows generally contain 5 to 15% quartz phenocrysts; feldspar phenocrysts are less common and range up to 15%. The matrix is aphanitic, and consists of sericite, chlorite, quartz, potassium feldspar and clay minerals; trace phases may include zircon, apatite, titanite, rutile, pyrite, and leucoxene after titanomagnetite. In more altered felsic volcanic rocks epidote and carbonate may be present. Spherules observed in the rock are composed of fine-grained, radiating intergrowths of quartz and feldspar, with the feldspar commonly altered to sericite and clay minerals.

The mafic volcanic rocks contain plagioclase phenocrysts up to 20% locally, although plagioclase phenocryst contents greater than 10% are rare. Primary mineralogy is particularly difficult to determine in mafic volcanic rocks of the KVC. Hart (1984) reported that sericite and epidote alteration of plagioclase does not allow for optical determination of their compositions. The matrix is generally chlorite, altered feldspar, amphibole, carbonate, epidote, possibly pyroxene and quartz; trace phases may include titanite, leucoxene after titanomagnetite, and sulphide.

Lower Volcanic Suite

The Lower volcanic suite occurs in central Whitesides, and southern Carscallen and Bristol townships. Rock types include massive and pillowed mafic volcanic rocks, and tuffaceous (?) rocks of intermediate and felsic composition. Mafic rocks predominate and constitute approximately 80% of the suite. At least one 2 to 10 m thick cherty sulphide-oxide-facies iron formation is intercalated with the Lower volcanic suite rocks (present in outcrop at the southeast end of Carscallen Lake), and a separate iron formation conformably overlies the suite. Ductile deformation is evident in many outcrops and obscures or obliterates primary textures (*see* "Structural Geology"). Where deformed, the mafic rocks form hornblende-actinolite-plagioclase schists. The felsic volcanic rocks are principally tuffaceous and are composed of sericite, quartz, and feldspar and clay minerals. Pervasive chlorite alteration is prevalent in the felsic volcanic rocks below the iron formation in western Carscallen Township, and is similar in appearance to synvolcanic alteration generally attributed to seafloor

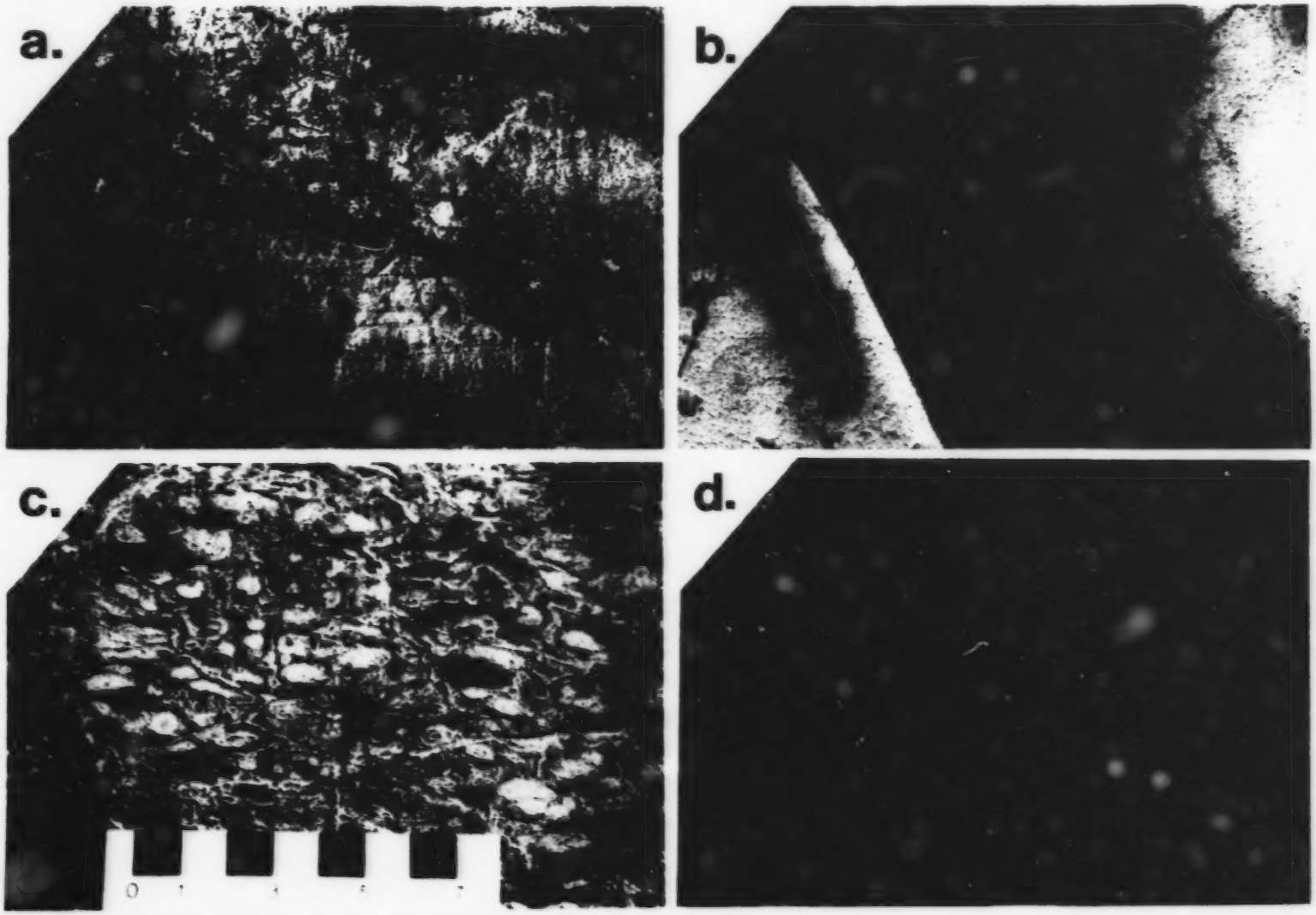

Plate 5. Textures in KVC rocks: a) rhyolite agglomerate, with blocks of flow-banded rhyolite, eastern Godfrey Township; b) rhyolite crystal tuff with quenched inclusions of andesitic material, providing evidence for coexisting felsic and intermediate liquids in magma chamber prior to eruption, southern Godfrey Township; c) spherulitic rhyolite, Kam-Kotia open pit, Robb Township; d) pillowed mafic metavolcanic rocks, with slight tectonic flattening parallel to hammer handle, Canadian Jamieson Mine property, northern Godfrey Township.

hydrothermal systems. Carbonate ± fuchsite alteration is present adjacent to quartz-carbonate-sulphide veins that cut deformed Lower volcanic suite rocks in several locations, including at the Union Mine property (*see* Figure 4).

Metasedimentary Rocks

Metasedimentary rocks are located in southern Bristol Township, and central Carscallen and Whitesides townships. They consist of metagreywacke, argillite, metachert, and oxide-sulphide-facies iron formation. At the Holmer Mine property in Bristol Township, the northeast part of the main outcrops is metagreywacke that consists of metre-thick layers with grain size that grades from coarse sand-sized to silt-sized, indicating that facing directions from graded bedding are to the south. These may represent thin turbidite horizons. Most iron formation and metachert occur in several outcrops along strike, from southern Carscallen Township to western Whitesides Township. This iron formation represents a single unit and contains up to 25% pyrite and 25% magnetite, either heavily disseminated throughout the metachert or as discrete layers up to 20 cm thick. In central Carscallen Township, the iron formation rests conformably on pillowed basalts of the Lower volcanic suite, with local magnetite and sulphide interstitial to relatively unaltered basalt pillows. Iron formation is also observed in outcrop in southwestern Carscallen Township, south of Carscallen Lake, that apparently form a separate unit.

Granitoid Rocks

The granitoid rocks described here are quartz bearing, leucocratic intrusive rocks that are not related to the KGC or the KVC. These are divided into four units. Three have been given informal names (*see* Map P.3396, back pocket): the Turnbull Township tonalite, the Côté Township tonalite, and the Groundhog River tonalite (in Enid, Frey, and western Massey and Whitesides townships). In this report, these masses are termed granitoids A, B, C, respectively; a fourth granitoid mass, in southern Whitesides and Carscallen townships, is termed granitoid D (*see* Figure 4). Other granitoid rocks are undifferentiated.

Granitoid A is characterized by mixed magma textures with chilled rocks of the KGC, and exhibits a wide variety of textural and modal characteristics. It is composed of medium- to coarse-grained tonalite and granodiorite, with subordinate quartz diorite, quartz monzodiorite, quartz monzonite and granite, and local quartz-feldspar aplite and pegmatite. Much of the granitoid A region is underlain by hybrid or agmatitic rocks where rocks of the KGC form blocks, fragments and pillow-like structures within a granitoid matrix (*see* Plates 3a-f).

Granitoids B and C consist of medium- to coarse-grained quartz diorite, tonalite, quartz monzodiorite, granodiorite, quartz monzonite, granite; and felsic aplite and pegmatite dikes or masses. Both intrusions have well-developed flattening fabrics along their margins, with foliations and locally, gneissic fabrics that parallel the intrusive contacts. Intrusive breccia zones up to 3 km thick containing flattened, angular blocks of wall rock characterize the margins. In granitoid B, angular blocks of anorthositic gabbro are found as far as 5 km from the southern margin, and it appears that much of the intrusion contains large fragments of gabbro.

Bristol Township Lamprophyre Suite

A lamprophyre suite is found within the DPFZ in southwestern Bristol Township, on the Croxall and Holmer properties (*see* Figure 4; *see also* Figures 32 and 34) (Plate 6). For this report, the suite is informally named the Bristol Township lamprophyre suite. The suite occurs within deformed and carbonate-altered metabasalts and metasedimentary rocks. Recently exhumed exposures on the Croxall property have revealed that the suite is greater than 60 m wide and has subvertical contacts. Ground magnetic surveys suggest that the suite extends under glacial cover to the southwest for several kilometres with widths up to 1 km. The suite is also present in outcrop 1.5 km to the northeast of the Croxall property on the Holmer property, where trace-element enriched, altered clinopyroxenites are found adjacent to gold mineralization.

The Bristol Township lamprophyre suite is unique in its mineralogy and geochemistry in the southern Superior Province. It consists of three principal lithologic types, with mutually gradational and/or crosscutting relationships. The most abundant (50% of the exposures) is biotite lamprophyre forming the margins of the suite composed of a groundmass of fine-grained ferroan carbonate, serpentine, biotite and apatite and minor to trace amounts of potassium feldspar, chlorite, magnetite, baddeleyite, sulphate and sulphide. The next most abundant lithology (47% of the exposures) is a diopside-rich rock, consisting of medium- to very coarse-grained diopside in a distinctive bladed crystal habit, with interstitial chessboard albite (after potassium feldspar), garnet, phlogopite, magnetite, and epidote. Garnetite and garnet-rich feldspathic dikes are the third lithology of the lamprophyre suite (3% of the exposures). These dikes contain from 7 to 85% red-brown garnet as fine-grained euhedra to very coarse-grained aggregates. Preliminary microprobe analyses indicate high calcium and iron contents, and greater than 5 weight % TiO_2 and up to 3500 ppm Zr. This indicates that they are melanite-andradite (with a kimzeyitic component), common to ultramafic lamprophyres (Rock 1986). Up to 30% light brown, anisotropic hydrogarnet or clinopyroxene rimming garnet is present in the rock. Other minerals present are diopside, calcite, biotite, apatite; and minor potassium feldspar, tremolite, titanite, allanite, magnetite, and chlorite and sulphides. There is one exposure of highly altered garnetite, with an octagonal-shaped, coarse-grained mineral (garnet?) as the principal constituent in fine-grained matrix of chlorite, biotite, epidote, magnetite, rutile and sulphides (pyrite, chalcopyrite). The garnet has been completely replaced by fine-grained calcite and dolomite, potassium feldspar, albite, sericite, and very fine-grained rutile, baddeleyite and/or zircon.

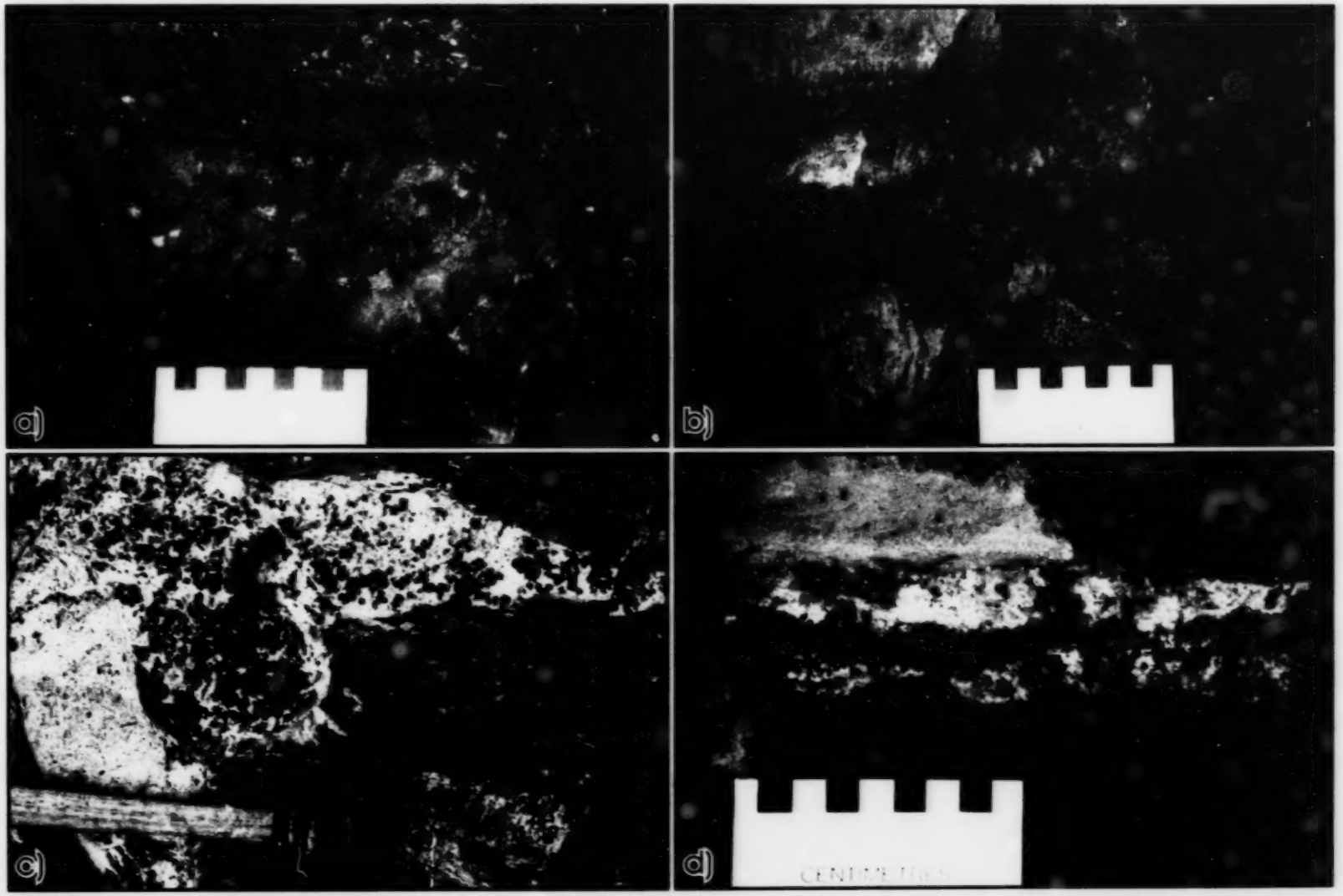

Plate 6. Croxall property ultramafic lamprophyre suite: a) undeformed biotite-rich lamprophyre; very coarse-grained, dark brown to black biotite in matrix of ferroan carbonate, chlorite, magnetite and apatite; b) contact between biotite ultramafic lamprophyre and melanite-bearing syenite dike; note alignment of biotite and magnetite (pseudomorphous after biotite) perpendicular to contact; c) melanite-bearing syenite dike (to left) and apophyses (to right), cutting carbonate-rich ultramafic lamprophyre; d) thin melanite-bearing syenite dike cutting medium-grained diopside-feldspar-melanite-biotite rock; note coxcomb-like growth of garnet toward dike center.

Structure

BEDDING AND LAYERING, AND REGIONAL FOLDING

Facing directions are observed in the metavolcanic strata and in KGC cumulates (*see* Figure 4). In the Lower volcanic suite, facing directions from pillowed mafic metavolcanic rocks are consistently to the north through Whitesides, Carscallen and Bristol townships. In several of these outcrops, bedding is overturned and dips steeply to the south. Grain size gradations in KVC pyroclastic crystal ash deposits indicate facing directions to the northeast in southern Godfrey Township, and face east in recently stripped outcrops in central Godfrey Township. These facing directions are in agreement with well-exposed outcrops of KVC pillowed mafic metavolcanic rocks, which are east-facing in central Godfrey Township, and face to the northeast in northern part of this township, and in southern Robb and Jamieson townships. Transposition of bedding is observed in the vicinity of the DPFZ, with a predominantly dextral displacement; and near the fault that parallels Highway 576, near the Canadian Jamieson Mine, also with a dextral sense of displacement. The transposed strata near the Canadian Jamieson Mine were originally more north-facing prior to transposition.

Facing directions in the KGC are based on modal gradations in layering, with "normal" mafic to felsic gradation in cumulus minerals pointing up stratigraphy (*see* Plate 1a). This is generally the case in most intrusions that exhibit cumulate layering, although postcumulus processes may create the opposite effect, and layering in alkaline intrusions commonly exhibits "reverse" gradations (Irvine 1982; Parsons 1979). Facing directions are also inferred from cross-bedding features. In western Whitesides Township, Lower Zone cumulates have east facing directions, with layering overturned and dipping steeply to the west (*see* Plate 1b). Facing directions are to the north in northeast Carscallen and northwest Massey townships. Upper Zone cumulates show a consistent northeast facing in southern Robb Township.

In a broad sense, the stratigraphy (Lower volcanic suite, metasedimentary rocks, KGC, KVC) forms a regional monocline that faces to the north and northeast. Thick glacial deposits cover a substantial portion of the MZ, which prevents a more detailed structural analysis. Granitoids B, C and D represent antiformal structures, and in general facing directions are away from their margins. It is possible that a synform, with a north-trending axis is present in the southwestern KGC. This may explain the apparent anomalous thickness of the KGC observed from central Whitesides Township to central Turnbull Township. The apparent anomalous thickness of the northern KGC in southern Robb Township may be due to a higher proportion of felsic intrusive material than is mapped; glacial deposits also cover bedrock in this area.

Linear features in the Kamiskotia area that are apparent on the Timmins area shadow-enhanced total magnetic field map (Barlow 1988) are depicted on the accompanying 1:50 000 scale map (*see* Map P.3396, back pocket). The shadow enhancement is designed to filter out the north-northwest-trending Matachewan dikes in the area. Several linear features on the shadow-enhanced magnetic map are used either to interpret or extrapolate significant geological features where there is poor bedrock exposure. Firstly, a north-northwest-trending linear feature is aligned with a 2 km left-lateral offset of the KGC–Lower volcanic suite contact in Carscallen Township. This linear feature is interpreted as a continuation of the fault that extends through western Turnbull Township into northwestern Robb Township, with 1 to 2 km of apparent sinistral displacement. Secondly, an oval, concentric magnetic pattern is apparent around granitoid B in Côté Township, consistent with granitoid B representing the core of a dome-like or antiformal structure. Thirdly, magnetic units in the Middle Zone of the KGC are interpreted to form a steeply plunging synform that opens to the west-southwest. This feature is present immediately south of granitoid B, in Massey Township, where there is a thick cover of glacial alluvium. These features are depicted on the 1:50 000 map (*see* Map P.3396). And fourthly, a prominent, northwest-trending linear feature extends from southeast Bristol Township to northwest Côté Township. This is interpreted as a post-Kenoran mafic dike that is not present at the surface in the Kamiskotia area.

STRUCTURAL FABRIC ANALYSIS

To determine the structural history of the Kamiskotia area, penetrative and non-penetrative foliations, lineations and L-S fabrics (Flinn 1965) were recorded, in addition to the bedding attitudes described above. The major planar fabric is schistosity (Figures 6, 7); however, gneissosity is present locally between the margins of granitoids B and C, within amphibolite-grade Lower volcanic suite rocks and leucocratic tonalite lenses. Lineations and L-S fabrics were recorded for outcrops with penetrative deformation wherever possible (Figures 8, 9). The L-S fabric scheme qualitatively estimates the prolateness factor of the strain ellipsoid by comparing the relative strength of lineation (L) with that of foliation (S - schistosity) for minerals or mineral aggregates, assuming that their initial state was quasi-spherical. For prolate strain ellipsoids, L is greater than S with the maximum extension direction parallel to the lineation measured in the field. When combined with regional lithologic, foliation and lineation patterns, the L-S fabric scheme has been used with success to discriminate between structural hypotheses in Archean terranes, particularly within and adjacent to granitoid intrusions (e.g., Schwerdtner et al. 1983; Stott 1985).

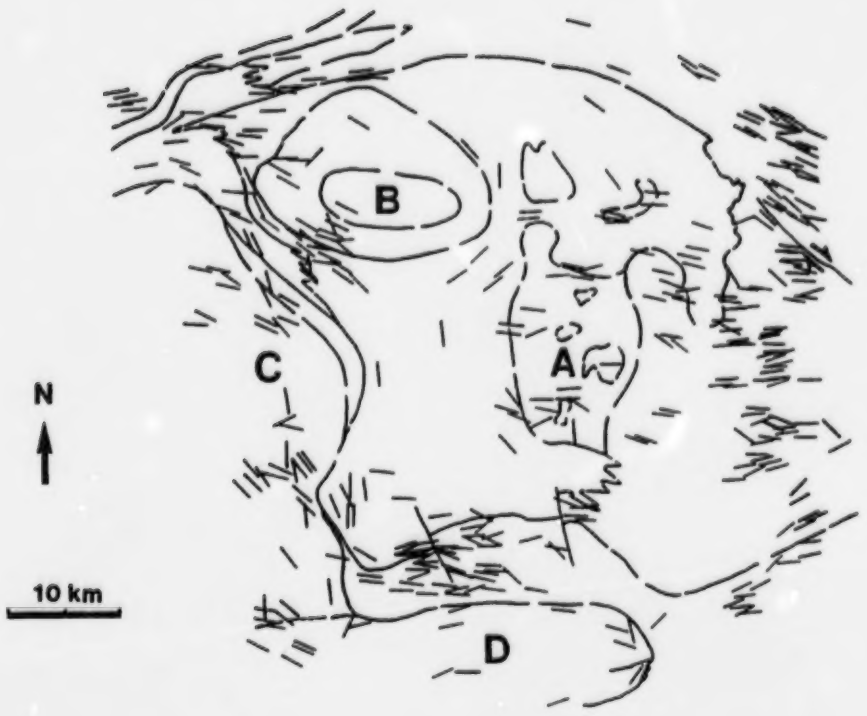

Figure 6. Foliation map. Outcrop exposure reflected by density of foliations. Bedrock in the region of granitoid B and the central KGC under glacial cover; bedrock in region of southern KVC covered by poorly drained area. All foliations are near vertical (90°±15°). No preferred dip directions are evident across the region.

Results

Two prominent features appear in planar fabric maps (*see* Figures 6, 7): zones of foliation that parallel the margins of granitoids B, C and D; and east-trending foliations, particularly in the KVC. The zones of foliation parallel to the margins of granitoids B, C and D extend up to 2 km on either side of the granitoid margins, and locally up to 5 km into the country rocks. The intensity of penetrative deformation (Plates 7a,b) diminishes with distance from the contacts. From the available outcrops, it appears that granitoid B is completely rimmed by penetratively deformed rocks. Fragments of gabbro and mafic metavolcanic rock are found within the foliated margins of granitoids B and C.

The second prominent feature noted in the planar fabric maps is the pervasive east-trending foliation across the Kamiskotia area, particularly in the metavolcanic rocks to the east (*see* Figures 6, 7). This fabric is generally nonpenetrative and cuts directly across the strike of the metavolcanic rocks. Furthermore it continues relatively undisturbed through granitoid A, in contrast to foliations that parallel the contacts of the other felsic intrusions. Penetrative fabrics are confined to local, east-northeast- and east-southeast-trending high strain zones that contain quartz ± pyrite veins in the region of granitoid A. The east-trending foliation is most pervasive in the vicinity of base metal mineralization, where the metavolcanic rocks have undergone hydrothermal alteration (sericite and chlorite alteration). In metavolcanic rocks to the north, the fabric strikes west-northwest and to the south, west-southwest.

A consistent, shallow west-plunging stretching lineation is pervasive in the Lower volcanic suite north of granitoid D, and at the C-D contact (*see* Figures 8, 9). This fabric extends to the east and merges with highly strained rocks within the westernmost extent of the DPFZ. Accompanying this fabric is a reasonably consistent dextral sense of displacement (5 observations of dextral sense to 1 observation of sinistral sense) noted on the subhorizontal plane in asymmetric, transposed fold hinges of siliceous material within strained Lower volcanic suite rocks, and within shear zones in granitoid D (Plate 7d). Between granitoids B and C, there are two prominent lineation trends, some plunging steeply to the north-northeast along the northwest contact of granitoid C, and the other with a shallow northwest plunge. Highly prolate (L>>S) fabrics are concentrated between granitoids B and C, and along the northern contact of granitoid D, extending toward a part of the westernmost DPFZ (*see* Figure 9). Highly strained rocks also occur in ductile shear zones that strike west-northwest with a dextral sense of displacement in KVC rocks near the Canadian Jamieson Mine (Plate 7c).

Highly prolate fabrics are present on the Holmer property in southwest Bristol Township. The Bristol Township lamprophyre suite on the adjacent Croxall property occurs

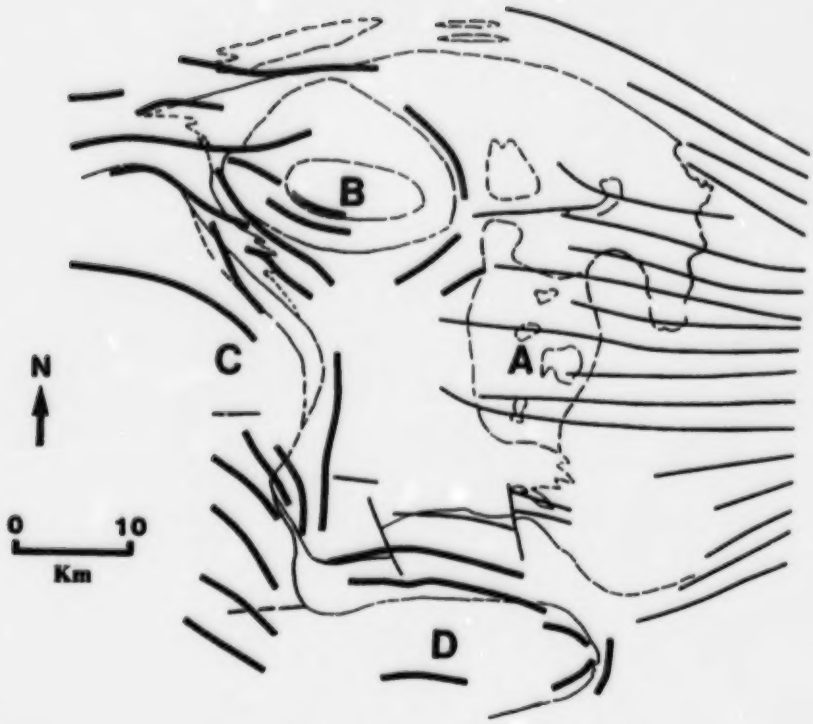

Figure 7. Foliation trajectory map. Visual estimate of foliation trends, based on foliations in Figure 6. Light lines represent predominantly non-penetrative foliations due to north-south compression; bold lines represent penetrative planar fabrics due to granitoid emplacement.

within deformed and carbonate-altered basalts in the DPFZ. The margins of the suite are highly deformed, with a well-developed, subvertical flattening fabric that exhibits a component of elongation locally. The central portion of the suite is nearly undeformed, but is cut by subvertical shear zones up to 50 cm thick, and by brittle fractures with minor displacements of up to 20 cm.

Interpretation

The foliations that parallel the margins of granitoids B and C define contact strain zones; for granitoid D, where the foliation apparently encircles the intrusion, it defines a contact strain aureole. These features may be the result of granitoid emplacement by diapirism and ballooning mechanisms. Schwerdtner et al. (1978) outlined three principal features that characterize diapiric structures. Firstly, an inverse density stratification is necessary for initial diapiric movement between a hot magma body and surrounding rocks. This is a common feature for granitic basement rocks, although densities may change after diapirism due to cooling of magma or an increase in metamorphism in the mantling material. This would pertain to the Kamiskotia area, where denser gabbroic rock (q = 2.85 to 3.12 g/cc) is cut by felsic intrusive rocks (q = 2.52 to 2.96 g/cc for granite to quartz diorite; 2.33 to 2.57 g/cc for rhyolite to andesite liquids: Daly et al. 1966) at the base of the KGC. Secondly, the plan of a diapiric structure should have a continuous, smooth oval outline. This would pertain to granitoid B, and may also be the case for granitoids C and D, considering their regional aeromagnetic signatures and topographic expressions. Poor outcrop to the west and south of the mapped area limits the use of these criteria for parts of granitoids C and D. Thirdly, subhorizontal stretching fabrics should be present across the crest line of the diapiric structure. However possible crest lines with a subhorizontal stretching fabric are not preserved or exposed for these intrusions. Granitoids B, C and D meet two of the three criteria for diapirism, and are interpreted to have been emplaced by diapiric processes.

As the flattening fabric in the margins of granitoids B, C and D and in mantling country rock is well-developed, ballooning may have occurred in addition to diapirism. After partial crystallization at their margins, these intrusions may have expanded and ballooned *in situ* as more magma entered the chamber, producing a radial compressive force that would create the observed tangential flattening fabric (e.g., Bateman 1985).

The fragments of gabbro and mafic metavolcanic rock within the foliated margins of granitoids B and C suggest that stoping of adjacent country rock may have been an operative process, in addition to diapirism and ballooning. Stoping is believed to be a common intrusive mechanism during the final stages of granitoid emplacement at high

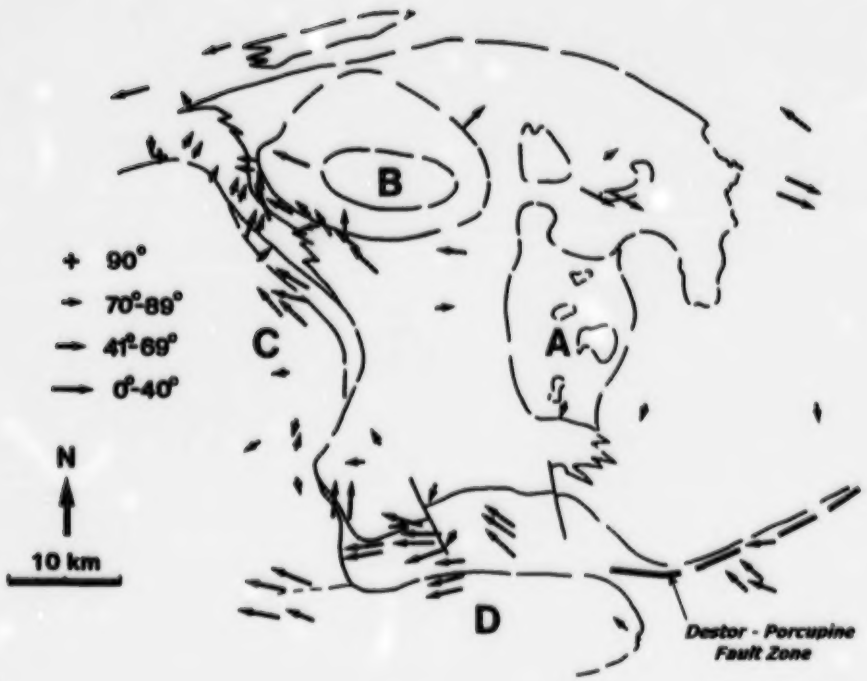

Figure 8. Mineral lineation map. Note that the western extent of the Destor–Porcupine Fault Zone extends to the east and north of Granitoid D; a splay continues to the north within the Lower volcanic suite.

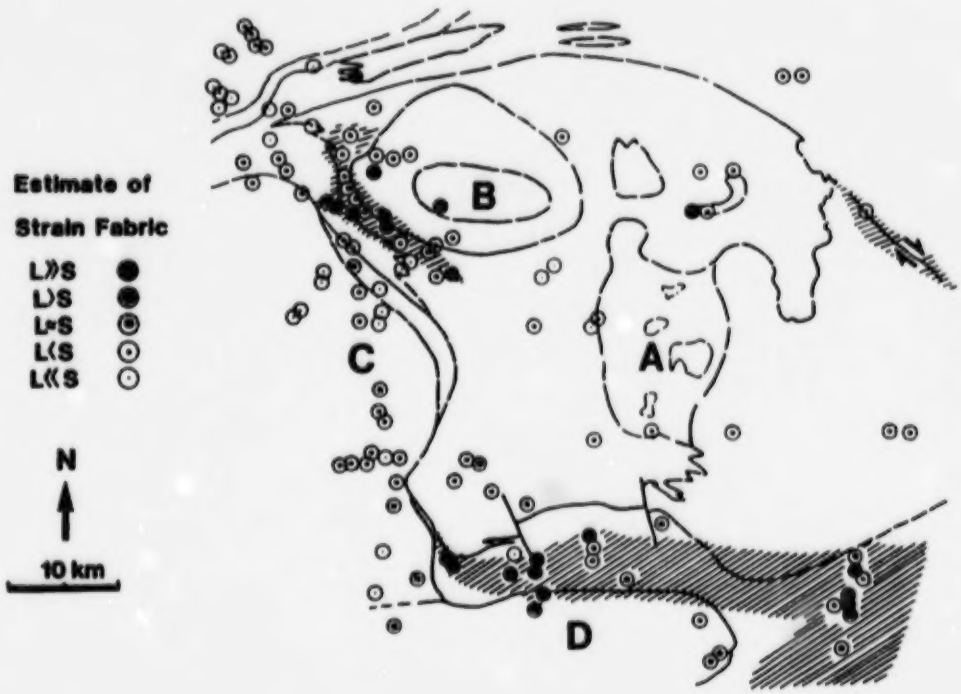

Figure 9. Map of apparent total strain fabric, based on field observations of mineral aggregates. Areas of high strain intensity shaded.

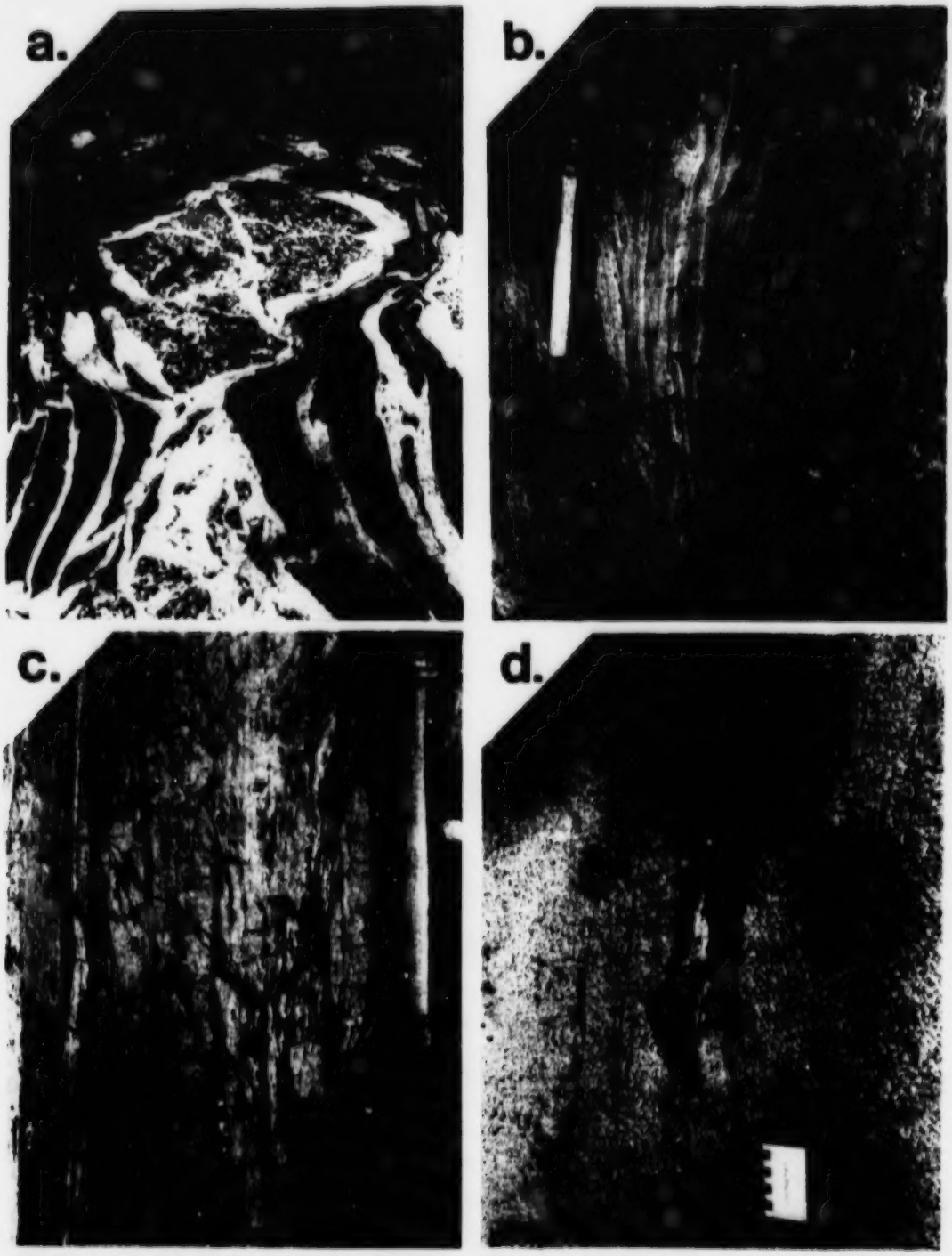

Plate 7. Deformation textures: a) boudinaged blocks of Lower Zone gabbronorite in migmatitic rocks in western part of contact strain zone of granitoid B, Enid Township; b) chevron folds in mafic metavolcanic rocks? of the Lower volcanic suite, situated between granitoids B and C, northwest Massey Township; c) ductile shear zone in KVC rocks on the Canadian Jamieson Mine property. Note possible pillow rims near hammer, now highly attenuated. Deformation intensity increases to left. These rocks occur 4 m away from those in photograph 5d; d) Small zone of ductile deformation in the eastern extent of granitoid D. Undeformed granodiorite is progressively deformed toward quartz-sulphide vein in center, with C fabric parallel to pens.

crustal levels (Bateman 1985), particularly by magmas with lower water contents (Marsh 1982).

The east-trending foliation may be a product of a late north-south compressional event that affected much of the southern Superior Province (Stott et al. 1987). The deflection of foliations away from an east-west trend in the metavolcanic rocks may be the result of a competency contrast between locally altered metavolcanic rocks and the more competent, relatively unaltered intrusions to the west. Within the contact strain zone of granitoid C, this fabric is manifested as a weak, non-penetrative foliation or parting cleavage which locally cuts the foliation produced by the emplacement of granitoid C. This provides evidence that at least some north-south compression post-dated the emplacement of granitoid C. Furthermore, the east-west fabric cuts across the strike of the subvertical KVC, indicating that north-south compression postdated a passive, bulk crustal rotation of the stratigraphy, that did not produce any rock fabric.

The observation that granitoid A is cut by the east-trending foliation indicates that it was emplaced in a manner entirely different from that of the other felsic intrusions. Granitoid A is characterized by a variety of mixed magma textures with the basal part of the Middle Zone of the KGC, indicating that it was emplaced during the solidification of the KGC and is therefore contemporaneous with it. Possible flexures on the western side of granitoid A may be related to strain from neighboring granitoid intrusions.

The two lineation trends between granitoids B and C may be related to granitoid C emplacement. The steep north-northeast-plunging lineations are consistent with an upward diapiric movement of granitoid C with respect to the surrounding rocks. In laboratory experiments of diapiric structures using plasticine, Dixon (1975) noted that subvertical prolate strain ellipsoids will develop along the flanks of diapiric structures of circular or oval plan. Similar features have been documented at the margins of crescentic granitoid plutons in northwestern Ontario (Schwerdtner et al. 1983). The shallow northwest-plunging lineations are found within granitoid C, within its intrusive breccia zone and into the KGC near granitoid B, overprinting any previous fabric formed from granitoid B emplacement. This fabric may be a product of ballooning by granitoid C against a competent wall of granitoid B, creating a subhorizontal stress regime where the less competent mantling material was attenuated parallel to the C axis of the strain ellipsoid. Alternatively, it may reflect strain created by flow of magma and crystal mush within granitoid C after the formation of a gneissic carapace and wall. Similar models have been proposed to explain subhorizontal stretching fabrics in crescentic granitoid plutons (Schwerdtner et al. 1983).

The shallow, west-plunging stretching (elongation) lineation within the Lower volcanic suite and at the margins of granitoid D may have resulted from 1) emplacement of granitoid D, 2) bulk north-south shortening, or 3) ductile shear along a splay of the DPFZ, possibly related to late north-south bulk shortening or transpression. Although this west-plunging fabric is parallel to the margin of granitoid D, it extends eastward for 10 km past the nose of granitoid D and on into the DPFZ. As the contacts of granitoid D are near vertical, it is unlikely that its contact strain effects would extend 10 km and beyond in one direction. Bulk north-south shortening could produce this fabric between two competent masses (granitoid D and the KGC) if, during deformation, the Lower volcanic suite was confined by competent material above and below. However, the continuation of this strain fabric in metavolcanic rocks to the east away from any competent intrusive masses argues against pure north-south compression. The third scenario is related to ductile shear along the DPFZ, this prolate strain regime predominates over any flattening fabric that could be attributed to granitoid D emplacement or pure north-south compression. Furthermore, this deformation zone contains numerous occurrences of lode gold mineralization, with syn- to posttectonic, quartz-tourmaline-sulphide gold veins and associated carbonate alteration, similar to occurrences found in the western DPFZ.

Summary

Based on geology and fabric analysis, the sequence of major magmatic and tectonic events in the Kamiskotia area are interpreted as follows: 1) formation of the Lower volcanic suite; 2) formation of the KGC–KVC, and coeval intrusion of granitoid A into the KGC during solidification; 3) regional bulk rotation of the stratigraphy about a subhorizontal axis, to form a northeast-facing monocline; possibly accompanied by 4) diapiric intrusion of granitoids B, C and D (timing with respect to each other not established), imparting their respective contact strain aureoles or zones on mantling material; 5) regional north-south compression, probably in part synchronous with, but locally postdated by 6) ductile shear along the western DPFZ, and a related splay through the Lower volcanic suite, that exhibits a consistent sense of dextral displacement.

Geochronology

Primary igneous ages from U-Pb geochronology and primary and secondary ages from Sm-Nd and Rb-Sr isochron systematics have been determined for Kamiskotia area rocks in studies by Barrie (1990), Barrie and Davis (1990), and Barrie and Shirey (1991). In this section, the results from these studies are reviewed, and then the chronologic constraints on the magmatic and structural history of the area are discussed. Sample locations are marked in Figure 10. Universal Transverse Mercator grid coordinates for the sample locations with brief petrologic descriptions are provided in Appendix I.

RESULTS OF U–Pb GEOCHRONOLOGY

A pegmatitic quartz gabbro sample taken from the Middle Zone of the KGC gave a U–Pb age of 2707±2 Ma. Zircons from a quartz- and feldspar-phyric flow-banded rhyolite sample of the Kamiskotia rhyolite gave an age of 2705±2 Ma. This age coincides, within the margin of error, with the age for the KGC.

Samples were obtained from a well-foliated tonalite forming the contact strain aureole of Granitoid B (Côté Township tonalite) and the contact strain zone of Granitoid C (Groundhog River tonalite). Zircons from granitoid C yield an age of 2696±1.5 Ma. A titanite fraction, from the same sample is nearly concordant, with a $^{207}Pb/^{206}Pb$ age of 2692±5 Ma. One zircon fraction from granitoid B has a $^{207}Pb/^{206}Pb$ age of 2926 Ma and is 4.6% discordant. This most likely represents an inherited component. Four more analyses of abraded, small zircon fractions are all slightly discordant, with $^{207}Pb/^{206}Pb$ ages ranging from 2704 to 2693 Ma. One grain with a $^{207}Pb/^{206}Pb$ age of 2704 Ma may be inherited from a slightly older component, and the preferred crystallization age is an average of the three lower $^{207}Pb/^{206}Pb$ ages at 2694±4 Ma.

In an attempt to provide for time-stratigraphic correlation with other the felsic volcanic rocks in region, U-Pb ages are reported for three felsic metavolcanic rocks in the Kidd Creek area, including the addition of one abraded, concordant fraction to previous analyses of the Kidd Creek rhyolite by Nunes and Pyke (1981), and two new ages. For the Kidd Creek rhyolite, the new age is more precise than the age previously reported, at 2717±2 Ma. Two other rhyolites, termed the Prosser (Township) rhyolite and the Reid (Township) rhyolite, are quartz- and feldspar-phyric tuffaceous horizons intercalated with metasedimentary rocks, located to the east and west of the Kidd Creek mine, respectively (*see* Figure 10). The Prosser rhyolite is 2716±4 Ma, and the Reid rhyolite is 2705 +5/-3 Ma. The Prosser rhyolite is coeval within error with the Kidd Creek rhyolite, whereas the Reid rhyolite is coeval with the KGC and Kamiskotia rhyolite 40 km to the south-southwest.

U-Pb isotopic data for two garnet fractions and one titanite fraction from a garnetite dike in the Bristol Township lamprophyre suite yield an age of 2687±3 Ma. The garnetite dike is undeformed; however, the lamprophyre suite is deformed along its margins, with the fabric parallel to the fabric in the DPFZ. The lamprophyre suite is interpreted to have utilized the DPFZ as a conduit, thus the age represents a minimum age for the early formation of the DPFZ in this area. The U-Pb system in garnet is apparently more resilient than other isotopic systems (Rb-Sr, Ar-Ar, Sm-Nd) for whole rock suites and minerals associated with lode gold mineralization within the DPFZ, which show evidence for resetting or disturbance (Kerrich et al. 1987; Bell et al. 1989; Wong et al. 1989; Barrie 1990).

Sm-Nd AND Rb-Sr ISOCHRON AND REGRESSION AGES

Mineral separates for four whole rock samples were analyzed for Sm-Nd and Rb-Sr isotopes to produce mineral-whole rock isochrons, which are summarized in Table 3. These isotope systems are set at the time of crystallization, but may be reset during subsequent metamorphic events. The McIntyre 1 regression model (McIntyre et al. 1966) has been used to calculate regression lines for these data. If the regression has an MSWD (mean square of the weighted deviates) of less than 3, the scatter in the data can be accommodated by analytical uncertainty, and the regression line is termed an isochron.

A seven point Sm-Nd isochron for rocks and mineral separates from the KGC and KVC, including plagioclase and clinopyroxene analyses, yielded an age of 2710±30 Ma (2-r), in complete agreement with the KGC and KVC U-Pb ages. An isochron from Rb-Sr analyses of a whole rock KGC ferroan gabbro and clinopyroxene and zircon fractions derived from the ferroan gabbro sample has an age of 2450±35 Ma. This age is identical within error to three U-Pb discordia ages from regressions of baddeleyite and zircon fractions, all at 2452 +3/-2 Ma, from the Hearst–Matachewan mafic dike swarm (Heaman 1989); and one baddeleyite fraction (2460 Ma: L. Heaman, personal communication, 1989) from a Matachewan dike 12 km from this location.

Regression of isotope data for mineral separates from samples of granitoids B and C produce ages younger than their zircon and titanite U-Pb ages in the Sm-Nd and Rb-Sr systems. For the granitoid B, a whole rock-plagioclase-apatite1-apatite2 (two separate apatite reactions) Sm-Nd isochron has an age of 2615±15 Ma, significantly younger than the 2696±4 Ma U-Pb age from the same rock. This age represents essentially a two point isochron, controlled by the apatite fractions with their similar isotopic ratios, and the precision of the age error should be considered with some caution. The Rb-Sr data did not yield meaningful results, indicating an open system behavior for Rb or Sr, or both were susceptible to remobilization after crystallization in this sample.

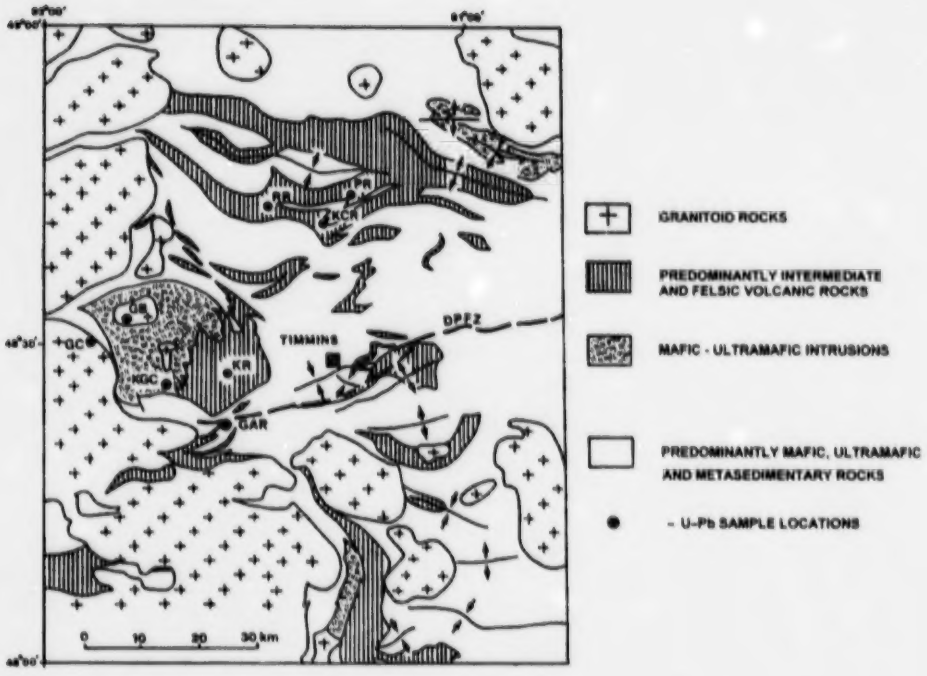

Figure 10. U-Pb sample locations, and general geology of the Kamiskotia–Kidd Creek area. KGC-Kamiskotia Gabbroic Complex; KR-Kamiskotia rhyolite of the Kamiskotia Volcanic Complex; GB-Granitoid B (Côté Township tonalite); GC-Granitoid C (Groundhog River tonalite); GAR-garnetite of the Bristol Township lamprophyre suite; KCR-Kidd Creek rhyolite; RR-Reid (Township) rhyolite; PR-Prosser (Township) rhyolite.

Table 3: Summary of Sm-Nd and Rb-Sr ages (*from* Barrie 1990).

Rock Unit	System	Age (Ma)[1]	MSWD[2]	Initial Ratio	Comments
Kamiskotia Gabbroic and Volcanic Complex	Sm-Nd Rb-Sr	2710±30 2450±35	2.77 0.42	0.50925±4 0.70085±4	Whole rock and mineral separates from Kamiskotia ferroan gabbro.
Côté Township tonalite (GB)	Sm-Nd	2615±15	2.24	0.50940±2	Whole rock and mineral separates.
Groundhog River tonalite (GC)	Sm-Nd Rb-Sr	2530±35 2530±35	14.0 8.7	0.50941±4 0.70124±2	Whole rock and mineral separates.
Bristol Township lamprophyre suite	Sm-Nd	2500±160	0.37	0.50959±7	Garnetite dike; whole rock and mineral separates.

[1] Ages and initial ratios with 2-sigma errors calculated using a McIntyre 1 model least squares cubic regression program (McIntyre et al. 1966), with 2-sigma errors for $^{143}Nd/^{144}Nd$ and $^{87}Sr/^{86}Sr$ =0.000040, $^{147}Sm/^{144}Nd$ = 0.3%, $^{87}Rb/^{86}Sr$ = 2.0%.

[2] Ages with MSWD values <3 indicate geological scatter inside of analytical error and represent isochrons. See text for discussion.

For granitoid C, regressions of the Sm-Nd and Rb-Sr data give ages that are identical at 2530±35 Ma, younger than the U-Pb zircon age of 2696±2 Ma for the same sample, and a U-Pb titanite $^{207}Pb/^{206}Pb$ minimum age of 2692±5 Ma. The agreement between the Sm-Nd and Rb-Sr isotope systems is strong evidence that this age has geological significance. Similar ages of 2530, 2508 and 2504 Ma have been reported for individual, concordant metamorphic titanite grains in granulite and upper amphibolite grade rocks of the nearby Kapuskasing Structural Zone, 40 km to the west (Krogh et al. 1988).

MAGMATIC AND STRUCTURAL HISTORY

A chronologic summary of the magmatism and deformation in the Kamiskotia–Kidd Creek area based on the U-Pb data is presented in Figure 11. Three periods of magmatic

activity occurred at approximately 10 million-year intervals: felsic volcanism in the Kidd Creek area from 2717±2 to 2716±4 Ma, volcanism and hypabyssal mafic and felsic intrusions at 2707±2 to 2705±2 Ma, and voluminous granitoid emplacement at 2696±1.5 to 2694±4 Ma. The timing of deformation events, constrained by geological relationships along with U-Pb ages, is in part coincident with and related to the magmatism, with regional crustal warping between 2705±2 and 2694±4 Ma, and with contact strain aureole and zone development. North-south compression postdated contact strain development for granitoid C. A minimum age for the early formation of the DPFZ may be provided by a U-Pb age for the garnetite dike from the Bristol Township lamprophyre suite, at 2687±3 Ma.

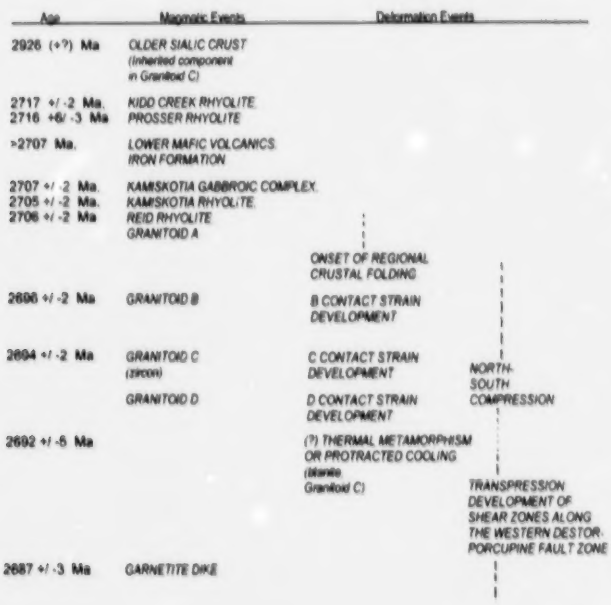

Figure 11. Summary of the U-Pb ages in the Kamiskotia–Kidd Creek area.

Geochemistry

Major, trace and rare earth element analyses for KGC, KVC, Lower volcanic suite rocks, granitoid rocks, and the Bristol Township lamprophyre suite are presented in this section. Particular emphasis is given to the characteristics and petrogenesis of the KGC, and its relationship to KVC basalts.

ALTERATION

Major and incompatible trace elements for the rock suites presented in this section plot as coherent trends on inter-element variation diagrams, and are believed to represent the primary compositions, despite postsolidus alteration and metamorphism. This is in accord with studies on the mobility of major and trace elements in greenstone belt rocks that have been subjected to greenschist facies metamorphism and normal surficial weathering processes (Menzies et al. 1979; Ludden et al. 1982; Beswick 1982). Variation diagrams for KGC cumulates and KVC basalts, using K_2O, Rb and Ba do not correlate well with other elements of similar geochemical affinities: Therefore, little emphasis is placed on these elements in the mafic rocks.

KGC CUMULATES

Whole rock major oxide and trace element compositions for 33 medium to coarse-grained cumulus samples are given in Table 4 and located in Figure 12. They include four olivine-bearing cumulates of the LZ: two peridotites (samples 1 and 2) and two troctolites (samples 3 and 4), other LZ cumulates (sample 15) and MZ cumulates (samples 16 to 23) which constitute the Western Traverse, and UZ cumulates (samples 24 to 33) which constitute the Northeastern Traverse (*see* Figure 12). The samples are assigned a stratigraphic height by projection along strike to the traverse lines. These heights have errors of approximately ±5 to 50 m, with larger errors for the UZ samples located far from the traverse lines. Sample locations are given by Universal Transverse Mercator grid coordinates in Appendix II.

A slightly enriched Nd isotopic signature of +1.0 (Barrie 1990) must be accounted for when considering the ultimate source of the Bristol Township lamprophyre suite. One possibility is that the suite was derived by magmatic or metasomatic processes, from a crustal material 200 million years older than the majority of rocks in the southern Abitibi Subprovince. This would require a very efficient scavenging of rare earth elements (REE) from the crust

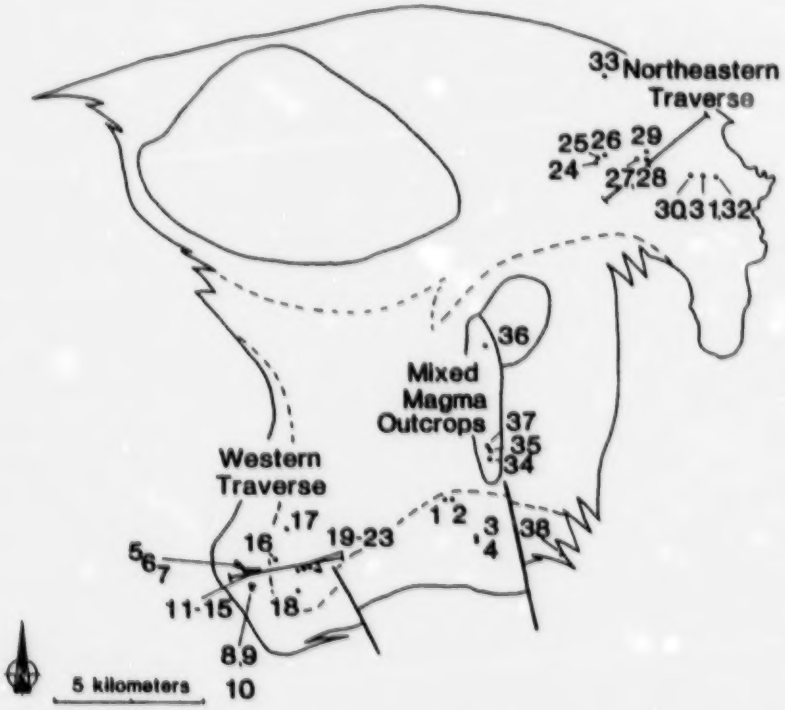

Figure 12. Locations of samples and traverses in the Kamiskotia Gabbroic Complex. Sample locations given by Universal Transverse Mercator grid coordinates in Appendix II.

Table 4. Geochemistry[1] of Kamiskotia Gabbroic Complex cumulates *(from* Barrie and Shirey 1989). Sample locations shown on Figure 12 and UTM coordinates given in Appendix II.

	WESTERN TRAVERSE															
Reference No.	1	2	3	4	5	6	7	8	9	10	11	12	13	14	15	16
Sample No.	86-260	84-12	84-18	84-19	86-309	86-310	86-311	84-271a	84-271b	84-271c	86-313	86-315	86-317	86-316	84-237	84-226
Major Oxides (wt %)																
SiO_2	44.3	40.7	40.3	38.1	48.1	43.0	41.6	49.9	49.7	49.8	43.6	42.9	41.8	43.0	41.0	48.0
TiO_2	0.07	0.05	0.07	0.04	0.14	0.13	0.06	0.18	0.18	0.19	0.08	0.09	0.11	0.09	0.09	0.28
Al_2O_3	7.36	9.89	21.70	15.00	20.30	23.00	21.40	14.90	15.80	14.20	23.60	20.80	17.00	20.30	21.00	16.80
Fe_2O_3	9.67	10.30	6.31	9.06	7.08	4.93	6.65	6.39	6.05	6.62	5.46	6.06	8.24	6.42	5.41	8.16
MnO	0.09	0.14	0.10	0.13	0.16	0.07	0.09	0.12	0.11	0.13	0.08	0.09	0.11	0.09	0.08	0.15
MgO	25.90	24.60	13.20	20.80	8.61	10.80	12.70	10.70	10.10	11.30	9.25	12.90	17.20	14.00	12.10	10.30
CaO	3.29	5.82	11.80	8.26	11.30	11.90	10.90	14.30	14.10	13.70	12.20	11.10	9.08	10.60	10.70	8.44
Na_2O	0.09	0.17	0.64	0.19	1.52	1.13	1.01	1.19	1.48	1.15	1.18	1.27	0.87	1.27	0.86	3.09
K_2O	0.03	0.01	0.06	0.05	0.33	0.20	0.21	0.09	0.25	0.08	0.03	0.10	0.15	0.11	0.16	0.25
P_2O_5	0.02	0.02	0.02	0.02	0.02	0.02	0.01	0.02	0.02	0.02	0.02	0.02	0.02	0.02	0.02	0.02
LOI	9.39	8.00	5.85	8.39	2.70	5.31	5.00	2.39	2.31	2.31	4.93	5.00	5.23	3.93	9.00	4.54
Total	100.2	99.7	100.1	100.0	100.3	100.5	99.6	100.2	100.1	99.5	100.4	100.3	99.8	99.8	100.4	100.0
Trace Elements (ppm)																
La	0.37	0.18	0.42	0.29	0.65	0.33	0.31	0.44	0.53	0.40	0.30	0.31	0.32	0.52	0.35	0.86
Ce	...	0.4	0.6	0.4	2.2	0.9	0.8	1.3	1.3	1.5	0.9	1.6	1.2	0.8	...	2.7
Nd	0.4	0.4	0.5	...	...	...	...	0.8	..	0.9	...	...	...	...	...	1.2
Sm	0.15	0.11	0.15	0.09	0.33	0.22	0.13	0.44	0.38	0.36	0.19	0.19	0.22	0.21	0.17	0.61
Eu	...	0.04	0.30	0.10	0.23	0.18	0.22	0.23	0.2	0.22	0.18	0.13	0.15	0.15	0.12	0.38
Tb	...	...	...	...	...	...	...	0.1	0.1	0.1	...	...	...	...	...	0.2
Yb	0.10	0.10	0.16	0.12	0.36	0.20	0.08	0.62	0.46	0.47	0.19	0.16	0.18	0.15	0.16	0.70
Lu	0.02	0.02	0.03	0.02	0.05	0.02	0.01	0.09	0.08	0.09	0.03	0.03	0.04	0.03	0.03	0.11
Zr	2	2	5	...	5	7	2	10	10	10	3	4	3	8	4	14
Y	2	1	...	2	4	3	2	6	5	6	2	2	4	2	2	5
Hf	...	0.1	0.1	0.1	...	0.2	...	0.3	0.2	...	...	...	...	0.2	0.1	...
Rb	...	...	...	...	6	5	9	...	...	...	...	...	3	5	...	...
Sr	7	6	31	128	136	119	128	94	98	86	125	114	55	104	86	106
Ba	...	...	...	...	74	...	...	...	...	...	30	...	37	39	19	20
Sc	5.6	7.1	4.7	5.0	17.4	7.8	4.5	46.0	40.3	39.6	6.3	8.1	8.3	5.2	6.3	48.3
V	18	15	18	11.5	...	45	17	172	151	174	41	36	40	26	39	180
Cr	105	205	114	115	707	105	31	383	353	381	71	108	125	64	224	279
Ni	1290	2300	400	680	370	540	820	110	310	100	430	610	380	530	600	220
Co	114	97	59	92	40	43	73	38	35	40	33	49	65	50	47	60
Zn	62	40	30	75	68	33	40	50	10	40	20	59	53	15	23	50
Mg'^2	86	85	82	84	73	83	81	79	78	79	79	83	83	83	84	74
Stratigraphic Height (m)[3]					300	340	400	400	401	402	540	660	680	710	725	1250

Table 4. (continued)

	WESTERN TRAVERSE							NORTHEASTERN TRAVERSE[4]									
Reference No.	17	18	19	20	21	22	23	24	25	26	27	28	29	30	31	32	33
Sample No.	84-227	84-219	86-295	86-296	86-297	86-298	86-300	84-402	84-406	TH-150	TH-172	TH-174	84-415	TH-85	TH-37	TH-133	TH-146
Major Oxides (wt %)																	
SiO_2	47.8	48.8	49.5	48.9	49.8	50.3	50.1	49.6	44.6	48.3	46.8	43.6	41.9	47.8	50.1	40.7	49.2
TiO_2	0.55	0.43	1.16	1.46	0.26	0.21	0.14	1.11	2.29	0.76	0.38	0.53	0.78	0.77	1.08	3.20	0.56
Al_2O_3	15.20	15.25	15.60	16.90	15.40	16.50	19.10	14.20	13.70	19.87	22.50	11.40	9.37	15.30	14.60	11.57	17.47
Fe_2O_3	10.90	9.97	11.10	9.21	9.94	9.29	8.08	12.80	17.30	9.55	7.64	17.53	19.50	10.53	12.56	24.49	11.15
MnO	0.19	0.18	0.16	0.12	0.18	0.18	0.16	0.21	0.21	0.15	0.10	0.21	0.28	0.09	0.17	0.22	0.12
MgO	8.74	8.96	7.37	6.04	8.49	8.00	6.14	7.79	6.60	5.33	6.02	14.00	15.20	8.33	6.32	6.25	5.29
CaO	10.10	11.80	8.90	11.50	11.20	9.24	10.70	12.10	11.10	10.64	11.00	8.02	7.84	8.46	10.20	7.58	11.26
Na_2O	2.44	1.54	2.29	2.51	1.64	2.53	2.51	1.90	1.65	2.17	3.17	0.79	0.12	2.47	1.78	0.81	2.44
K_2O	0.20	0.30	0.12	0.19	0.19	0.41	0.12	0.10	0.11	0.18	0.55	0.05	0.03	0.23	0.63	0.44	0.32
P_2O_5	0.02	0.01	0.04	0.02	0.01	0.02	0.02	0.13	0.02	0.06	0.05	0.05	0.05	0.02	0.17	0.10	0.10
LOI	3.00	2.89	3.08	2.93	3.16	3.62	3.31	0.39	0.77	3.20	2.87	4.63	5.16	6.77	2.75	5.80	2.02
Total	99.1	100.1	99.3	99.8	100.3	100.3	100.4	100.3	98.4	100.2	101.1	100.8	100.2	100.8	100.4	101.2	99.9
Trace Elements (ppm)																	
La	0.98	0.48	0.99	0.62	0.57	0.55	0.63	2.40	0.76	1.30	1.80	1.30	0.91	3.20	6.20	2.30	3.30
Ce	3.0	...	2.5	1.5	1.9	1.4	1.2	8.1	2.6	4.1	4.6	...	2.2	7.2	18.3	7.0	10.4
Nd	2.3	0.8	2.4	2.4	1.7	1.1	...	4.0	2.6	2.4	2.7	2.3	1.3	3.5	11.7	...	5.8
Sm	1.04	0.62	0.88	0.82	0.60	0.47	...	1.82	1.00	0.74	1.00	0.77	0.60	1.42	3.10	1.68	2.38
Eu	0.64	0.39	0.77	0.59	0.51	0.46	0.37	0.78	0.57	0.59	0.79	0.39	0.32	0.44	1.03	0.94	0.90
Tb	0.2	0.2	0.2	0.2	0.2	...	0.1	0.4	0.2	0.2	0.3	0.2	0.2	0.3	0.7	0.4	0.5
Yb	1.19	0.91	0.83	0.58	0.89	0.71	0.42	1.98	1.25	0.71	0.77	0.90	0.76	1.57	2.82	1.94	2.05
Lu	0.17	0.14	0.12	0.09	0.14	0.10	0.06	0.26	0.21	0.15	0.14	0.16	0.13	0.25	0.45	0.34	0.35
Zr	15	14	10	11	7	5	2	53	23	16	17	22	15	21	110	36	45
Y	9	8	8	6	8	5	3	20	10	7	7	8	6	12	26	18	19
Hf	0.5	0.2	0.6	0.3	0.3	...	...	1.4	0.6	0.5	0.4	0.6	0.3	0.4	2.2	1.0	1.1
Rb	...	...	...	...	...	10	...	...	...	2	14	1	...	9	14	22	5
Sr	137	114	188	288	135	162	184	104	99	142	205	64	34	155	110	75	116
Ba	30	40	32	41	58	92	42	300	200	26	148	37	...	76	189	127	82
Sc	40.4	40.4	24.9	31.8	39.1	34.7	18.8	48.8	52.1	24.2	17.3	21.7	23.7	28.5	39.2	44.7	35.3
V	236	273	203	255	193	117	91	318	860	...	...	...	219	...	...	...	...
Cr	165	445	314	210	291	224	101	307	197	130	...	...	221	...	...	...	...
Ni	220	290	230	72	150	150	200	170	240	90	...	...	630	105	70	120	55
Co	60	44	35	32	43	37	37	45	61	46	40	67	124	...	51	102	47
Zn	80	10	29	...	68	26	65	5	30	...	...	...	150	...	...	...	...
Mg'[2]	64	67	60	60	66	66	69	58	46	56	64	64	64	64	53	37	52
Stratigraphic Height (m)[3]	2150	2325	2550	2700	2875	3000	3100	100	275	300	1075	1150	1275	1975	2300	2375	2500

[1] Major elements by XRF at X-Ray Assay Laboratories, Toronto; trace elements by XRF and INAA at the University of Toronto: see Barrie (1990) for accuracy and precision of analyses.
[2] Mg' = molecular percent MgO x 100/ MgO+FeO, with $FeO/FeO+Fe_2O_3 = 0.85$.
[3] Height - estimated stratigraphic height from base of the Western or Northeastern traverses (Figure 12); see text for details.
[4] Samples with TH prefix from Hart (1984).

into a melt or fluid in order to account for the incompatible element enrichment of the lamprophyre suite. Two processes that may account for this are CO_2 fluid streaming through the lower crust during granulite facies metamorphism; and fluxing by fluid, rich in H_2O, derived from subducting oceanic slabs (Sorensen and Grossman 1989). It is noted that there are no known rock suites associated with subduction zones that are as enriched in the light rare earth elements (LREE) as the Bristol Township lamprophyre suite. A second possibility is that the lamprophyre suite was derived from a part of the mantle that had undergone significant LREE enrichment, approximately 200 million years prior to the separation and emplacement of the lamprophyre suite (Barrie 1990). At present, it is difficult to distinguish between isotopically enriched mantle, or lower crustal sources for the lamprophyre suite.

Samples 8, 9 and 10 were taken 3 to 5 m apart from the same outcrop of moderately altered gabbronorite in the LZ as a test for trace element mobility. Their primary modes of plagioclase, clinopyroxene and orthopyroxene, respectively, have the following estimate: sample 8, 45-40-20; sample 9, 50-25-25; and sample 10, 45-25-30. Their similar trace element geochemistry suggests that the REE, the high field strength elements (HFSE), V, Cr and Sr have not been disturbed by postsolidus alteration or metamorphism. Variation in Sc content is proportional to modal clinopyroxene content, as Sc partitions favorably into clinopyroxene (Irving 1978). Nickel is higher in sample 9; this may be due to trace amounts of sulphide not detected in hand specimen or thin section.

The modes for the traverse samples are presented in Figure 13. These samples are meso- and adcumulates, with anhydrous silicates comprising the bulk of the cumulus and postcumulus phases. One exception is sample 13 where hornblende comprises 11% of the mode as a primary, postcumulus phase. Magnetite, titanomagnetite and ilmenite are postcumulus phases in the Western Traverse, and they are both cumulus and postcumulus phases in the Northeastern Traverse. Biotite and apatite are present as postcumulus phases in sample 24; apatite may be a cumulus phase as well. Sulphides (pyrite, pyrrhotite, chalcopyrite) occur as trace phases interstitial to the silicates commonly in the olivine cumulates in the Western Traverse. They also occur sporadically in the Northeastern Traverse.

Whole rock Mg numbers and normative An, TiO_2 and P_2O_5 contents versus stratigraphic height are presented in Figure 14. Broadly, Mg numbers and normative An contents decrease from 82 to 86 and 91 to 96, respectively in the olivine-bearing cumulates to 37 to 53 and 60 to 76, respectively for the upper four UZ cumulates. This is consistent with normal fractionation and iron-enrichment trends observed in many large layered intrusions such as the Bushveld and Skaergaard complexes (Wager and Brown 1968). The contents of TiO_2 and P_2O_5 are low in LZ cumulates and increase sporadically in the MZ and UZ cumulates, reflecting the presence of oxide phases and apatite, respectively.

Nickel contents are highest in LZ cumulates, consistent with the presence of olivine and sulphide which strongly favor nickel (Figure 15). Scandium abundances are low in the olivine-bearing cumulates and the majority of LZ rocks (*see* Figure 15). Scandium partitions favorably into clinopyroxene and oxide phases but not into olivine, orthopyroxene or plagioclase under reasonable magmatic temperatures and oxygen fugacities (Lindstrom 1976).

In Figure 16, incompatible elements and incompatible element ratios are plotted versus stratigraphic height. The abundances of the REE and high field strength elements in cumulus rocks are in a general sense proportional to the amount of intercumulus liquid trapped during postcumulus crystallization. It is apparent from Figure 16 that the majority of LZ cumulates have very low La, Yb, Zr and Y contents and thus contain low amounts of intercumulus material. This observation is consistent with their adcumulus and mesocumulus textures. In comparison, the MZ and UZ cumulates are relatively enriched in these elements. In the MZ, more closely spaced samples from 2000 to 3000 m

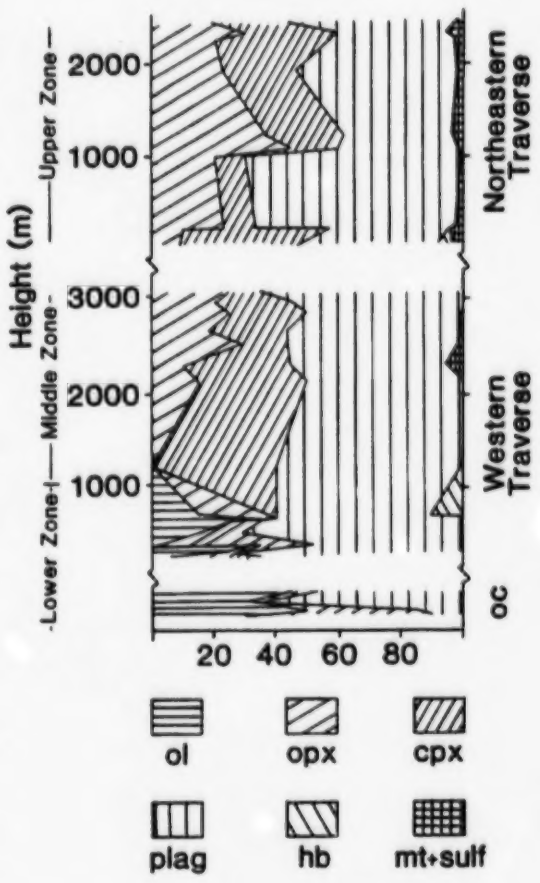

Figure 13. Petrographic traverse for cumulate rocks. The abbreviations used for minerals are as follows: ol-olivine; opx-orthopyroxene; cpx-clinopyroxene; plag-plagioclase; hb-hornblende; mt+sulf-magnetite and sulphide; oc-olivine-rich cumulates. Traverse locations shown in Figure 12.

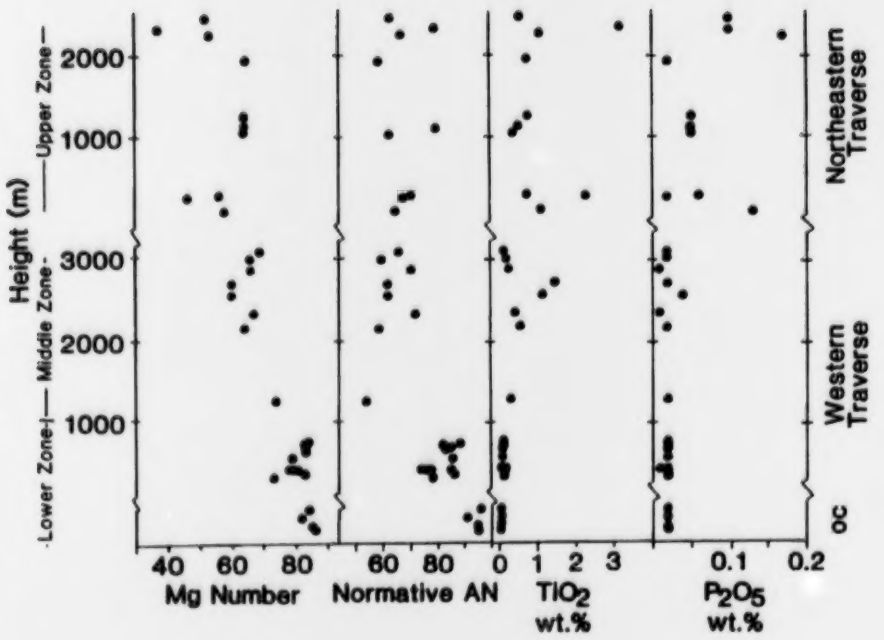

Figure 14. KGC cumulates; whole rock magnesium number, normative anorthite composition, TiO_2 and P_2O_5 versus stratigraphic height.

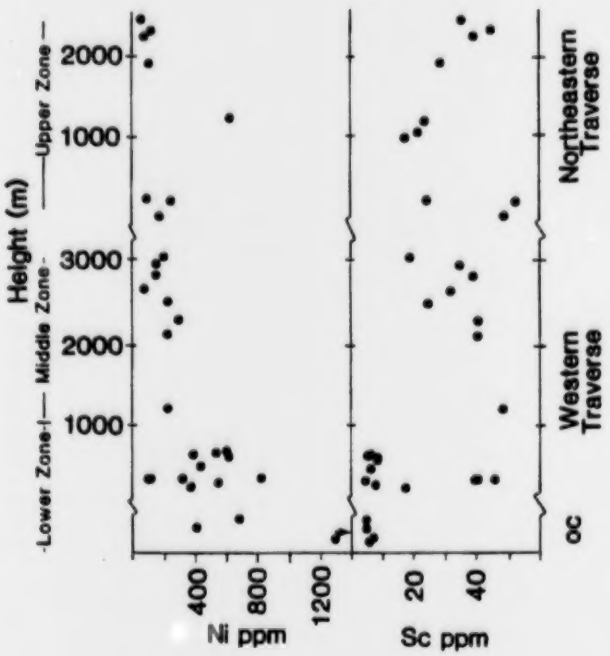

Figure 15. Ni and Sc versus stratigraphic height in the KGC.

show a consistent trend toward lower concentrations upsection. Three samples at the base of the UZ decrease in incompatible element abundances in a generally similar manner. This may reflect a decrease in the mode of intercumulus phases upsection which is not detectable petrographically. In both cases, Zr/Y follows the decrease in incompatible element contents; this may be due to Y^{3+} behaving more compatibly in clinopyroxene than Zr^{4+}. Lanthanum in the MZ samples remains relatively constant from 2000 to 3000 m, contrary to the behavior of the other trace elements. One explanation for the constant La content would be that cumulus pyroxenes are present in greater abundance where there is more trapped liquid. In the UZ, Yb, Zr and Y increase from 1000 to 2500 m, accompanied by a decrease in Mg number from 64 to 37-52 (*see* Figure 16), and corresponding decreasing Mg numbers in clinopyroxene and An contents of plagioclase (*see* Figure 5, samples G-I). These trace element trends in the UZ are consistent with normal fractionation accompanied by assimilation of trace element-enriched siliceous material (discussed in detail below).

The cumulates of all three zones have flat REE patterns, with La_N/Yb_N = 0.4 to 2.6, and increasing total REE abundances upsection (Figure 17a, b). There is a strong negative correlation between La_N/Yb_N and Sc and clinopyroxene content, consistent with lower K_Ds for the LREE between clinopyroxene and basaltic liquids (Irving 1978). Europium anomalies are positive in the LZ with Eu/Eu* of 1.2 to 5, and show a progressive depletion upsection to Eu/Eu* of 0.8 to 0.85 for the upper four UZ cumulates. In general the REE are consistent with enrichment due to fractionation of plagioclase and mafic phases from a tholeiitic parent, accompanied by the addition of REE-enriched material (discussed below). Except for the upper four UZ samples, the KGC cumulates have REE contents similar to anorthositic gabbronorites from the Shawmere anorthosite of the Kapuskasing Structural Zone (Simmons et al. 1980) and massive gabbros from the Bad Vermilion anorthosite, northwestern Ontario (Ashwal et al. 1985). Their REE contents are distinct from ophiolitic gabbro cumulates which are characterized by LREE-depletion (e.g., Pallister and Knight 1981 and references therein).

KGC CHILLED ROCKS

Geochemistry for KGC chilled samples and average compositions of KVC basalts and evolved basalts are given in Table 5, and the sample locations are given in Appendix II.

There are several locations where chilled KGC gabbroic rocks are exposed. Samples 34 to 37 are from the mixed magma outcrops; sample 38 is from a contact with felsic metavolcanic rocks that interdigitate with the KGC margin, where the felsic rocks show no textural evidence of melting due to the juxtaposition of the hot gabbroic liquid (*see* Figure 4). Care was taken to ensure that no felsic material was included during sample collection. These samples are composed of aphanitic basalt 1 to 2 cm in from the margin, to medium-grained gabbro, 50 cm in from the contact. They have similar geochemical characteristics, with Mg numbers from 54 to 58, TiO_2 from 0.88 to 1.01 weight %, and generally similar REE and trace element compositions (*see* Table 5).

Sample 34 has 8 to 12 times higher K_2O, Ba and Rb contents, but less than half the Sr content of an average of the other four samples. This may be attributed to preferential diffusion of the alkalis and Ba from the adjacent felsic liquid into sample 34 during (and after?) solidification. Experiments in basaltic liquids at 1200 to 1400°C indicate

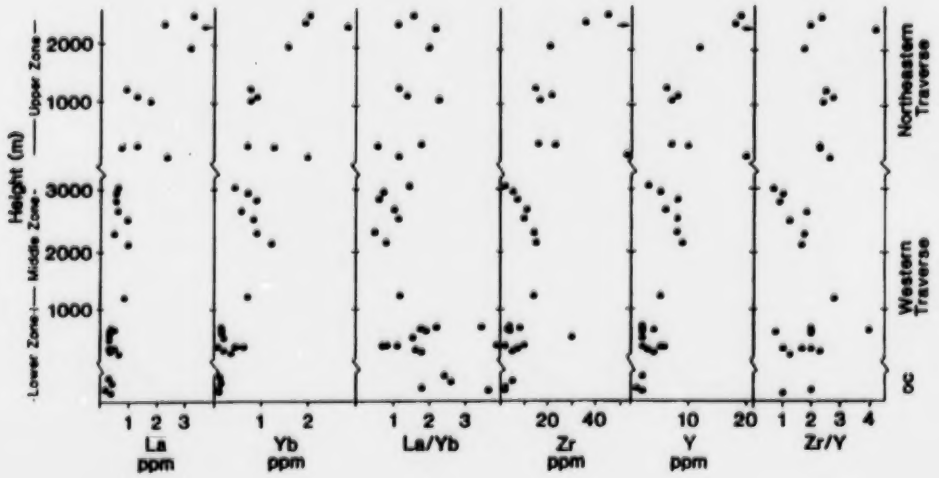

Figure 16. Incompatible trace elements and trace element ratios: La, Yb, La/Yb, Zr, Y and Zr/Y versus stratigraphic height in the KGC.

that initially, potassium diffuses much more rapidly than other melt species until the basalt has contents of around 1.5 weight % K_2O, after which the basalt is buffered from further potassium diffusion (Watson 1982). With their similar cation charge to radius ratios, Rb and Ba would behave in a similar manner. In granitic melts, the rates of diffusion of the alkalis are known to be two or more orders of magnitude greater than for more highly charged cations (e.g., Ce, Eu) under a wide range of temperatures (Jambon 1982).

Watson's experiments (1976) on element partitioning between coexisting mafic and felsic melts indicate that the REE and HFSE should partition into the less polymerized mafic melt by factors of 3 to 13. Wholesale REE and HFSE enrichment does not seem likely for the KGC mixed magma chilled samples for two reasons. Firstly, whereas their major element compositions are similar to N-MORB, they have slightly lower abundances of the REE and HFSE in comparison to N-MORB. Secondly, their concentrations are nearly identical to sample 38, taken from outcrops away from the mixed magma outcrops. It seems probable that mixed magma chill samples quenched rapidly enough to prevent the diffusion of the REE and HFSE from the felsic liquid under liquid-liquid equilibrium conditions.

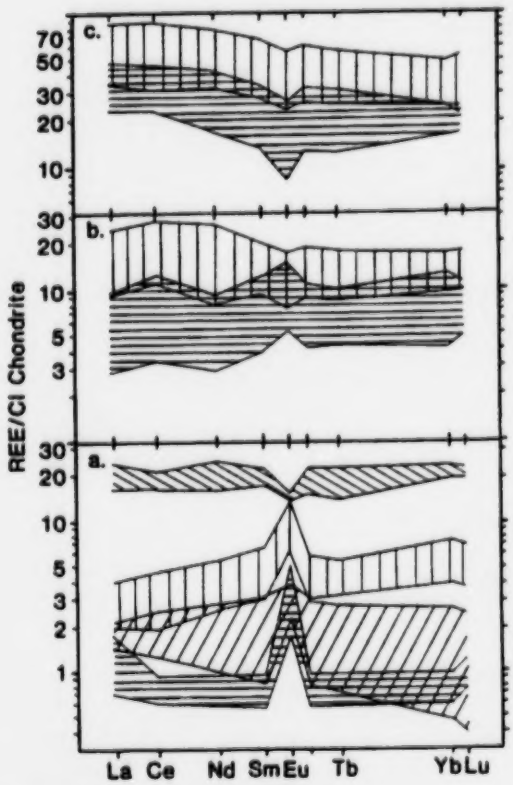

Figure 17. Rare earth element profiles, normalized to Cl chondrite values of Evensen et al. (1978). Gd values determined from interpolation between Sm and Tb.
a. Olivine-rich cumulates (samples 1 to 4): horizontal-ruled; LZ cumulates (samples 5 to 15): northeast-southwest diagonal-ruled; MZ cumulates (samples 16 to 23): vertical-ruled; chilled samples 33 to 38 -diagonal-ruled.
b. Lower UZ cumulates (samples 24 to 29): horizontal ruled; upper LZ cumulates (samples 30 to 34): vertical-ruled.
c. Range for Kamiskotia basalts: horizontal ruled; range for Kamiskotia evolved basalts: vertical-ruled.

The REE for the KGC chill samples are plotted along with the range of the REE for the LZ in Figure 17a. They have a restricted range, with flat REE profiles (La_N/Sm_N = 0.9 to 1.3; La_N/Yb_N = 0.8 to 1.2) at 15 to 20 times chondritic values, and consistent negative Eu anomalies. In comparison to southern Abitibi Subprovince basalts, these REE abundances are most similar to parts of the lower Skead Group south of Kirkland Lake, Ontario (Figure 1i *in* Capdevila et al. 1983). Many of the Skead Group basalts are interpreted as the products of partial melting of a slightly depleted mantle where the degree of melting is sufficiently high to leave only olivine and orthopyroxene in the residue, followed by minor fractional crystallization of olivine and plagioclase (Capdevila et al. 1983). The KGC chill samples are distinguished from LREE-depleted, N- MORB (e.g., Schilling et al. 1976; Frey et al. 1974) and many ophiolite-related basalts (e.g., Pallister and Knight 1981 and references therein) by their flat REE patterns and consistent Eu anomalies. They have flatter REE patterns than the LREE-enriched parental ultramafic or basaltic liquids of the Bushveld Complex (average Ce_N/Yb_N = 12 and 3, respectively: Sharpe and Hulbert 1985) and the majority of gabbronorite sills of the Stillwater Complex (average La_N/Yb_N = 3.5: samples 3 to 10 in Helz 1985).

GRANOPHYRIC ROCKS

A brief characterization of the KGC felsic granophyric rocks is given here, based on 14 samples from Godfrey Township collected and analyzed by Hart (1984). Felsic granophyres are characterized by high silica contents, (64.5 to 77.4 weight % SiO_2), low magnesium contents (0.3 to 1.5 weight % MgO), and relatively low alkali and alkaline earth contents (2.5 to 5.6 weight % Na_2O, 0.3 to 2.6 weight % K_2O, 4 to 39 ppm Rb, 19 to 84 ppm Sr). They have high REE contents (33 to 74 ppm La, n=13) and flat REE patterns (La_N/Yb_N = 1.6 to 2.6) with negative Eu anomalies, and very high Zr contents (525 to 825 ppm, n=13).

The majority of granophyric rocks of intermediate composition are interpreted as altered felsic granophyres. Ten samples from Godfrey Township analyzed by Hart (1984) have incompatible element concentrations very similar to the felsic granophyric rocks, and differ from them only in their lower silica contents (60 to 68 weight % SiO_2) and higher magnesium contents (1.2 to 4.5 weight %, n=9). This may be attributed to chlorite alteration, probably related to subseafloor hydrothermal alteration (*see* "Economic Geology").

Table 5. Geochemistry* of chilled gabbros and Kamiskotia basalts.

Reference No.	34	35	36	36	37	Prim. Basalt	Evolved Basalt
Sample No.	87-14	87-15	87-18	84-186	86-285	Average	Average
Major Oxides (wt %)							
SiO_2	47.4	46.9	47.3	46.7	49.7	50.1	49.2
TiO_2	0.92	0.90	0.93	0.88	1.01	1.36	2.47
Al_2O_3	16.00	16.00	15.70	15.60	14.4	13.4	12.2
Fe_2O_3	13.40	13.30	14.10	13.10	13.3	14.0	15.5
MnO	0.21	0.20	0.20	0.19	0.21	0.25	0.24
MgO	8.11	8.09	7.49	7.98	6.89	6.32	4.73
CaO	7.01	9.81	9.64	9.93	8.87	7.10	6.79
Na_2O	1.15	1.78	1.78	1.28	1.55	2.56	2.49
K_2O	2.36	0.34	0.18	0.33	0.19	0.31	0.74
P_2O_5	0.09	0.09	0.09	0.09	0.09	0.14	0.54
LOI	3.23	2.54	2.70	3.16	3.77	3.96	5.10
	99.9	100.0	100.1	99.2	100.0	99.3	99.3
Trace Elements (ppm)							
La	5.02	4.83	3.76	3.80	5.51	7.30	14.5
Ce	12.4	12.8	10.6	10.0	11.7	18.4	37.2
Nd	6.6	7.7	6.9	7.4	10.3	11.2	25.1
Sm	2.51	2.63	2.51	2.47	3.19	3.67	7.13
Eu	0.83	0.75	0.82	0.74	0.83	1.09	2.30
Tb	0.6	0.5	0.5	0.5	0.8	0.8	1.5
Yb	2.99	3.08	3.10	3.03	3.61	3.35	5.87
Lu	0.48	0.49	0.47	0.46	0.49	0.54	0.90
Zr	61	62	61	55	69	102	302
Y	23	22	23	22	31	30	60
Hf	1.6	1.9	1.7	1.8	1.8	2.6	3.4
U	0.1	0.2	0.1	0.1	0.2	...	0.4
Th	0.5	0.1	0.1	0.4	0.4	0.6	1.6
Ta	...	0.2	0.2	0.2	0.3	0.2	1.1
Rb	88	11	11	10	...	6	18
Sr	65	136	133	112	188	70	130
Ba	770	110	39	70	34	121	285
Sc	42.5	44.9	44.4	44.0	46.4	40.0	38.0
V	236	237	243	239	344	...	315
Cr	194	200	229	301	230	...	139
Ni	170	170	140	170	80	42	49
Co	54	60	58	60	40	...	43
Zn	68	145	145	55	43	...	140
Mg'[1]	57	58	56	58	54	49	42

* Kamiskotia primitive basalt average of samples TH-2, TH-8, TH-25, and TH-208 from Hart (1984); evolved basalt average of samples TH-225, TH-233, TH-244 from Hart (1984), and 88-17, 88-18, 88-19 from Barrie (1990). Locations for gabbro chill samples in Appendix II; see Hart (1984) and Barrie (1990) for other sample locations.

[1]Mg'=molecular percent MgO x 100 / MgO + FeO, with FeO/FeO + Fe_2O_3 = 0.85

Kamiskotia Volcanic Complex

BASALTS, EVOLVED BASALTS AND ANDESITES

Kamiskotia basalts are predominantly massive or pillowed flows that contain less than 15% plagioclase and pyroxene phenocrysts. Hart (1984) has divided them into "primitive" and "evolved" basalts on the basis of geochemistry. The averages listed in Table 5 are from samples taken away from chlorite alteration zones related to copper-zinc mineralization (locations given in Hart 1984; and Barrie 1990). Kamiskotia primitive basalts are mildly enriched in TiO_2, P_2O_5, REE and HFSE in comparison to the KGC chill samples, and in comparison to N-MORB. "Evolved" basalts consist of basalts, basaltic andesites and andesites, that are significantly enriched in TiO_2, P_2O_5, REE and HFSE; they are transitional with highly enriched andesites similar in composition to basaltic andesites and icelandites of eastern Iceland (e.g., Wood 1978). The "evolved" basalts have flat REE patterns (average La_N/Yb_N = 1.47 and 1.60, respectively) with moderately negative to no Eu anomalies (Figure 17c).

One of the andesitic fragments with apparent quenched margins from within KVC welded rhyolite tuffs (*see* Plate 5b) has been analyzed for major elements by XRF (same sample as plotted in Figure 12 of Comba et al. 1986; P. Binney, Falconbridge Limited, personal communication, 1988). The oxides for this sample are, in weight %, SiO_2 = 54.5, TiO_2 = 2.15, Al_2O_3 = 12.8, Fe_2O_3 = 11.0, MgO = 1.9, MnO = 0.34, CaO = 5.19, Na_2O = 2.25, K_2O = 2.9, P_2O_5 = 0.36, LOI = 6.23, and Total = 99.7. The Mg number for this sample is 34, and Zr = 290 ppm, determined by a semiquantitative, fast-count XRF method. This sample has similar TiO_2 and P_2O_5 contents, but higher potassium and loss on ignition (LOI) contents than the incompatible element-enriched andesites described above.

RHYOLITES

The Kamiskotia Volcanic Complex rhyolites occur as quartz and feldspar-phyric pyroclastic flows, tuffs and agglomerates, with phenocryst content up to 15%. Hart (1984) analyzed 15 rhyolite samples taken away from hydrothermal alteration associated with the copper-zinc deposits, in south Jamieson and north Godfrey townships (also reported in Lesher et al. 1986). These samples are characterized by high silica contents, with SiO_2 = 71.9 to 78.6 weight % (average of 74.8 weight % SiO_2, n = 14), and very high immobile, incompatible element contents, with La = 39 to 67 ppm, Yb = 7 to 18 ppm, Zr = 215 to 410 ppm, and Th = 6 to 11 ppm (n=15). The rhyolites exhibit a range in K_2O and Rb contents, with K_2O = 2 to 9 weight % and Rb = 30 to 130 ppm (n=15). Rhyolite samples with higher K_2O and Rb contents are located from 1 to 2 km upsection to the northeast from the Canadian Jamieson and Genex Mine properties, and are also within 1 km of the main Kamiskotia Highway fault. Rhyolite flows and welded tuffs in central and southern Godfrey Township have similar chemical characteristics with those to the north. The rhyolites in north Carscallen and southeast Turnbull townships do not have as high abundances of these elements. However, they have identical incompatible element ratios as those in Godfrey and Jamieson townships and are included as part of the KVC (unpublished data).

Hart (1984) and Lesher et al. (1986) have noted that the incompatible element-enriched chemistry of the KVC rhyolites is similar to the chemistry of Kidd Creek agglomeratic rhyolites from the east outcrops of the Kidd Creek mine site. One of the notable characteristics for both Kamiskotia and Kidd Creek rhyolites is their relatively flat, chondrite-normalized REE patterns with large negative Eu anomalies (Figure 18a). These REE patterns are distinctive from many other felsic metavolcanic sequences in the southern Superior Province, which generally have steeper chondrite-normalized REE patterns with lower heavy REE contents (e.g., Types "FI" and "FII": Figure 18b). Kamiskotia and Kidd Creek rhyolites are also distinguished by their high Y contents (Figure 18c,d). In these respects they are similar to high silica rhyolites in Tertiary and Recent bimodal volcanic fields. Examples occur in the Basin and Range Province, U.S.A. (e.g., Coso volcanic field, California: Bacon et al. 1981; Kaiser Spring volcanic field, Arizona: Moyer and Esperanca 1989); and in eastern Iceland (e.g., eastern Iceland rift zone: Wood 1978; 1875 eruption of Askja volcano: Macdonald et al. 1987).

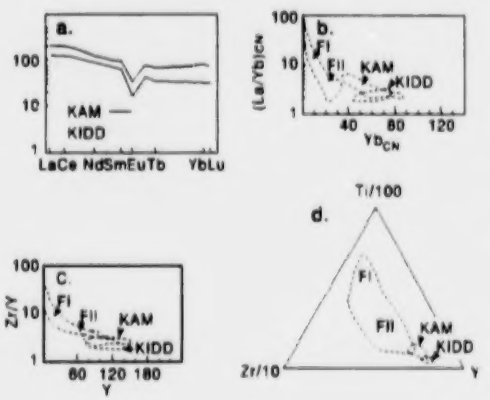

Figure 18. REE and trace element plots for Kamiskotia and Kidd Creek rhyolites, and felsic metavolcanic rocks that are not known to be the host to copper-zinc deposits (FI and FII from the southern Superior Province): a) rare earth element profiles for Kamiskotia and Kidd Creek; b) $(La/Yb)_{CN}$ versus Yb_{CN}; c) Zr/Y versus Y; and d) Ti/100-Zr/10 - Y ternary (*after* Lesher et al. 1986).

Lower Volcanic Suite

Twelve samples from the Lower volcanic suite range in composition from basalts to andesites; no felsic compositions were present (Table 6). The samples contain from 43.8 to 59.6% SiO_2, and have Mg numbers from 30 to 64. They have relatively low REE contents, with La from 1.9 to 10.5 ppm, Yb from 0.6 to 3.6 ppm; and variable REE patterns, with La_N/Yb_N from 0.6 to 4.3. The variable REE patterns along with a range in incompatible element ratios is interpreted to reflect heterogeneous sources for the suite. It is possible that several basalt samples which have chemical characteristics similar to KVC basalts or KGC chilled samples, are part of the KVC (e.g., samples 84-72, 84-265, 86-12).

Granitoid Rocks

Major element analyses are reported for eleven granitoid samples taken from granitoids A, B, C and D, and trace element analyses are given for six of these (Table 7). On normative Q-A-P and Or-Ab-An diagrams, these rocks plot in the diorite, monzodiorite, tonalite and granodiorite fields. Chondrite-normalized REE profiles for two samples from each of granitoids A, B and C show distinguishable patterns (Figure 19). Samples of granitoid A, from the mixed magma outcrops, have higher REE abundances and flat REE patterns, with La_N/Yb_N = 2.9 and 6.3, and negative Eu anomalies. These REE patterns are similar in character to KVC rhyolites, and KGC granophyre rocks, although

they have lower concentrations. These samples may represent KGC felsic liquids from that mixed with KGC mafic liquids in the MZ, although it is noted that several other tonalitic samples of granitoid A have much steeper REE patterns that cannot be related to the KGC–KVC suite (Barrie 1990). Samples of granitoid B have steeper patterns, La_N/Yb_N = 6.3 and 7.9, with no Eu anomalies. The major and trace element chemistry of the granitoid B samples is typical of Archean tonalites that are interpreted to be derived from partial melting of tholeiitic material with hornblende and garnet in the residuum (e.g., Arth and Hanson 1975; Martin 1987).

Table 6. Geochemistry of Lower volcanic suite mafic and intermediate volcanic rocks* (*from* Barrie 1990).

Sample No.	84-48	84-72	84-86	84-136	84-217	84-265	86-6	86-7	86-12	86-93	86-306	86-307
Major Oxides (wt %)												
SiO_2	48.30	49.00	55.10	59.60	54.20	43.80	48.50	49.60	50.40	46.60	52.40	53.40
TiO_2	1.16	0.81	0.93	0.56	0.65	0.70	1.28	1.23	0.97	1.96	0.55	0.25
Al_2O_3	13.50	14.70	16.40	12.80	15.80	14.40	13.30	14.50	13.60	12.50	15.00	15.80
Fe_2O_3	15.30	12.70	6.87	12.80	11.80	11.80	16.10	16.00	14.00	20.10	10.20	9.26
MnO	0.23	0.19	0.10	0.60	0.50	0.18	0.26	0.25	0.20	0.28	0.19	0.15
MgO	6.96	6.87	3.42	2.43	5.00	8.06	5.57	5.14	7.13	5.63	6.48	7.44
CaO	9.66	12.70	6.44	6.23	6.94	8.75	8.78	8.18	9.96	10.30	8.60	9.73
Na_2O	2.29	1.33	3.65	3.26	3.60	0.88	3.07	3.44	1.65	1.15	3.54	2.36
K_2O	1.17	0.32	1.22	0.54	0.26	0.61	0.49	0.15	0.39	0.35	0.87	0.25
P_2O_5	0.08	0.06	0.16	0.09	0.12	0.05	0.10	0.10	0.07	0.18	0.05	0.02
LOI	1.39	1.16	5.35	0.39	1.31	10.70	1.77	1.23	1.31	1.08	1.62	1.47
Total	100.0	99.8	99.6	99.3	100.2	99.9	99.2	99.8	99.7	100.1	99.5	100.1
Trace Elements (ppm)												
La	2.49	2.48	8.83	8.98	4.88	1.90	4.07	4.24	2.52	1.24	10.50	6.87
Ce	6.1	6.4	18.5	21.2	7.0	6.0	14.2	7.8	7.8	2.5	27.4	17.4
Nd	5.90	4.60	10.80	9.20	4.30	3.60	9.50	9.10	5.00	1.70	17.90	11.60
Sm	2.48	1.97	3.00	2.18	1.40	1.45	3.06	3.17	1.80	0.58	4.80	3.54
Eu	0.69	0.75	0.72	0.72	0.66	0.62	1.16	0.70	0.73	0.39	1.17	0.72
Tb	0.4	0.4	0.4	0.4	0.2	0.3	0.8	0.5	0.4	0.1	0.6	0.7
Yb	2.69	2.20	1.75	1.42	1.13	1.40	3.24	3.44	1.93	0.62	3.93	3.63
Lu	0.41	0.32	0.27	0.22	0.19	0.23	0.51	0.53	0.29	0.09	0.60	0.52
Zr	65	46	111	92	23	40	80	60	60	124	160	54
Hf	1.3	1.4	2.0	2.2	0.4	1.4	2.7	1.6	1.5	0.2	4.2	1.7
Y	24	17	18	14	10	13	28	19	19	41	36	32
Nb	3	2	4	3	1		4	2	2	6	11	3
Ta	0.2	0.1	0.3	0.4	0.1	0.1	0.3	0.2	0.1	0.0	0.7	0.1
Th	6.6	0.2	0.8	1.4	0.2	0.1	0.5	0.3	0.2		0.8	0.2
Sc	37.0	48.6	17.9	17.2	23.6	34.7	47.8	52.5	44.6	24.2	26.8	28.0
V		259	209	116	175	24					159	177
Sr	132	171	150	92	222	88	118	405	89	93	134	118
Ba	270	90	180	250	200	90	90	80	62		300	203
Rb		8	33	1	3	18	13	47	9		18	
Cr	168	326	135	273	265	292	105	69	148	686	120	143
Ni	112	148	98	49	107	195	80	37	220	170	137	162
Cu	48	78	58	14	38	5						
Co	40.2	53.8	16.4	16.2	19.4	51.5	54.0	36.8	46.4	42.7	38.3	39.1
Zn	40	110	20	70	32	130	150	35	60	110	125	
Au (ppb)	6				3	5	4	6	8	6		4
Mg'[1]	57	55	53	30	50	61	44	42	53	39	59	64

* See Appendix II for sample locations.
[1]Mg'=molecular percent MgO x 100 / MgO + FeO, with FeO/FeO + Fe_2O_3 = 0.85

Table 7. Geochemistry of regional granitoid rocks* (*from* Barrie 1990).

	Granitoid A		Granitoid B			Granitoid C		Granitoid D		
Sample No.	84-31	86-267	86-101	84-246	84-174	84-43	86-220	84-266	84-01	84-130
Major Oxides (wt %)										
SiO_2	68.1	69.5	73.9	76.8	75.3	71.4	71.9	66.1	67.4	66.8
TiO_2	0.36	0.36	0.35	0.32	0.11	0.17	0.15	0.45	0.36	0.59
Al_2O_3	15.5	15.1	12.5	11.6	13.5	15.6	15.7	15.7	16.1	14.6
Fe_2O_3	3.74	3.26	3.26	3.01	1.45	1.75	0.84	3.76	3.22	4.55
MnO	0.06	0.06	0.06	0.04	0.03	0.03	0.02	0.06	0.04	0.07
MgO	1.41	1.02	0.78	0.63	0.27	0.70	0.41	1.70	1.84	1.45
CaO	3.10	3.61	2.64	0.74	1.28	2.82	2.00	4.00	1.97	3.08
Na_2O	4.48	4.56	4.00	3.62	4.52	5.25	6.48	4.86	5.78	4.51
K_2O	1.95	1.59	1.24	0.82	2.34	1.75	1.91	1.31	1.10	1.61
P_2O_5	0.10	0.08	0.07	0.06	0.04	0.06	0.06	0.13	0.15	0.15
LOI	1.62	1.08	1.00	1.54	1.08	0.39	0.54	1.62	2.23	1.31
Total	100.4	100.2	99.8	99.2	99.9	99.9	100.0	99.7	100.2	98.7
Trace Elements (ppm)										
La	24.80	8.97	13.70	11.50		5.88	3.31			
Ce	49.0	19.1	32.7	25.3		10.2	11.8			
Nd	18.4	8.4	10.3	12.2		3.6	4.6			
Sm	4.49	2.40	2.05	2.05		0.75	1.14			
Eu	1.08	0.55	0.72	0.66		0.28	0.43			
Tb	1.2	0.8	0.3	0.3		—	0.1			
Yb	2.65	2.09	1.17	1.23		0.25	0.15			
Lu	0.46	0.31	0.25	0.19		0.05	0.05			
Zr	154	125	183	157		98	91			
Hf	5.0	3.0	5.0	3.6		1.9	2.9			
Y	17	22	13	11		3	4			
Nb	8	7	12	4		—	—			
Ta	1.4	0.9	0.8	0.7		0.3	0.2			
U	1.1	0.6	0.6	0.3		1.1	0.5			
Th	8.8	3.8	6.0	1.4		1.2	1.1			
Sr	213	222	160	173		405	811			
Ba	1090	365	540	260		620	640			
Rb	87	55	56	39		47	40			
Cr	22	6	15	70		25	—			
Ni	28	—	—	21		—	—			
Co	14	7	6	71		2	3			
Zn	32	62	43	26		80	—			
Sc	9.0	6.2	6.3	5.1		1.7	1.4			
V	46	—	30	—		9	—			

*Sample locations given in Appendix II.

Samples of granitoid C, obtained from the contact strain zone, have relatively low incompatible element contents; and steep REE patterns, with La_N/Yb_N = 14.9 and 15.9, and slight positive Eu anomalies (*see* Figure 19). These samples have a high modal content of plagioclase and alkali feldspar, reflected in their high Na_2O, K_2O, Sr and Ba and Eu contents (*see* Table 6). The high alkali and alkaline earth but low incompatible element contents can be explained by either of two processes. Firstly, if the feldspars represent meso- to adcumulus phases, then cumulus and/or postcumulus processes, normally considered for mafic cumulates, may have been active in granitoid C and led to the removal of any incompatible element-enriched intercumulus liquid. A second process to explain the low incompatible element contents is *in situ* deformation. If these rocks were deformed *in situ* prior to total consolidation during diapiric emplacement, then a filter-pressing effect may have squeezed out any incompatible element-rich liquid.

Bristol Township Lamprophyre Suite

Geochemical analyses for 14 samples (and one duplicate) of the Bristol Township lamprophyre suite, and three samples of adjacent, altered basalts are given in Table 8. Sample locations are given in Figures 32 and 33, and in Appendix II. Two biotite-rich lamprophyres, three garnetite samples and one altered garnetite sample have been analyzed by ICP-MS for the REE, after total dissolution was achieved with a lithium metaborate flux.

The lamprophyre suite is characterized by very low silica contents (averaging 38.4 weight % SiO_2, n=14); high titanium and phosphorous contents (1.9 weight % TiO_2 and 2.4 weight % P_2O_5, n=14) and very elevated, HFSE and LREE contents (e.g., 970 ppm Zr n=13; 157 ppm Y, n=14; 40 ppm Th, n=13; 680 ppm Ce, n=6; 660 ppm Nd, n=6). The biotite-rich lamprophyres have up to 6 weight %

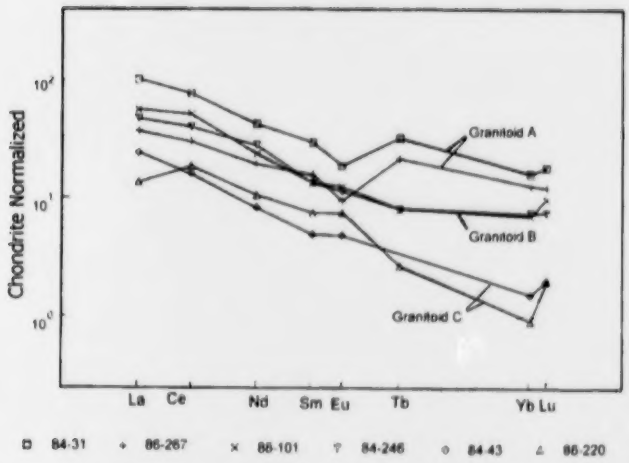

Figure 19. Rare earth element profiles for selected granitoid rocks from the Kamiskotia area.

P_2O_5, and up to 4.5 weight % K_2O, reflecting their high apatite and biotite contents. The garnetite samples are highly enriched in TiO_2, Zr and the LREE. The altered garnetite samples are very highly enriched in these elements, and also contain appreciable S and Cu (*see* Table 8).

Selected major and trace elements are plotted versus zirconium in Figure 20. With its high charge (+4) and small ionic radius (0.79 by 10^{-10} m), zirconium is a highly incompatible element in the crystal structures of the common rock-forming silicates. Because of this, zirconium is an excellent indicator of silicate mineral fractionation in most magmatic systems. Additionally, it can be used to track HFSE and LREE enrichment in certain volatile-rich systems. Volatile activity is believed to have contributed to the HFSE and LREE enrichment in this lamprophyre suite, considering the high carbonate (and halogen: unpublished data) contents in many of these rocks.

The MgO, Ni, K_2O and P_2O_5 contents all decrease with increasing Zr contents in the lamprophyre suite (Figure 20a). Enrichment in Zr is accompanied by increasing TiO_2, Y, Th and S contents (Figure 20b). This is interpreted to reflect the fractionation of a magnesium-rich silicate, possibly diopside, in addition to biotite and apatite fractionation. Diopside has a mineral to liquid partition coefficient of between 1 and 3, much lower than that of olivine at 10 to 20 for sulphide (200 or greater) in basaltic magmas (Irving 1978). Olivine or sulphide fractionation would cause the nickel contents to drop precipitously. Titanium and yttrium are present along with zirconium in the melanite garnets, and they form linear trends with zirconium due to the addition of garnet in this suite. It is interesting to note that sulphur and copper increase with zirconium, which suggests that the sulphide phases became saturated and precipitated along with garnet, during the late stages in this system.

Chondrite-normalized REE profiles for six samples from the lamprophyre suite are steep, with no Eu anomalies (Figure 21). They have La_N = 400 to 1500, Nd_N = 350 to 2900, and Yb_N = 5.5 to 19. The flattest pattern is also the most enriched sample, an altered garnetite, with La_N/Yb_N = 8; and the steepest pattern is for a biotite lamprophyre with La_N/Yb_N = 90 (*see* Figure 21). The patterns are elevated in comparison to tholeiitic and calc-alkalic rocks, and are higher than most alkalic suites, including lamprophyres (Rock 1987). They are similar to the patterns found in some fluorapatite-rich rocks found along the DPFZ in Taylor Township (King and Kerrich 1987); and to some of the less enriched carbonatites in the Oka Complex, Quebec (Eby 1975). They are also similar to estimates of average kimberlite, lamproite and metasomatic fluids believed to be in equilibrium with richteritic amphiboles from veined mantle nodules (e.g., Figure 4b *in* Menzies et al. 1987).

Geochemical Modeling of KGC Supracrustal Magmatic Processes

In this section, the relationships between the LZ, the upper UZ and their parental liquid compositions, represented by the KGC chill rocks, and the Kamiskotia evolved basalts, respectively, are established. This is followed by assimilation-fractional crystallization (AFC) modeling of the parental liquids using their trace element contents.

CMAS-TYPE PHASE DIAGRAMS

The phase relations and major element compositions of the KGC chill samples and the evolved basalts suggest that they are parental to LZ and upper UZ cumulates, respectively. The chill samples and evolved basalts are similar to abyssal basalts in their major element geochemistry, and as such can be represented in the CMAS-type (CaO-MgO-Al_2O_3-SO_2) diopside + olivine + plagioclase + silica tetrahedron of Walker et al. (1979). The chill samples plot in the olivine- (samples 34 to 37) or orthopyroxene- (sample 38) saturated fields at one bar (and fO_2 at QFM buffer) when projected from plagioclase, and in the plagioclase-saturated field when projected from silica (Figure 22). At

Table 8. Geochemistry of Bristol Township lamprophyre suite and nearby rocks.

Sample No.	87-4	87-6	88-2	88-3	88-4	88-4D	88-5	88-6
Major Oxides (wt %)								
SiO_2	36.10	32.60	38.0	35.0	40.0	40.2	39.8	34.2
TiO_2	2.27	1.35	1.17	2.38	2.45	2.57	4.85	1.25
Al_2O_3	7.68	4.44	3.88	9.74	8.34	8.40	10.8	6.54
Fe_2O_3	20.30	15.70	14.1	18.1	18.9	18.7	10.1	13.6
MgO	0.46	0.13	11.0	1.66	1.38	1.49	1.79	12.0
MnO	1.78	10.60	0.15	0.43	0.42	0.42	0.16	0.13
CaO	25.70	16.90	20.1	23.7	22.8	22.9	11.7	13.9
Na_2O	1.44	0.12	0.19	0.99	1.37	1.32	5.03	0.06
K_2O	1.16	2.98	0.64	1.02	1.66	1.70	0.35	4.52
P_2O_5	2.32	2.30	5.81	0.29	0.24	0.26	1.90	2.02
S	0.59	0.04	0.04	0.61	0.42	0.43	0.79	0.07
LOI	1.6	2.3	4.8	3.6	0.7	0.7	7.4	9.7
CO_2	5.6	4.07	4.73	2.91	0.33	0.32	8.02	8.99
TOTAL*	99.9	99.6	99.9	97.5	98.7	99.1	94.7	98.0
Trace Elements (ppm)								
La	234	133	-	218	165	155	377	99
Ce	772	332	-	809	664	617	1252	248
Pr	156	47.3	-	155	133	127	244	36
Nd	840	202	-	762	745	753	1272	156
Sm	188	35.8	-	128	187	189	302	29.3
Eu	46.4	9.13	-	27.5	42.9	43.4	64.1	6.8
Gd	110	24.8	-	54.4	107	103	190	18.7
Tb	8.9	2.2	-	4.8	9.6	10.0	19.5	1.7
Dy	38.2	8.6	-	15.5	41.1	40.2	96	7.2
Ho	5.07	1.08	-	2.12	5.8	5.6	16.3	0.9
Er	11	2.3	-	4.0	13	12.1	40	1.8
Tm	1.6	0.3	-	0.7	1.5	1.6	5.3	0.1
Yb	8.3	1.0	-	3.8	10.3	9.5	32	0.9
Lu	1.2	bdl	-	0.7	1.5	1.5	4.9	0.1
Zr	2100	67	-	1200	1586	1599	3070	138
Y	160	26	58	88	210	204	522	23
Hf	49	4	-	-	-	-	-	-
Nb	18	bdl	-	24	15	9	17	bdl
Ta	3	bdl	-	-	-	-	-	-
Th	44.5	11.2	-	41	35	38	72	12
U	9.5	0.7	-	-	-	-	-	-
Sr	998	1181	1293	3830	1320	1318	1249	1150
Ba	698	2200	-	-	-	-	-	-
Rb	30	93	-	28	30	27	6	125
Cs	2	13	-	-	-	-	-	-
Cr	bdl	32	-	-	-	-	-	-
Ni	11	77	9	-	-	-	-	-
Cu	190	9.5	11	-	-	-	-	-
Co	39	49	43	-	-	-	-	-
Zn	110	110	102	-	-	-	-	-
Sc	bdl	36	52	-	-	-	-	-
V	56	34	92	-	-	-	-	-
Trace Elements (ppb)								
Au	2	bdl	-	3	5	5	4	bdl
Pt	-	-	-	bdl	bdl	bdl	bdl	-
Pd	-	-	-	bdl	bdl	bdl	bdl	-

Table 8. (continued)

Sample No.	89-5	89-7	89-8	89-9	89-10	89-13	89-14	89-15	89-18	89-19
Major Oxides (wt%)										
SiO_2	37.8	45.6	49.6	35.2	39.3	49.6	42.5	37.6	53.0	61.9
TiO_2	1.25	1.18	0.84	2.2	1.48	0.99	0.82	4.38	0.73	0.53
Al_2O_3	3.85	13.7	5.42	4.76	11.5	14.6	5.66	10.2	19.3	18.5
Fe_2O_3	14.2	13.3	11.8	24.1	12	9.5	10.1	14.2	7.31	6.41
MgO	10.9	5.70	8.79	9.72	4.16	2.19	8.70	2.54	2.62	2.78
MnO	0.15	0.21	0.19	0.24	0.22	0.22	0.23	0.17	0.1	0.07
CaO	20.0	10.1	14.6	13.2	13.2	13.5	23.7	11.2	3.68	0.93
Na_2O	0.23	2.49	2.6	0.01	4.77	4.85	0.49	3.98	4.5	3.59
K_2O	0.65	0.17	0.20	3.16	2.70	0.86	0.34	0.42	0.20	0.78
P_2O_5	1.90	0.15	2.13	1.07	0.78	1.11	6.06	1.8	0.14	0.12
S	0.04	0.12	0.32	0.66	0.18	0.11	0.05	2.34	0.14	0.07
LOI	4.8	7.2	3.7	6.3	9.4	1.2	1.4	5.4	5.2	2.5
CO_2	4.74	5.6	3.96	6.04	7.91	0.89	0.86	6.85	4.07	1.83
TOTAL*	99.7	99.9	00.2	100.6	99.7	98.7	100.1	94.2	96.9	98.2
Trace Elements (ppm)										
Zr	224	104	261	254	635	340	218	3081	140	227
Y	74	21	61	45	129	129	79	569	25	78
Nb	bdl	6	bdl	bdl	16	25	bdl	9	bdl	7
Th	29	bdl	17	15	54	54	36	86	bdl	30
Sr	1425	358	566	935	1409	3050	2864	1328	356	1413
Rb	11	5	bdl	107	82	20	7	6	6	14
Ni	9	289	49	88	31	23	27	12	93	69
Cu	14	87	91	237	34	51	12	12000	41	40
Co	44	54	42	68	24	25	38	88	23	18
Zn	102	94	98	187	89	78	136	174	69	74
Sc	55	25	22	33	12	9	40	64	19	16
V	94	20	147	333	247	208	175	328	135	130

*Using LOI as total volatile content. Samples with low totals contain high concentrations of trace elements and/or halogens.

Geochemistry from OGS analytical laboratories except for samples 87-4 and 87-6 from X-Ray Assay Laboratories, Toronto. Major elements by XRF; REE by ICP; other trace elements by XRF and ICP except Pt, Pd and Au by AA. For sample 88-2 Sr and Y by ICP, other Sr and Y data from XRF. Zr data by XRF: samples 88-3, 88-4, 88-5, and 89-15 have significantly (15 to 30 %) higher Zr contents by ICP-MS. bdl- below detection limits (not analyzed).

Lamprophyre samples: 87-4: Carbonate-rich biotite lamprophyre; 88-2: Carbonate-apatite rock; 88-3: Garnetite; 88-4: Garnetite (88-4D = duplicate from separate powder); 88-5: Highly altered garnetite(?) with 3% sulphides; 88-6: Biotite lamprophyre; 89-5: Diopside-rich lamprophyre; 89-8: Diopside-rich lamprophyre; 89-9: Biotite- and carbonate-rich lamprophyre; 89-10: Syenite dike with biotite; 89-13: Plagioclase-garnet dike; 89-14: Diopside-rich lamprophyre; 89-15: Highly altered garnetite(?) with 5% sulphides; 89-17: Biotite-carbonate-apatite rock. **Other rock types**: 89-7: Epidotized basalt; 89-18a: Tourmalinized basalt; 89-19: Silicified and tourmalinized basalt.

Samples are from Croxall property except for samples 89-5, 89-7, 89-18 and 89-19, from Holmer property: *see* Figures 32 and 33 for locations.

atmospheric pressure, the average chill composition would crystallize plagioclase at An_{81-78}, orthopyroxene at En_{83-79} and olivine at Fo_{82-80}, at ratios of approximately 6:3:1 (McBirney 1985, *after* Nathan and Van Kirk 1978). These values and ratios compare favorably to LZ mineral compositions (*see* Figure 5) and the average LZ mode (60% plagioclase, 12% orthopyroxene, 13% clinopyroxene, 16% olivine). The average Kamiskotia primitive and evolved basalts plot in the olivine, and the plagioclase and olivine fields, respectively (*see* Figure 22). The primitive basalt average would crystallize olivine at Fo_{81}. The evolved basalt average would crystallize orthopyroxene at En_{69-65} and plagioclase at An_{59} at a ratio of 4:1 at one atmosphere (McBirney 1985, *after* Nathan and Van Kirk 1978), which closely approximates mineral compositions in the UZ (*see* Figure 22).

MASS BALANCE CALCULATIONS USING RARE EARTH ELEMENTS

If the major element geochemistry of the mixed magma and contact chill samples are candidates for a LZ parental liquid, then mass balance calculations using trace elements should provide supporting evidence for this relationship.

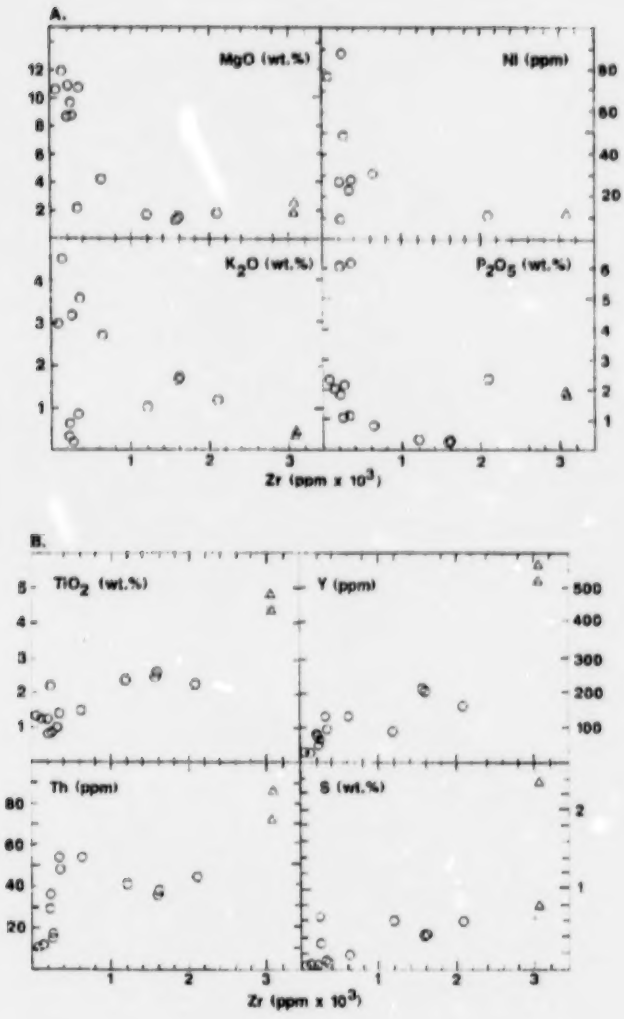

Figure 20. X-Y plots for Brisiol Township lamprophyre suite. Biotite-carbonate-apatite lamprophyres are represented by circles; garnetite samples by hexgons; altered garnetite samples by triangles. A) MgO, Ni, K_2O, and P_2O_5 versus log Zr; B) TiO_2, Y, Th and S versus log Zr.

One approach is to use mass balance equations to estimate the REE content of the LZ cumulates using the average chill composition, where:

$$Chill_{REE} \times (Bulk\ K_D \times M_{cum} + M_{TL}) = Cum_{REE},$$

with $Chill_{REE}$ as the REE content in the average chill composition, Bulk K_D as the bulk distribution coefficient for the average cumulus mineralogy of the LZ, M_{cum} and M_{TL} as the estimated average mass of the cumulate phases and trapped liquid in the LZ cumulates, respectively, and Cum_{REE} as the average REE content of the LZ cumulates. The trapped liquid composition is assumed to be the same as the chill composition, and density differences between liquids and cumulates are considered insignificant. Models that use mass balance calculations are highly dependent on the K_Ds chosen. For these calculations, the values have been chosen conservatively, and are near the lowest of the range for basalt to mineral K_Ds in the literature. Using trapped liquid contents of zero (C_1) and 5 (C_2)%, the model LZ cumulates bracket the average LZ cumulate composition for the REE, including the positive Eu anomaly (Figure 23). They closely approximate the overall slope of the REE pattern, with La_N/Yb_N = 1.01 and 1.05 respectively, in comparison to the average LZ cumulate with La_N/Yb_N = 0.99.

A similar set of models have been calculated for the upper four UZ cumulates, using the average evolved basalt as a model parental liquid (*see* Figure 23). For these models, trace amounts of cumulus apatite and titanomagnetite are included in the average cumulus mineralogy, the K_Ds

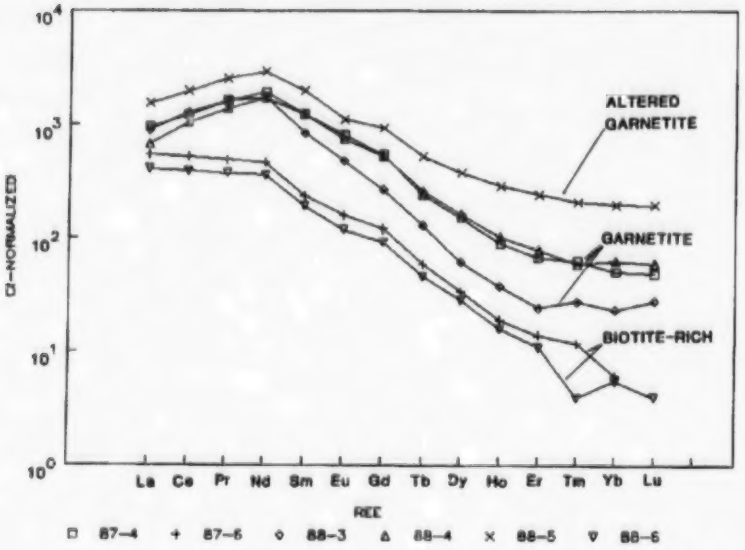

Figure 21. REE profiles for Bristol Township lamprophyre suite rocks.

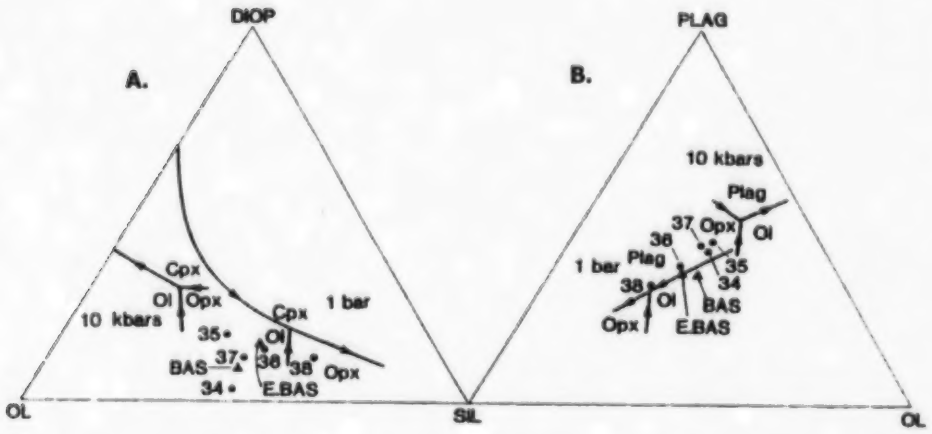

Figure 22. CMAS-type tetrahedron projections for KGC chill samples and Kamiskotia basalt (BAS) and evolved basalt (E.BAS) (*after* Walker et al. 1979). A) Projection from plagioclase; B) projection from silica.

for orthopyroxene and plagioclase are slightly higher (Appendix III), and trapped liquid contents of 10 (C_1) and 25 (C_2)% are used (higher amounts of trapped liquid which may be applicable to UZ orthocumulates would require lower REE contents in the liquid: discussed below). As in the example above, the cumulate REE pattern (except for Nd) is bracketed by the model cumulate compositions. For C_1 and C_2, La_N/Yb_N = 1.15 and 1.38, respectively, in comparison to the average upper UZ cumulates with La_N/Yb_N = 1.21. These mass balance calculations indicate that LZ cumulates and upper UZ cumulates may be derived from the KGC chill average and Kamiskotia evolved basalts, respectively, consistent with the phase relationships using the major elements described above.

ASSIMILATION-FRACTIONAL CRYSTALLIZATION MODELING

Variation diagrams are used to determine the nature of the supracrustal magma chamber processes, with trace elements, and TiO_2 and P_2O_5 contents plotted versus Zr on the abscissa (Figure 24a-f). Zirconium is used to monitor trace element enrichment or depletion as it behaves incompatibly in this system, forming coherent enrichment trends

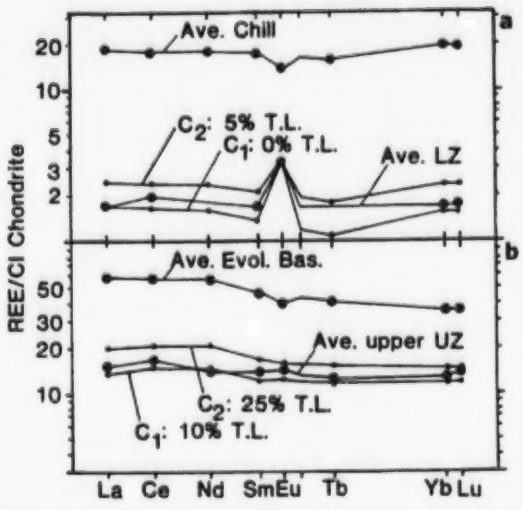

Figure 23. Mass balance calculations using the REE: a) model LZ cumulate compositions from average KGC chill average composition, using 0% trapped liquid (C_1) and 5% trapped liquid (C_2); b) model upper UZ cumulate compositions from average Kamiskotia evolved basalt composition, using 10% trapped liquid (C_1) and 25% trapped liquid (C_2).

with other incompatible elements (Th, Hf, Y, Yb). There is a systematic increase of TiO_2, P_2O_5, Th, La and Eu contents.

Nickel (also MgO and Cr, not shown) is highest for the KGC chill rocks and decreases systematically through the evolved basalts, with increasing Zr (*see* Figure 24a). However, the Ni contents of the primitive basalts are low. The low Ni contents may be explained by the fractionation of olivine or sulphide which lowers the Ni content of the liquid prior to extrusion of the primitive basalts. This would have to be followed by recharge of a primitive liquid during fractionation before the extrusion of evolved basalts, in order to explain the Ni and Zr contents in the evolved basalts (e.g., sample 88-16 with 100 ppm Ni and 180 ppm Zr: *see* Barrie 1990, Figure 24a). An alternative explanation, that the evolved basalts are derived from a separate source with different trace element characteristics, seems unlikely for several reasons. Firstly, the Kamiskotia primitive and evolved basalts are intimately interbedded on a scale of tens of metres at different stratigraphic levels, in several locations. Chemically-similar hypabyssal sills are found in the footwall of the evolved basalts on the Canadian Jamieson property. Secondly, there is clear evidence for the coexistence of magmas of intermediate (more fractionated equivalents of the enriched basalts) and felsic composition

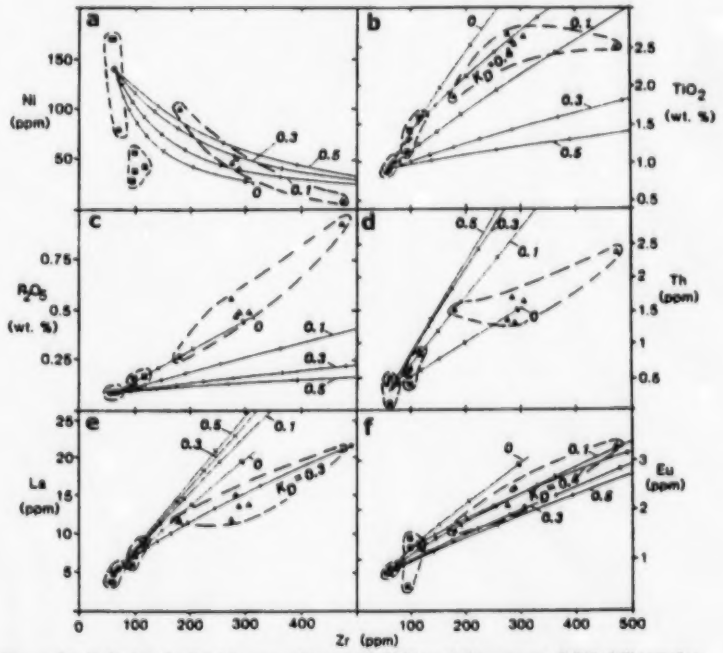

Figure 24. X-Y plots for liquid compositions with AFC modeling curves. KGC chill samples: dots; Kamiskotia "primitive" basalts: squares; Kamiskotia evolved basalts: triangles. AFC curves using equations of DePaolo (1981a) labeled by ratio of mass assimilated (MA) to mass fractionated (MF), with 0 representing fractionation only. Tick marks represent 10% fractionation increments; double-tick marks are for 80% fractionation. Assimilant used is average of 9 granites and tonalites from the KGC granophyre, with 6 ppm Ni, 0.29 wt.% TiO_2, 0.04 wt. % P_2O_5, 9.2 ppm Th, 58 ppm La, 2.9 ppm Eu and 643 ppm Zr (Hart 1984). Bulk K_Ds used: Ni: 2; TiO_2: 0.2; P_2O_5: 0.01; Th: 0.001; La: 0.1; Eu: 0.2; Zr: 0.01. For TiO_2, La and Eu, secondary FC curves from 100 ppm Zr use bulk K_Ds as labeled. Additional data from Hart (1984) and Appendix III. a) Ni versus Zr, b) TiO_2 versus Zr, c) P_2O_5 versus Zr, d) Th versus Zr, e) La versus Zr, f) Eu versus Zr.

in outcrop: trace element-enriched, quenched andesitic globules are found within ignimbritic rhyolites in southern Godfrey Township (Comba et al. 1986). One fragment of the enriched andesitic material has 54.5% SiO_2, 2.15% TiO_2, 0.36% P_2O_5, 290 ppm Zr and 120 ppm Y (unpublished data). And thirdly, the mass balance modeling between the evolved basalts and upper zone gabbros described above infers a cogenetic relationship.

The trajectories marked on Figure 24 are for bulk assimilation-fractional crystallization (AFC) models. An average of roof rock granophyre samples from Hart (1984) is used for the material assimilated. This composition is used for two reasons. Firstly, there is field evidence for partial assimilation of large granophyric blocks in and adjacent to the UZ cumulates. Secondly, the granophyres are highly enriched in incompatible elements, and have relatively flat REE patterns with negative Eu anomalies. Other material considered to be assimilated are the mixed magma outcrop tonalites and granodiorites, and average Archean continental crust compositions (Taylor and McLennan 1985; Shaw et al. 1986). However, all of these have low incompatible element contents in comparison to the granophyre that would require greater amounts of assimilation (increasing silica and K_2O contents). Furthermore, their P_2O_5 contents are too low and their REE patterns are too steep which is not consistent with the high P_2O_5 contents and flat REE patterns of the Kamiskotia basaltic andesites. Ratios of assimilation/fractionation used in the models range from 0 to 0.5. Generally, assimilation/fractional crystallization rates for mafic-ultramafic systems range from 0.01 for parts of the Kiglapait intrusion, which is hosted in refractory gneisses and anorthosites (DePaolo 1981a) to 0.5 for komatiites in supracrustal environments (Sparks 1986). Rates of 0.1 to 0.3 are considered normal for supracrustal tholeiitic intrusions (DePaolo 1985; Sharpe 1986; Sparks 1986).

The AFC models with ratios of 0.1 to 0.3 work well for some of the elements, but they do not approximate the enrichment for P_2O_5. Assimilation of the granophyric rocks with low P_2O_5 contents depresses the enrichment due to fractionation. Furthermore even small amounts of granophyre assimilation will cause significant increases in silica content which are not observed.

Bulk fractionation of 70 to 80% provides a reasonable approximation for these trends, particularly Ni, P_2O_5 and Th (*see* Figure 24a, c, d). Deviations from the data may be due to variation in the bulk K_Ds during fractionation. For TiO_2, an increase in the bulk K_D from 0.2 to 0.4 after 40% fractionation, provides a close approximation of the data (*see* Figure 24b). This may reflect the onset of iron–titanium oxide fractionation. Higher bulk K_Ds provide a better fit for La and Eu also (*see* Figure 24e). Higher K_Ds for the La and Eu could reflect minor apatite fractionation and/or greater partitioning into plagioclase with decreasing An content (Schnetzler and Philpotts 1970). If higher bulk K_Ds for the REE are necessary, then the average evolved basalt composition may be too enriched to be parental to the upper UZ cumulates (considering the mass balance calculations described above), and the upper UZ cumulates may have been derived from a composition intermediate between the primitive and evolved basalts.

Fractionation also explains decreasing Mg numbers and the relatively constant silica contents. Bulk fractionation of 70 to 80% from the KGC average chill composition causes Mg numbers to decrease from 56 to 29 to 30 (Nathan and Van Kirk 1978), within the range for the evolved basalts (Hart 1984; Barrie 1990). Silica contents are enriched only slightly during fractionation, in contrast to the five-fold enrichment in Zr. In general terms, if a bulk K_D for silica is estimated from $SiO_{2(LZ)}$ divided by $SiO_{2(chill)}$ at slightly less than unity, then only slight silica enrichment would result, even at high levels of fractionation. This is a well-known characteristic of tholeiitic fractionation trends, where iron enrichment is accompanied by essentially no silica enrichment in the liquid prior to significant iron-titanium oxide fractionation (e.g., Skaergaard Intrusion: Wager 1960; Hunter and Sparks 1987).

Other geochemical models for trace elements that may pertain to the Kamiskotia magma system, but not considered in detail here, are fractionation-recharge and -discharge models. In fractionation-recharge models, incompatible element enrichment and compatible element depletion are enhanced in comparison to FC models due to higher degrees of cumulates removed for a given volume of liquid in the system. Thus, their trajectories would follow the fractionation-only trajectories in Figure 24 but extend to greater degrees of enrichment for a given volume of residual liquid in the system (O'Hara 1977). If discharge from the system is incorporated into the model, then enrichment or depletion may eventually reach a steady state, as originally envisioned for mid-ocean ridge systems by O'Hara (1977). Such a model could account for greater variation in incompatible element ratios (e.g., Zr/Hf), if the amount of magma discharged is small in comparison to the amount fractionated (O'Hara 1977).

Trace element enrichment by two-liquid chemical diffusion and thermal (Soret) diffusion should also be considered at Kamiskotia, as there is geological and textural evidence for the coexistence of mafic and felsic liquids in both intrusive and metavolcanic rocks. Basalt flows and rhyolite tuffs interdigitate on a scale of metres in several locations, and quenched andesitic enclaves are found within rhyolite crystal lithic tuffs at one location (*see* "Geology").

Two-liquid chemical diffusion models predict that the large ion lithophile elements (LILE) prefer more polymerized acidic liquids, and just the opposite for the HFSE (Watson 1976; Ryerson and Hess 1978). However, the entire Kamiskotia suite (excepting one extremely fractionated rhyodacite) shows normal enrichment trends with increasing SiO_2 content, which would not be the case if chemical diffusion were a dominant process. Thermal diffusion models predict that the LILE will generally partition into the hotter silicate liquid whereas most HFSE will partition in the opposite direction (Lesher 1986). For mid-oceanic-ridge basalt (MORB) compositions, the REE are enriched by a factor of 2.5 under temperature gradients of 50 to 80°C (at 1 GPa, 1380 to 1535°C: Lesher 1986). This

suggests that in addition to fractionation, thermal diffusion may have been an operative process in the formation of the Kamiskotia evolved basalts.

Nd Isotope Signatures

In a related study of Kamiskotia area rocks, Barrie and Shirey (1991) investigated the geochemistry and Nd-Sr isotope systematics of several rock suites. They used geochemistry and Nd isotopic compositions to characterize mantle and crustal sources, and to provide constraints on petrogenetic models for tholeiitic, calc-alkalic and lamprophyric suites in the Kamiskotia area. One of the purposes of the study was to identify and characterize potentially distinct mantle and crustal sources for the supracrustal rocks using whole rock geochemistry and Nd isotopic compositions. Previous trace element and radiogenic isotope studies for Abitibi mantle-derived rocks have indicated that the mantle was variably depleted in Sm/Nd, Rb/Sr, and U/Pb with respect to a reservoir with chondritic ratios for these elements. When considered on a subprovince scale, mantle-derived Abitibi tholeiitic and komatiitic intrusions appear uniformly depleted in their Nd and Sr isotopic compositions (e.g., Machado et al. 1986). However, other investigations have detected different isotopic signatures (Basu et al. 1984), even within "cogenetic" suites (Cattell et al. 1984), and mantle heterogeneites have been found in Archean rocks elsewhere in the southern Superior Province (Shirey and Hanson 1986). Crustally derived Abitibi rocks show primitive and slightly enriched Pb isotopic signatures (*see* Gariepy and Allegre 1985; for review), and isotopic heterogeneities have been found in crustally derived rocks in northwestern Ontario (e.g., Hanson et al. 1971; Morrison et al. 1985; Shirey and Hanson 1986; Smith et al. 1987).

The KGC and KVC are represented by two ferroan gabbros, a dacitic granophyre, a rhyolite and a basalt. The suite is characterized by relatively flat REE patterns and a restricted range of $\varepsilon_{Nd(t)}$ values (defined as the deviation in parts per 10 000 from a chondritic uniform reservoir of the same age, with ages from U-Pb data) from +2.2 to +2.6. This is essentially identical to the best estimates of the MORB-like, isotopically depleted Abitibi mantle at 2.7 Ga (Dupre et al. 1984; Machado et al. 1986).

Three basalts of the Lower volcanic suite have flat to slightly LREE-enriched REE patterns, with Ce/Yb ranging from 2.3 to 10.6, and $\varepsilon_{Nd(t)}$ values ranging from +1.7 to +3.0.

Lamprophyric rocks in the Kamiskotia area are best represented as dikes in the Montcalm gabbroic complex, located 25 km west of the KGC; and by the Bristol Township lamprophyre suite (*see* Figure 4 for location). The lamprophyre samples are characterized by high Th, LREE and P_2O_5 values, and steep REE patterns. Both Montcalm lamprophyre dikes have nearly identical $\varepsilon_{Nd(t)}$ values of +2.8 and +2.5. A garnetite sample from the Bristol Township lamprophyre suite has a whole rock $\varepsilon_{Nd(t)}$ value of +1.0, slightly isotopically enriched in comparison to the Abitibi mantle at 2.7 Ga.

Petrogenesis of the KGC Gabbros and KVC Basalts

The KGC average chill composition is compared to N-MORB and Alexo komatiites (located 140 km east of the Kamiskotia area, within the Abitibi Subprovince) on a primitive mantle-normalized diagram (Figure 25). The elements are ordered according to their compatibility with primitive mantle peridotite, with the most compatible elements to the right. Generally, a melt formed from single stage partial melting would curve downward toward the compatible elements to the right and would be flat toward the incompatible elements at the left. A two stage model is required for the abundances of N-MORB, which has a concave-down pattern. The first stage has approximately 1.5% melting that depletes the mantle in the most incompatible elements, and the second stage has 8 to 10% partial melting of the first stage residue (Hofmann 1988). For Alexo komatiites, Barnes (1984) and Brugmann (1985) have noted that the elemental abundances (except K_2O) also correspond to a two stage model, with a higher degree of melting during the second stage (up to 40%).

The KGC chill average has compatible element concentrations nearly identical to N-MORB; however, the incompatible elements exhibit a flat pattern (except for K_2O, Rb and Ba: *see* below). The most straightforward explanation is a derivation by single-stage partial melting of a chemically primitive mantle. A first order approximation for the minimum degree of single stage partial melting can be determined using a simplified equation for bulk partial melting: $F = C_0/C_l$, where F is the fraction of melt, C_0 is concentration in the primitive mantle before melting and C_l is the concentration of the element in the melt. Using the 13 elements in Figure 25 from La to Lu, an average value for the KGC chill average of 15.9% (1 sigma = 2.6%) partial melting is required; excluding P_2O_5, TiO_2 and Eu, 14.7% (n=10, 1 sigma = 1.2%) partial melting is required.

This approximation does not account for fractionation that must have occurred, after mantle melting and prior to emplacement. Negative Eu anomalies and liquidus phase relationships (Nathan and Van Kirk 1978) for the KGC chill samples imply a previous history of plagioclase fractionation. Furthermore, primitive magmas must be in equilibrium with mantle olivine compositions of $Fo_{86\text{-}90}$ (Green 1970). Given the olivine-liquid K_D^{Fe2+}/Mg of 0.30 to 0.33 (Roeder and Emslie 1970; Roeder 1974; Longhi et al. 1978), the minimum Mg number for primitive magmas are 68 to 75. Using an FeO/FeO_{total} of 0.9, which is appropriate for mantle-derived magmas, the KGC chill average would have an Mg number of 51. This is significantly lower than the minimum required for a primitive magma, implying that olivine and possibly pyroxene fractionation occurred after mantle extraction in addition to plagioclase. A reasonable estimate for the amount of fractionation can be made by combining the average olivine-bearing adcumulate composition (samples 1 to 4: average Mg number = 81, using FeO/FeO_{total}=0.9) with the KGC chill average to obtain a liquid in equilibrium with mantle olivine. A 1:1 mix of these components produces a composition with an Mg number of 70. This liquid would have 27.9 weight %

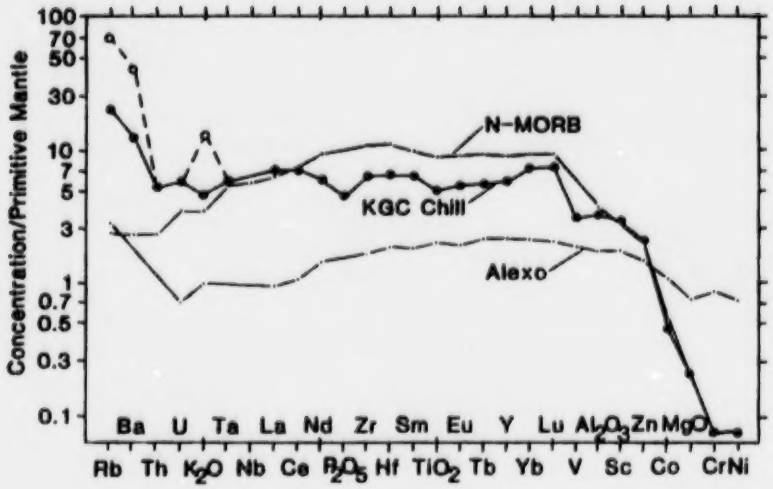

Figure 25. Primitive mantle-normalized profiles for Kamiskotia Gabbroic Complex average chill composition in comparison to Alexo, Ontario, komatiites (data *from* Brugmann 1985; Barnes 1984; and Whitford and Arndt 1978), and average N-MORB. KGC chill average for Rb, Ba and K_2O including sample 34 marked with open circles; without sample 34 marked in closed circles. Normalizing values and average N-MORB as listed in Hofmann (1988).

normative olivine (24.7 mole %) and a flat REE pattern at 9 to 10 times chondrites. The degree of partial melting of primitive mantle required to produce this composition would be 34% (using the partial melting equation and the REE without Tb). The normative olivine content of this liquid and the degree of partial melting can be used to estimate the temperature and pressure of anhydrous melting from a spinel lherzolite primitive mantle composition. This corresponds to melting at 17 kilobars pressure and 1550°C (*see* Jacques and Green 1980, Figure 9).

An alternative explanation is that, like the Alexo komatiites and N-MORB, the KGC chill was derived from a mantle source that previously had been depleted in the most incompatible elements but has subsequently undergone enrichment to form, perhaps fortuitously, the flat pattern on the primitive mantle-normalized diagram (*see* Figure 25). Selective enrichment would be due to either diffusion from the adjacent felsic liquids in the mixed magma and contact chill outcrops (Watson 1976), which as previously discussed seems unlikely, or by selective contamination en route through the lower crust as suggested by Watson (1982). Selective contamination processes cannot be ruled out, although at present there is no supporting experimental evidence for selective contamination involving HFSE in mafic liquids.

Petrogenesis of KVC Rhyolites

Considering the exposures of coeval mafic and felsic, intrusive and extrusive rocks, the Kamiskotia area is ideal for investigating the petrogenesis of high silica rhyolites in bimodal (basalt-andesite and rhyolite) volcanic fields. For this discussion, high silica rhyolites are defined as a suite of rhyolites having greater than 73 weight % SiO_2, high HFSE and REE contents, flat REE patterns with negative Eu anomalies, and Rb/Sr ratios greater than unity.

The petrogenesis of high silica rhyolites in bimodal volcanic fields as in the Kamiskotia area is a contentious issue. There are two main hypotheses. The first hypothesis, proposed particularly for high silica rhyolites of the Basin and Range Province, USA, is that high silica rhyolites represent partial melts of a felsic granulite source in the lower or middle crust, and have undergone little or no modification by supracrustal magmatic processes (e.g., Doe et al. 1982; Christiansen et al. 1986). The second hypothesis is that high silica rhyolites are the product of high degrees of fractional crystallization from a MORB-like, mantle partial melt, possibly accompanied by significant assimilation of roof rock partial melts, and by chemical and/or thermal diffusion-related enrichment processes within supracrustal magma chambers. Variations of this hypothesis have been proposed by numerous authors for the bimodal volcanic fields of eastern Iceland (e.g., Wood 1978; Macdonald et al. 1987; and by Hart 1984) for the Kamiskotia rhyolites. A third hypothesis, involving the separation of an immiscible, siliceous liquid from tholeiitic parent, has been proposed for rhyolites similar to high silica rhyolites in the Uchi–Confederation Lake area of the Superior Province (Thurston and Fryer 1983). Experimental studies (e.g., Watson 1976) on coexisting basaltic and silicic liquids indicate that incompatible elements will partition strongly into the mafic liquid, a phenomena that is not observed at Uchi–Confederation lakes in particular, or

in bimodal volcanic suites generally. Thus liquid immiscibility is not considered in this discussion.

The first hypothesis is proposed most elegantly for a variety of high silica rhyolites, the topaz rhyolites of the Basin and Range Province (e.g., Christiansen et al. 1986). Topaz rhyolites are characterized by high silica contents, high F, Rb, U and Th contents, low Sr, Ba and Eu contents, and flat REE patterns with strong negative Eu anomalies. Christiansen et al. (1986) proposed that siliceous magmas with high F contents are the result of partial melting of a metamorphosed felsic protolith, due to the passage of hot mafic magmas through the lower or middle crust, with the decomposition of small amounts of fluorine-rich biotite to give high F contents. The siliceous melts then migrated into supracrustal magma chambers, and extruded along with the contemporaneous mafic magmas. A similar hypothesis has been proposed for a suite of Archean high silica rhyolites, those that overlie the Bad Vermilion Anorthosite Complex in the Rainy River area of the southern Superior Province. Shirey (1984) postulated that partial melting of a tonalitic source with a relatively flat and elevated REE pattern, at either shallow or deep levels, as the most likely mechanism to generate these rhyolites.

The second hypothesis is a combination of several shallow level magma chamber processes: fractionation, assimilation of roof rock partial melts, and chemical and/or thermal diffusion. Fractionation of olivine, two pyroxenes, plagioclase and an iron-titanium oxide phase from a Kilauea basalt (Mg number = 53), under hydrous conditions at 1 kilobar, has been shown to generate rhyolites nearly identical in major element geochemistry to the high silica rhyolites of eastern Iceland (Spulber and Rutherford 1983). These experiments required 90% fractionation of these phases in cotectic proportions. A similar, high degree of fractionation would account for incompatible element enrichment also. For example, using a reasonable bulk partition for Ce of 0.2 over the range of magma compositions, a tenfold enrichment from 12 ppm Ce (typical MORB) to 120 ppm Ce (average KGC rhyolites from Hart 1984) requires greater than 90% equilibrium crystallization (using the equation: $C_l/C_o = 1/K_D$ (1-F), with C_l the concentration in liquid remaining, C_o the concentration in the liquid initially, K_D the bulk distribution coefficient, and F the fraction of system that is liquid).

If fractionation is the primary mechanism to produce the high silica rhyolites, then a spectrum of volcanic rock compositions would be expected. This is clearly not the case for most of the high silica rhyolites, which are found in bimodal volcanic fields, including those in the Kamiskotia area. One explanation for the compositional gap found in the bimodal fields may be provided in a petrologic and theoretical study of the Pleistocene to Recent Medicine Lake Volcano, California (Grove and Donnelly-Nolan 1986). At Medicine Lake, a compositional gap between andesites and rhyolites is explained by a three-stage fractionation process from a basaltic precursor. The first phases to fractionate were olivine, plagioclase and augite, and then olivine was replaced by orthopyroxene and amphibole. This led to an andesitic liquid, enriched in iron, titanium and phosphorous (and incompatible elements). Fractionation continued with apatite and magnetite crystallization joining the plagioclase, augite and amphibole, producing a liquid of rhyolite composition. Grove and Donnelly-Nolan (1986) noted that during magnetite and apatite crystallization, fractionation proceeds over a limited temperature interval (i.e., the liquidus surfaces have shallow slopes). Considering the rapid change in liquid composition over such a restricted temperature interval, the possibility of preserving an andesitic to rhyolitic liquid is diminished.

Fractionation from andesitic to rhyolitic liquids over a restricted temperature interval should be accompanied by a rapid increase in volatile contents. High volatile contents can aid chemical and thermal diffusion processes, which can lead to incompatible element enrichment in siliceous systems. This process is ensured, provided that the magma chamber is compositionally stratified and convecting (e.g., Hildreth 1981).

Hart (1984) favoured partial melting over fractionation as the principal mechanism to produce the KVC rhyolites and the KGC granophyres. Using a fractional melting model, and partition coefficients for andesitic liquids, Hart found that the REE concentrations in model rhyolites were generally similar to a 10% partial melt of a KVC primitive basalt composition, or a 30% melting of a KVC evolved basalt. In both cases, however, the resulting model rhyolite had significantly higher Ce/Yb ratios than the average KVC rhyolites, and these models may not adequately represent the Kamiskotia system.

Radiogenic isotope studies can provide a way to distinguish between the mantle or crustal origins for high silica rhyolites. The ideal locations for differentiating between mantle and crustal sources are where old sialic basement is present, such as across much of the Basin and Range Province. In a study of the Yellowstone bimodal volcanic field, Doe et al. (1982) found that the initial Pb and Sr isotope ratios of basalts were significantly less radiogenic than the coeval rhyolites. They interpreted the basalts as mantle-derived, and the high silica rhyolites as partial melts of a siliceous lower crust, based principally on the Sr isotope ratios. Halliday et al. (1989) obtained nearly the opposite results for the young (1.2 to 0.8 Ma) basalts and high silica rhyolites of the Long Valley Caldera, California. From a detailed Nd-Sr-Pb isotopic study, they found that these rhyolites are relatively unradiogenic, and identical to coeval, mantle-derived basalts. Other studies have found a spectrum of isotopic ratios for high silica rhyolites, particularly in the Rb-Sr system (e.g., Bacon et al. 1984; Christiansen et al. 1986). It is noted that a significant problem with the high Rb/Sr ratios that characterize high silica rhyolites, and topaz rhyolites in particular, is that it is very difficult to obtain accurate initial ratios, due to long, age-dependent extrapolations on isochron diagrams.

There is some evidence of an older sialic basement in the Kamiskotia area, from an inherited zircon fraction in granitoid B, and from a regional Sm-Nd isotope study in the Kamiskotia–Montcalm area (Barrie 1990; Barrie and Davis 1990). However, geochemical and radiogenic iso-

tope studies have shown that there is no evidence for assimilation or contamination of an older sialic basement for any part of the KGC or the KVC (Barrie 1990). This provides supporting evidence to the field and geochronological data that support a coeval, cogenetic relationship between mafic and felsic, intrusive and extrusive rocks in the Kamiskotia area.

To summarize, there are several lines of evidence to support a coeval and cogenetic relationship between the KVC high silica rhyolites and the KGC, with no involvement of an older crustal component: 1) coeval, high precision U-Pb ages for KGC and KVC rhyolite samples; 2) abundant field evidence for the coeval nature of the KVC rhyolites and basalts; 3) geochemical evidence for a cogenetic relationship between the KGC and KVC basalts; and 4) initial Nd isotope ratios for KGC and KVC rocks that are compatible with a derivation from a depleted mantle source, with no evidence for contamination from any enriched crustal component. Fractionation-dominated magma chamber processes at low pressures adequately explain the composition of the KVC rhyolites, although more rigorous modeling is necessary to test this hypothesis. Partial melting of KVC basalts, and chemical and/or thermal diffusion processes within the Kamiskotia magma chamber may have played minor roles in the generation of the KVC rhyolites.

Petrogenesis of Bristol Township Lamprophyre Suite

Perhaps the closest analogs to the Bristol Township lamprophyre suite are ultramafic lamprophyres, and particularly those with alkalic affinities. Ultramafic lamprophyres (UML) are characterized by their low SiO_2, and high K, Sr, Ba, REE, Mg, Cr, Ni, and volatile contents; they are distinguished from other lamprophyre types by an unusual mineralogy, including olivine (Fo_{92-78}), phlogopite (rich in Ti, Fe^{3+}, Ba or F) and sodic amphiboles as phenocrysts, and carbonates, feldspathoids, Ca-Fe-Ti-Zr garnets in groundmasses (Rock 1986, 1987). Aillikites are a carbonate-rich variety of UMLs. Classic examples of aillikites are found at Aillik Bay, Labrador (Malpas et al. 1986); and associated with carbonatites at Oka, Quebec (Treiman 1982) and Magnet Cove, Arkansas (e.g., Steele and Wagner 1979). Ultramafic lamprophyres are rare: the only other UML rocks documented in the Superior Province are the 1650 million-year-old McKellar Harbour dikes near Marathon, Ontario (Platt et al. 1983), and biotite-olivine-carbonate dikes at the northern end of Lake Nipigon, believed to be *circa* 1500 Ma (Sutcliffe 1988).

Many UMLs are believed to represent primary, mantle-derived magmas, generated at depths of 100 to 150 km, probably derived from metasomatized, LREE-enriched mantle material (e.g., Malpas et al. 1986; Rock 1986). The primary melts may have been extensively modified by fractionation or interaction with alkali- and volatile-rich fluids (Rock 1986). It is noted that the Bristol Township lamprophyre suite differs from most UML in that it is not known to have magnesium-rich olivine, high Ni and Cr contents, and it is more enriched in the HFSE and REE than most UML (Rock 1986). In these aspects, it is similar to zones of phosphorus and fluorine-rich metasomatism along the DPFZ, which have been compared with fenitization associated with volatile-rich, mantle-derived alkaline magmas (King and Kerrich 1987). Additionally, it is chemically and mineralogically similar to parts of the Oka carbonatite, Quebec, believed to represent upper mantle partial melts rich in CO_2 (Eby 1975).

A slightly enriched Nd isotopic signature of +1.0 (Barrie 1990) must be accounted for when considering the ultimate source of the Bristol Township lamprophyre suite. One possibility is that the suite was derived by magmatic or metasomatic processes, from a crustal material 200 million years older than the majority of rocks in the southern Abitibi Subprovince. This would require a very efficient scavenging of REE from the crust into a melt or fluid in order to account for the incompatible element enrichment of the lamprophyre suite. Two processes that may account for this are CO_2 fluid streaming through the lower crust during granulite facies metamorphism; and fluxing by a fluid rich in H_2O derived from subducting oceanic slabs (Sorensen and Grossman 1989). It is noted that there are no known rock suites associated with subduction zones that are as enriched in the LREE as the Bristol Township lamprophyre suite. A second possibility is that the lamprophyre suite was derived from a part of the mantle that had undergone significant LREE enrichment, approximately 200 million years prior to the separation and emplacement of the lamprophyre suite (Barrie 1990). At present, it is difficult to distinguish between isotopically enriched mantle, or lower crustal sources from the lamprophyre suite.

Economic Geology

Volcanogenic copper-zinc ± gold ± silver mines and deposits, mesothermal gold deposits, magmatic nickel-copper occurrences and one REE occurrence are present in the Kamiskotia area (*see* Figure 4). This section describes the most economically significant of these mineral concentrations. New assays and chemical data are provided for several nickel-copper occurrences within the KGC, and a previously undocumented REE occurrence in the Bristol Township lamprophyre suite.

VOLCANOGENIC COPPER-ZINC DEPOSITS

Four massive sulphide deposits hosted in the KVC have been mined for their copper-zinc ± gold ± silver contents: the Kam-Kotia Mine, the Jameland Mine, the Canadian Jamieson Mine, and the Genex Mine (*see* Figure 4). In general terms, all four orebodies have the following characteristics: 1) they are composed of several smaller lenses or masses of sulphide material; 2) the lenses or masses are generally within a restricted stratigraphic interval (<150 m) at each mine site: their host metavolcanic rocks are broadly correlative from deposit to deposit; 3) their host rocks are predominantly mafic metavolcanic rocks, with subordinate felsic tuffs located on the mine properties; and 4) they exhibit strong chlorite alteration in the stratigraphic footwall, and a more widespread sericite alteration pattern. The sulphide minerals for the deposits are pyrite, pyrrhotite, chalcopyrite, sphalerite, and minor magnetite; trace galena has been reported for the Kam-Kotia mine (Pyke and Middleton 1970). Interestingly, incompatible element-enriched, basaltic andesite and andesite flows and sills, generally uncommon in the KVC, are present at each mine property, in close proximity to the ore. These rocks apparently postdate ore formation, as they are generally less-altered than other KVC rocks, and they cut the other metavolcanic rocks and the orebodies locally. The geochemistry of the basaltic andesites and andesites are described above (*see* "Geochemistry").

Kam-Kotia and Jameland Mines

The Kam-Kotia mine is located in eastern Robb Township (Figure 26, and *see* No. 1 in Figure 4). Pyritized, rhyolitic breccias and tuffs are the immediate host rocks to the mine, and these are found within a sequence of predominantly mafic metavolcanic rocks which are north-facing, have a strike of 315°, and dip 75°N. Massive pyrite lenses, up to 2 m in thickness, are exposed at the southern wall of the open pit. They are found within foliated mafic metavolcanic rocks that have been subjected to strong chlorite and carbonate alteration. Spherulitic rhyolite with apparent flow banding occurs in a prominent outcrop within the southern

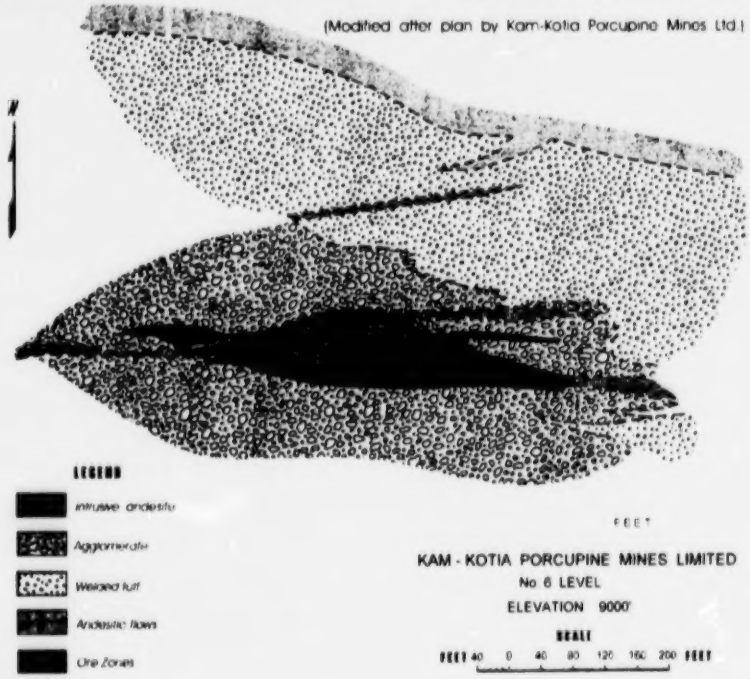

Figure 26. Geology of the number six mine level at Kam-Kotia Porcupine Mines Limited. From Pyke and Middleton (1970).

half of the open pit. The following description of the orebody is paraphrased from Somerville (1967), Pyke and Middleton (1970) and P. Binney (Falconbridge Limited, personal communication, 1990):

> The Kam-Kotia orebody consisted of seven lenses or irregular-shaped masses. The mineralized zone appeared to be steeply dipping. It consisted of six copper-rich lenses and one zinc-rich lens that had a strike slightly more westerly than the host rocks, and a plunge at 30°NW. The lower lenses were predominantly massive sulphide, whereas the upper lenses contained more stringer zone material (quartz - sulphide stockwork, with 10 to 25% sulphide). In general, copper was concentrated in closer to the surface and zinc at depth. Chloritic and sericitic alteration halos are present and surround the ore lenses. Andesite dike and sill-like masses apparently cut both ore lenses and altered metavolcanic rocks [*see* Figure 26]. The andesites are fine-grained, and unmineralized, with well-defined chilled margins. Mineralization predated andesite dike-sill emplacement and may have influenced their emplacement.

The Jameland Mine is in Jamieson Township, 1.2 km to the southeast and along strike with the Kam-Kotia Mine (*see* No.2 in Figure 4). The following description of the orebody is taken from Pyke and Middleton (1970) and Middleton (1973b):

> The deposit was situated within sheared, chloritized and brecciated basalts, andesites and rhyolite tuffs. The deposit consisted of ten lenses or irregular-shaped masses, and in its entirety plunged 30 to 35° to the southeast. At the west end, the orebody was a single lens with a horizontal width of 15 m, whereas 300 m to the east, near the center of the zone, numerous sulphide masses are distributed over a horizontal width of 100 m. As with the Kam-Kotia mine, stringer-type copper-rich ore was confined to the upper lenses and massive zinc-rich ore to the lower lenses. A zone of massive pyrite, without significant base metal content, occurs between the Kam-Kotia and Jameland Mines.

Ore from the Kam-Kotia Mine was recovered briefly during World War II (186 000 tons (169 000 tonnes) recovered). The mine produced again from 1961–1972. During the second period of mining, 6 436 000 tons (5 840 000 tonnes) were recovered (including minor production from the Jameland deposit), with average grades of 1.1% Cu, 1.2% Zn, and 0.1 ounces of silver per ton (totals of 143 351 665 pounds (6.5 by 10^6 kg), 156 000 000 pounds, (7.1 by 10^6 kg) and 663 136 ounces (20 600 kg), respectively; also 5604 ounces (174 kg) of gold (Canadian Mines Handbooks 1961–74)).

Canadian Jamieson Mine

The Canadian Jamieson Mine is located in northwest Godfrey Township (Figure 27, and *see* No. 3 in Figure 4). The orebody was situated within predominantly mafic metavolcanic rocks that face to the northeast, with lesser rhyolite tuffs and flows(?). Basaltic andesites are found 100 m south of the mill foundation (*see* Figure 27). Shear zones up to 1 m wide and ductile deformation in the metavolcanic rocks are present on the northeast outcrops. Deformation is probably related to a major fault zone located 100 m to the northwest (striking 130 to 140°, near-vertical dip: *see* Figure 27), which postdated KVC formation and massive sulphide mineralization. A description of the mine site stratigraphy and of the orebody is given here, based on the descriptions of Comba et al. (1986), and P. Binney and B. Filbey (Falconbridge Limited, personal communication, 1985–90):

From surface exposures, the base of the stratigraphic succession in Figure 27 consists of pillowed mafic flows that are intercalated with thin felsic ash beds, a mafic fragmental unit and several, thin massive mafic flows or sills. Felsic lapilli tuff overlies the mafic metavolcanic sequence, which is, in turn, overlain by a sulphidic, iron carbonatized, mafic fragmental unit. The base of the south ore zone appears to comprise a pyritic, cherty exhalite with stringer and colloform pyrite in a black, siliceous matrix. The south ore zone is overlain by bleached and altered pillowed mafic flows. These are in turn overlain by a spherulitic flow banded rhyolite and lapilli tuff or flow breccia unit. All felsic units are sodium-depleted, iron-carbonatized, and strongly foliated. A sulphide clast-bearing, iron-carbonatized, mafic fragmental unit overlies the felsic metavolcanic rocks and forms an extension along strike to the north ore zone. These rocks are capped by massive mafic flows, which have relatively little alteration.

The orebody consisted of three strata-bound sulphide lenses: the south, central and north zones. From observations made during underground mining, hangingwall rocks were usually barren, but footwall rocks were pyritic and locally contained sufficient chalcopyrite to be mined. Zoning was recognized within individual orebodies, which were copper-rich near their stratigraphic bases and more zinc-rich near their tops. Footwall rocks have been altered to sericite and chlorite.

The Canadian Jamieson mine operated from 1966 to 1971, producing 816 000 tons (740 000 tonnes) of ore averaging 2.4% Cu and 4.2% Zn (Northern Miner Handbooks, 1965–74).

Genex Mine

The Genex Mine is located in central Godfrey Township (Figure 28, and *see* No. 4 in Figure 4). The mine is located near a contact between KVC felsic breccia and mafic units composed of massive and pillowed mafic metavolcanic rocks and mafic sills. The stratigraphy here is near-vertical and faces to the east. Legault (1985) studied the geology and alteration associated with the Genex deposit. He compiled the results of surface geological mapping with mine plans from Genex Mines Limited (Figures 29, 30 and 31). The following description is based largely on the work of Middleton (1975) and Legault (1985):

> Four synvolcanic felsic intrusions are present on the Genex property. They have a general east-trend, perpendicular to stratigraphy, and range in apparent thickness from 40 m to 150 m. They may represent synvolcanic rhyolite flow domes. They taper to the east, and may be gradational with larger granophyric felsic intrusive masses to the west. The synvolcanic felsic intrusions are physically and texturally similar to nearby massive felsic metavolcanic rocks: both have spherulitic and flow-banded margins, quartz and feldspar phenocrysts, local brecciated areas with flow

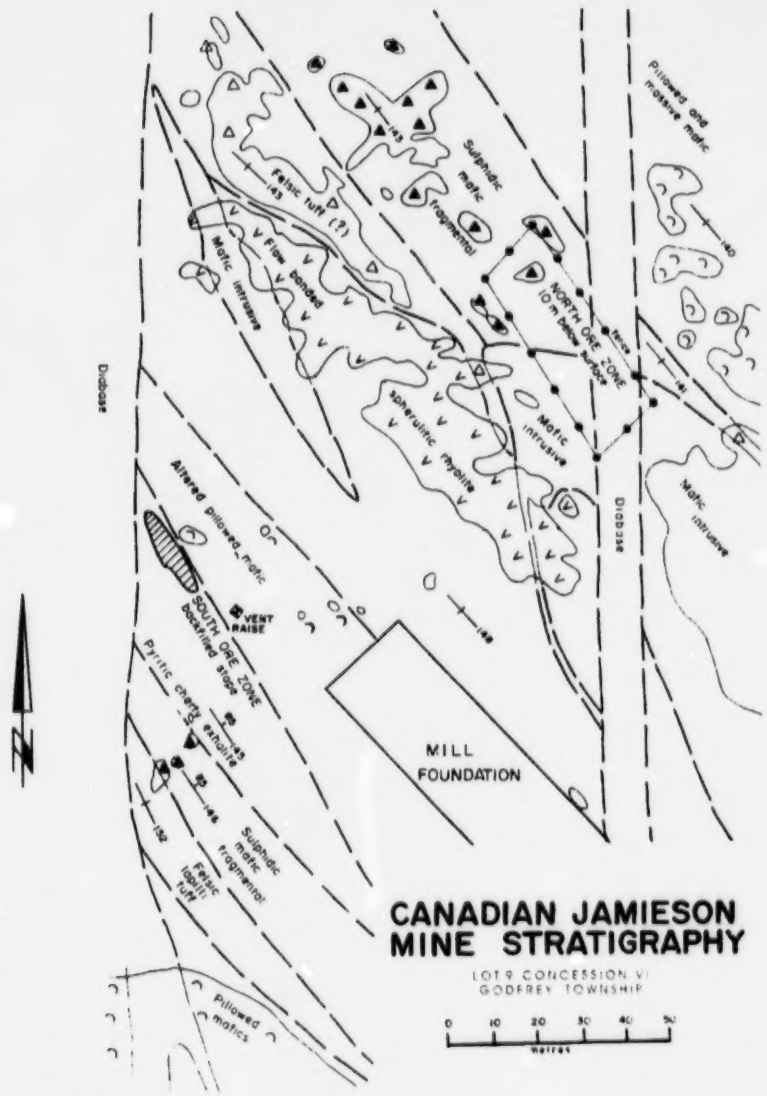

Figure 27. Geology of the Canadian Jamieson Mine property (*modified after* Comba et al. 1986).

banded clasts, and xenoliths of mafic metavolcanic material. Three of the four synvolcanic masses are strongly altered and mineralized, and one was the host rock for some of the "H" stringer ore zone (described below). Large sill-like mafic bodies are found stratigraphically below and above the Genex deposit [*see* Figure 29]. These rocks are possible feeder dikes in the area. Some of these intrusions apparently truncate patterns of alteration and mineralization that cross stratigraphy, but the intrusions are not visibly altered or mineralized.

The deposit is divided into several zones, with the A, C, and H zones comprising the most economic parts of the deposit [*see* Figures 29, 30, 31]. The A and H zones represent copper-rich, quartz stockwork stringer mineralization. They have a strike that crosses stratigraphy, and are situated within in felsic metavolcanic breccia and massive to pillowed mafic metavolcanic rocks. The C zone is conformable, and is located at a contact between a mafic pillow breccia and a massive mafic intrusion.

Production at Genex was minor, with approximately 120 000 tons (109 000 tonnes) of ore at 2.2% Cu recovered (Middleton 1975). Diamond drilling and underground exploration indicated reserves of 133 000 tons (121 000 tonnes) with an average grade of 2.2% Cu, with resources at 385 000 tons (349 000 tonnes) of 1.7% Cu by one estimate (Middleton 1975).

MESOTHERMAL GOLD DEPOSITS

Holmer Property

The Holmer gold property is located in southwest Bristol Township (Figure 32, and *see* No. 6 in Figure 4), within highly deformed rocks of the DPFZ, at a contact between mafic metavolcanic rocks of the Lower volcanic suite, and metasedimentary rocks. The Bristol Township lamprophyre suite occurs on the mine property, 50 m southeast of the main shaft, away from the gold mineralization (*see* "Geochemistry" for description, and sample 89-5 in Table 8 for geochemical analysis).

The rocks on the property are variably deformed. Primary volcanic and sedimentary textures are observed in less-deformed rocks in several locations. Hyaloclastite textures are preserved 25 m southwest of the main shaft. Graded layering, with coarse sand-sized to silt-sized grains are present in turbiditic metagreywacke 60 m northeast of the main shaft. Facing directions are difficult to determine in the metagreywacke because of chlorite alteration concentrated along fractures that parallel bedding. One bed, in which coarse to fine gradation is observed, strikes 105°, dips 80°S and faces to the south. Elsewhere, the rocks are moderately to highly deformed. The most intense de-

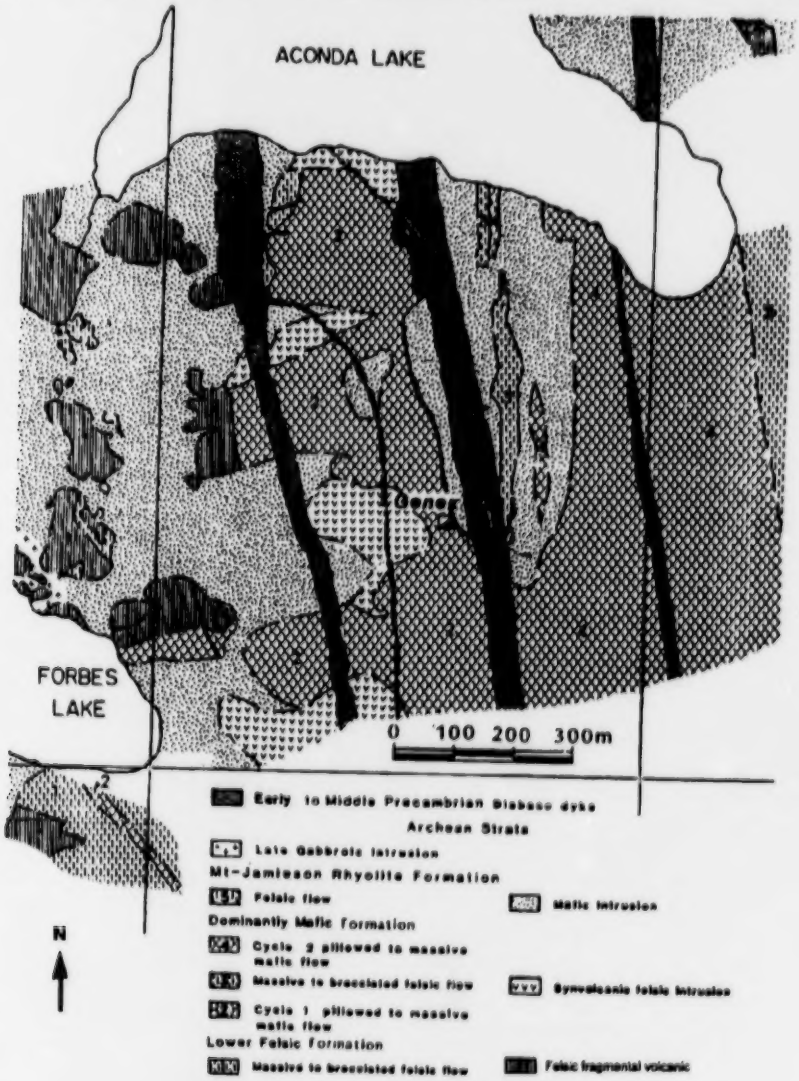

Figure 28. Geology of the Genex Mine area (*modified after* Legault 1985).

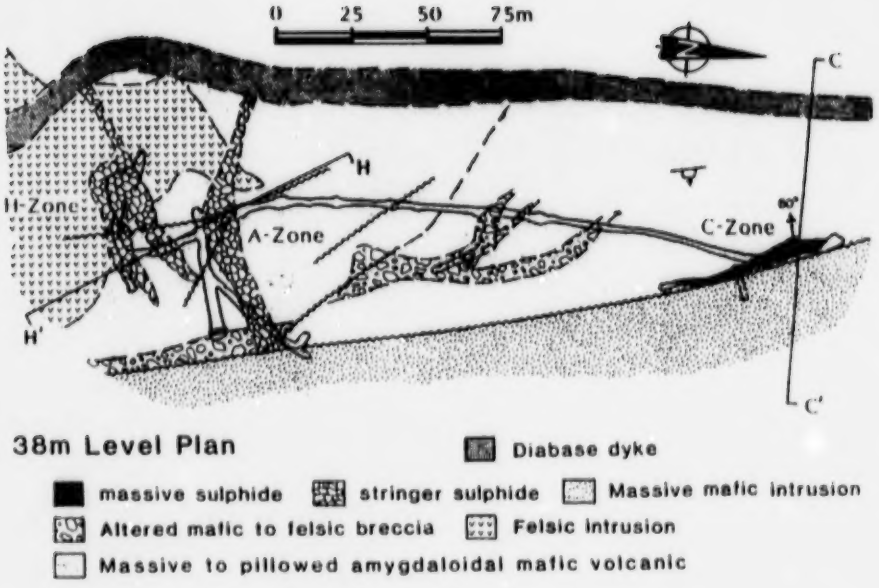

Figure 29. Geology of the Genex Mine, 38 m level (*modified after* Legault 1985).

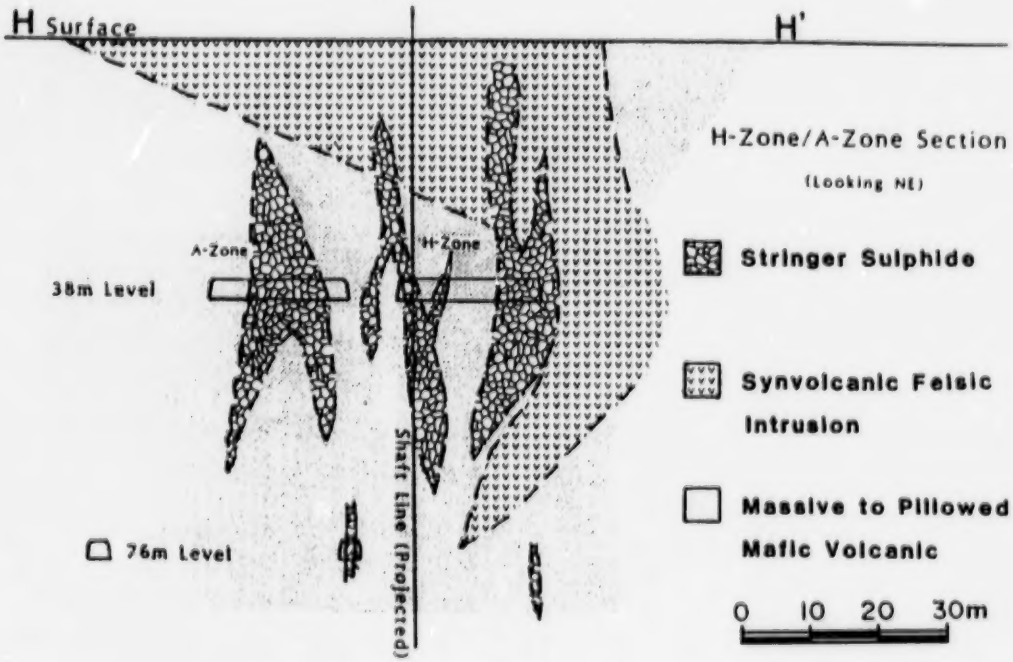

Figure 30. Cross-section of the H and A zones, Genex Mine, looking northeast (*modified after* Legault 1985).

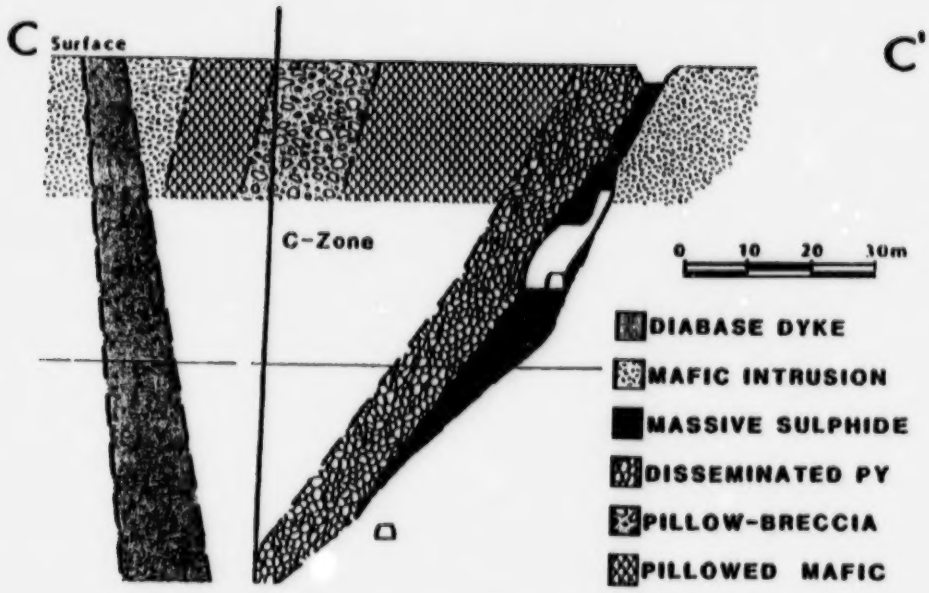

Figure 31. Cross-section of the C zone, Genex Mine, view looking north (*modified after* Legault 1985).

formation is located in the nose of a west-plunging fold hinge, manifested as rods or pencils (L>>S) of carbonatized metasedimentary rock, 25 m northeast of the main shaft.

Mineralization is found in quartz + tourmaline + sulphide (pyrite, chalcopyrite, and minor arsenopyrite, galena and sphalerite) veins and the enveloping tourmalinitized, carbonatized and locally silicified metasedimentary and metavolcanic wallrocks.

The property has been investigated intermittently since 1911, with no known production. Recent estimates of probable reserves range from 720,000 tons (650 000 tonnes) at 0.124 ounces (3.85 g) of gold per ton to 865 000 tons (785 000 tonnes) at 0.08 ounces (2.5 g) of gold per ton (Canadian Mines Handbook, 1987–88; S. Fumerton, Chevron Resources Limited, personal communication, 1989).

Gold-REE Occurrence: The Croxall Property

The Croxall gold-REE property (also known as the Rusk property) is located 1.5 km to the southwest of the Holmer property (Figure 33, and *see* No. 9 in Figure 4). The main showing has excellent exposures of the Bristol Township lamprophyre suite along three trenches and adjacent outcrops (*see* "Geology" and "Geochemistry" for detailed descriptions of the lamprophyre suite, and Table 8 for geochemical analyses). Lower volcanic suite metabasalts are present on the northwestern part of the main showing, and continue to the west for several kilometres. Excellent exposures of hyaloclastic metabasalts are located 0.7 km to the west of the main showing. Metasedimentary rocks are present to the east, and a granite porphyry stock is located to the south-southeast (Ferguson 1957a).

Several of the Bristol Township lamprophyre suite samples are highly enriched in the REE and Zr (*see* Table 8). Sample 88-5, an altered garnetite dike, contains of 0.43 weight % total rare earth elements (REE_t), and 3070 ppm Zr. Preliminary microprobe work by D. Wark (Rensellaer Polytechnical Institute, Troy, New York) indicates that the majority of the REE in garnetite rocks are located in fluorine-rich apatites and epidotes, which have up to 9 and 13 weight % REE_t, respectively. In general the melanite garnets have relatively low REE, with up to 0.15 weight % Sm_2O_3 (only measurable REE), and they average approximately 3000 ppm Zr. These rocks are possibly the most REE-enriched rocks of Archean age in the entire Superior Province.

The property has been worked as a gold prospect intermittently since 1941, including trenching, numerous blast pits, and 39 diamond drill holes. Gold mineralization occurs in two areas. One area is a minor, stockwork quartz-sulphide vein network, within the north-northeast part of a granite porphyry on the property (J.C. Pederson, Highwood Resources, unpublished report). The second gold occurrence is the main showing, where hand samples up to 0.18 ounces (5.5 g) of gold per ton have been reported from quartz-carbonate-sulphide veins (LeBaron 1985).

De Santis Property

The De Santis property is located in southwest Turnbull Township (Figure 34, and *see* No. 7 in Figure 4). The property lies entirely within the granitoid A region, and both KGC gabbros and quartz-feldspar porphyry (granitoid A) are exposed. A north-trending Matachewan dike cuts the gabbro and quartz-feldspar porphyry. The dike is parallel

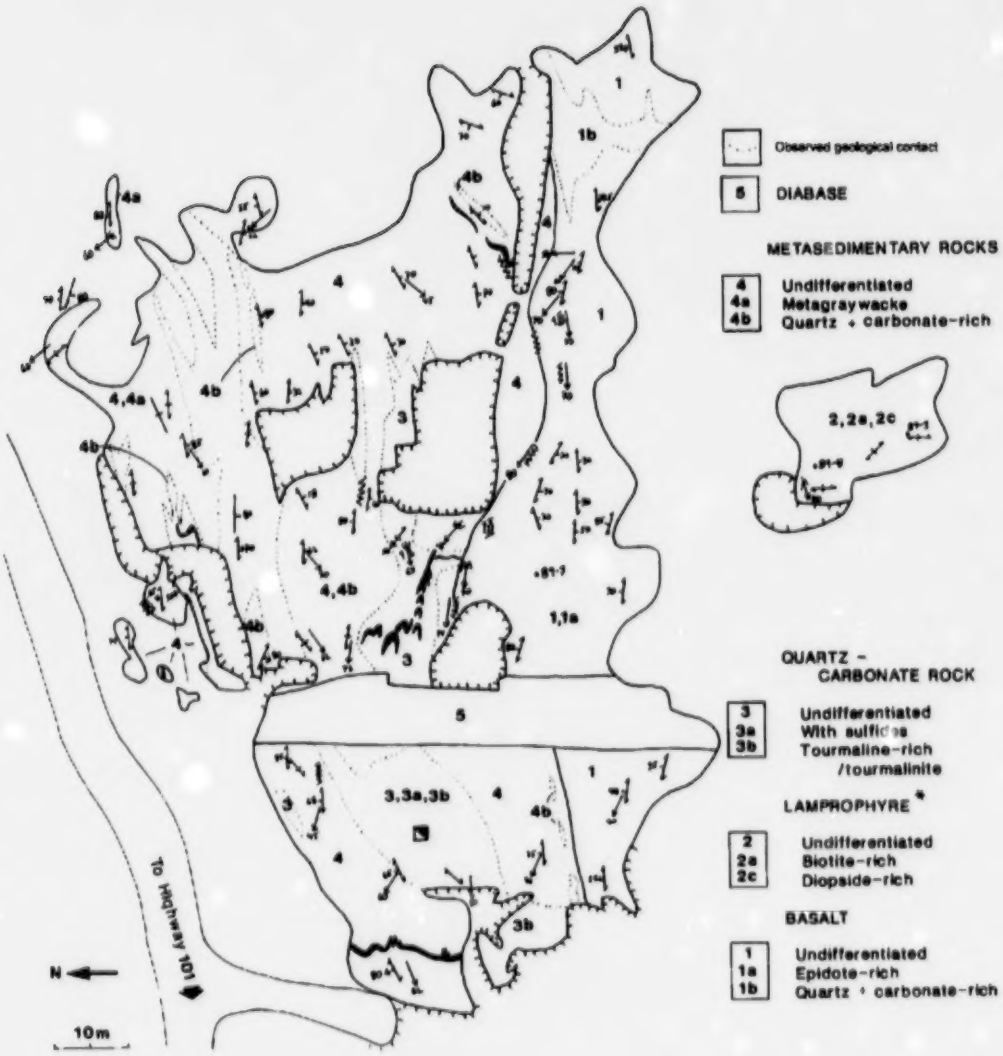

Figure 32. Geology of the Holmer gold property main outcrops. Quartz veins marked in black.

and adjacent to the main quartz vein, which is up to 1.5 m in width at the surface, and also cuts the gabbro and quartz-feldspar porphyry. The vein is generally barren of sulphide, but may contain up to 1.5 % sulphides (pyrite, chalcopyrite) locally. The gabbro and quartz-feldspar are locally deformed, with a well-develcped flattening fabric parallel to the margins of vein, near the shaft. Mineral lineations (alignment of actinolite-chlorite) on altered gabbro surfaces are nearly horizontal, plunging 10° to the north. It is noted that the vein attitude, along the trend of the adjacent Matachewan dike, is unusual: there are few quartz veins having this orientation and with gold mineralization in the entire Porcupine District. (The Lally gold property, located in east-central Turnbull Township, within the eastern margin of the granitoid A region, is parallel to a north-trending Matachewan dike also: Middleton 1975.) Considering the structural history of the Kamiskotia area, the vein may occupy a dilational fracture that formed during a north-south compressional regime, the same stress regime that was responsible for the predominant east-west fabric through the KVC and the granitoid A region at approximately 2700 to 2685 Ma (*see* Figures 6, 7; *see* "Structural Geology").

The property was discovered in 1920 by Mr. P. De Santis. In 1923–24, De Santis recovered a total of 2.8 tonnes of hand-picked ore, with an average grade of 250 g/t (Middleton 1975). The property has a shaft and several hundred metres of underground workings. There has been no production since 1924.

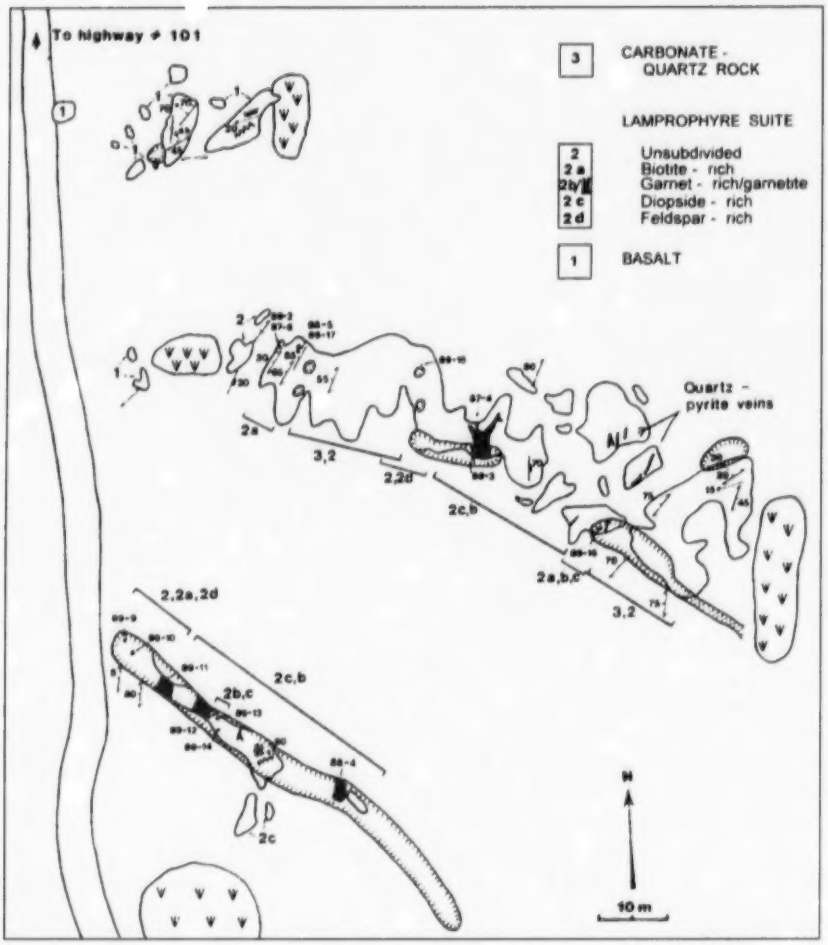

Figure 33. Geology of the Croxall gold-REE property, with sample locations.

MAGMATIC NICKEL-COPPER OCCURRENCES

Several nickel-copper (and very low PGE) sulphide occurrences are located within the more magnesian cumulates of the KGC. The three most significant are termed the northwest Carscallen occurrences, Bean Lake–Pirsson Lake occurrences, West Whitesides Township occurrences, and correspond to numbers 10, 11 and 12, respectively, in Figure 4. Samples from these localities have been analyzed for Ni, Cu, Co, and in some cases S, Pt, Pd, Au, and the remaining platinum group elements: Os, Ir, Ru, and Rh. These data are reported in Table 9.

West Whitesides Township Occurrences

In central west Whitesides Township, 500 m west of the Kamiskotia River, eight trenches and numerous drill holes have outlined sulphidic pods with low grade copper-nickel mineralization. The mineral occurrences are generally aligned parallel to the cumulate banding in the host rocks, with trenches oriented east-west, parallel to a weakly developed, non-penetrative structural fabric. A standard magmatic mineral assemblage of pyrrhotite, chalcopyrite, pentlandite and magnetite occur interstitial to silicate minerals in a net texture, and also injected into the host rock along jointing or fault planes locally. Graham (1931) reported 0.6 weight % Ni, in a pyrrhotite-rich grab sample from this area. Samples 86-321 to 86-329 (*see* Table 9) are considered representative of the mineralization in the trenches at surface; they do not contain any appreciable base or precious metal values.

Bean Lake–Pirsson Lake Occurrences

Two low grade magmatic sulphide occurrences are present in central Whitesides Township: one 0.5 km west of Bean Lake, and another 0.5 km west of Pirsson Lake. The Bean Lake occurrence was visited for this study. Extensive stripping in 1955 exposed iron formation, in contact with the base of the KGC. Sulphide mineralization occurs in

both the iron formation, and in the gabbro, 50 m to the north. Previous sampling of outcrop and drill core in this area determined very low Cu, Ni and Au abundances in net-textured and semi-massive sulphide (Wolfe 1970), although silver assays up to 3.3 ounces. (100 g) per tonne have been reported (Leahy 1968). Low base and precious metal values are found in one surface grab sample in this study (e.g., sample 86-27: *see* Table 9).

Northwest Carscallen Township Occurrences

Magmatic sulphide mineralization is found in northwest Carscallen Township and northeast Whitesides Township, located immediately south of the prominent (stands in high relief) peridotite outcrop in the area. Here net-textured chalcopyrite and pyrrhotite are present within altered olivine gabbro. Twelve diamond drill holes encountered disseminated sulphides with low Cu and Ni values (Wolfe 1970). Samples 84-14a and 84-175 are typical of the net-textured sulphide material; they have very low Ni, Cu and PGE contents (*see* Table 9).

POTENTIAL FOR MINERALIZATION

In this section, the potential for the discovery of volcanogenic copper-zinc deposits, mesothermal gold deposits, REE deposits and magmatic copper-nickel-PGE deposits is discussed. Additionally, lithogeochemical exploration strategies for each of these deposit types are outlined briefly.

Volcanogenic Copper-Zinc Deposits

The potential for the discovery of volcanogenic copper-zinc deposits in the Kamiskotia area is considered high. The four deposits of the Kamiskotia copper-zinc camp are located within the KVC, within a stratigraphic sequence less than 2 km thick, of mixed mafic and felsic metavolcanic rocks. Incompatible element-enriched basalts, basaltic andesites and andesites are present in close proximity to the massive sulphide lenses, forming footwall and hanging wall flows and sills; relatively fresh andesite dikes and sills cut the lenses at the Kam-Kotia mine (Pyke and Middleton 1970). These incompatible element-enriched mafic rocks have been shown to be the product of high degrees of fractional crystallization in a tholeiitic system, with the residual cumulus phases represented in the KGC to the south. High silica rhyolites in the KVC may be the product of more advanced fractionation. The cooling postulated to occur in high level magma chambers has been modeled quantitatively by Cathles et al. (1983), who demonstrated that this mechanism is adequate to drive base metal-precipitating, hydrothermal convection through overlying volcanic strata.

Exploration for volcanogenic base metal deposits should focus on the KVC, particularly where the stratigraphy is composed of mixed, coeval, incompatible element-enriched mafic and felsic metavolcanic rocks. These areas should be characterized by evidence for synvolcanic faulting, and mineralogical (chlorite, sericite, pyrite addition) and chemical modifications (e.g., proximal sodium depletion, magnesium and iron enrichment) typical of low-CO_2 (e.g., carbonate and chloritoid not significant in Kamiskotia camp), volcanogenic massive sulphide-precipitating hydrothermal systems.

Mesothermal Gold Deposits

The potential for mesothermal gold deposits is considered moderate. Efforts to locate mesothermal gold mineralization in the Kamiskotia area should focus on late-tectonic structures: along the DPFZ and south of granitoid D in Bristol and Denton townships; along the splay of the DPFZ through the Lower volcanic suite in southern Carscallen and Whitesides townships; or along the Kamiskotia highway fault, in north Godfrey and southern Jamieson townships. The vast majority of gold mineralization in the southern Abitibi Subprovince is found along late-tectonic deformation zones (e.g., Colvine et al. 1988). North-trending vein systems, such as at the De Santis and Lally properties, are considered less prospective. They are interpreted to have developed during regional north-south compression, prior to the late tectonic events in the Kamiskotia area.

Gold mineralization on the Holmer and Croxall properties, within the DPFZ, is proximal to the incompatible element-enriched, Bristol Township lamprophyre suite. In this respect, the mineralization is similar to gold mineralization associated with rocks enriched in LREE and P_2O_5 in Taylor Township, and elsewhere along the DPFZ and Kirkland–Larder fault zone to the south (King and Kerrich 1987). The gold-bearing quartz-tourmaline veins cut the lamprophyre suite on the Croxall property, and are believed to be genetically distinct from the lamprophyre suite. Both gold mineralization and LREE enrichment are believed to be produced during similar, regional tectonic processes, such as late transpression and crustal underplating by mafic magmas, that affected the crust and upper mantle in this region (discussed further below).

The potential for economic REE concentrations in the Bristol Township lamprophyre suite is considered low to moderate, considering 1) its high REE concentrations, of up to 0.43 weight % REE_t; 2) that the REE are principally in apatite, which is easily dissolved in HCl; and 3) the size of the lamprophyre suite, interpreted from ground and air magnetic surveys to extend for several kilometres. However, it is difficult to envisage competing with current REE producers, such as deposits with bastnaesite ($(Ce,La)CO_3(F,OH)$) as the primary REE mineral. The carbonatite at Mountain Pass, California is an example of a primary bastnaesite producer. The Mountain Pass deposit has approximately 31 million tonnes of ore, and contains, on average, approximately 12% bastnaesite (containing 74

weight % REE_t), or an average grade of 8.9 weight % REE_t (O'Driscoll 1988).

Magmatic Nickel-Copper-PGE Deposits

The potential for magmatic nickel-copper-PGE deposits in the KGC is considered low. All sulphide occurrences in the Lower Zone contain very low copper, nickel and PGE contents. Primary modal layering, an indictor of magma chamber processes that are favorable to reef-type PGE mineralization (e.g., establishment of stable convection within the magma chamber), is only poorly developed in the KGC. There are no known, stratiform horizons of pegmatitic-textured gabbros in the KGC, such as those found in the Bushveld and Stillwater Complexes. A reconnaissance program (52 samples), designed to test the potential for PGE mineralization in pegmatitic gabbros of any type, did not detect any significant enrichment in Pt, Pd or Au (Barrie, unpublished data).

The low Ni, Cu and PGE contents are interpreted to be the result of limited and passive contamination of KGC mafic liquids by footwall rocks. This is consistent with the fractionation-dominated, geochemical trends in the KGC–KVC system (*see* "Geochemistry"). Assimilation of siliceous, iron-rich or sulphur-rich rocks by mafic-ultramafic magmas causes sulphide immiscibility, and Ni, Cu and the PGE partition strongly into the resulting immiscible sulphide liquid. Under turbulent flow conditions in the magma chamber, the sulphide liquid can scavenge greater quantities in the siderophile elements and become increasingly enriched in them (e.g., Naldrett 1981).

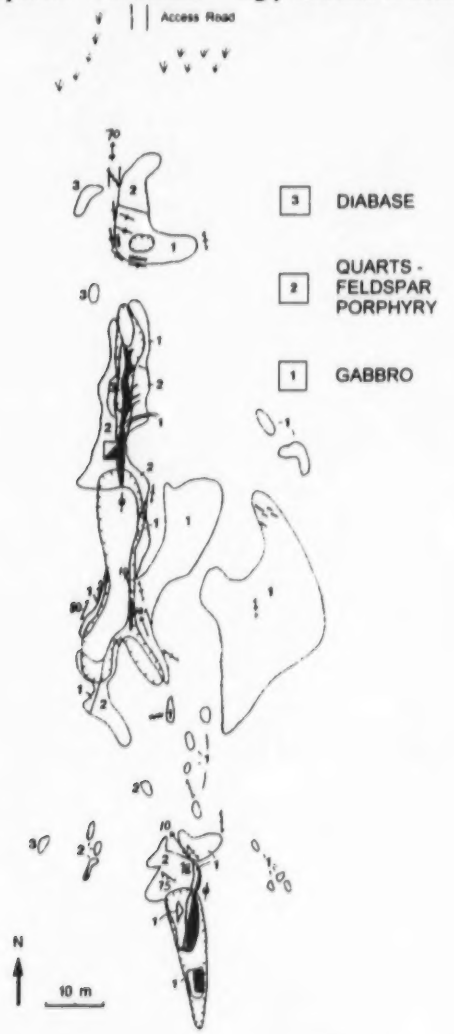

Figure 34. Geology of the De Santis gold property outcrops. Quartz vein marked in black.

Table 9. S, Ni, Cu, PGE, Au and REE abundances for KGC sulphide occurrences.

Sample No.	84-2a	84-2b	84-2c	84-2f	84-14a	84-63c	84-135	84-175	86-27	86-27a	86-27b	86-321	86-322	86-324	86-326	86-327	86-328	86-329
S (wt %)				12.9	2.04	14.1	1.53	22.0	1.32	17.1	15.1	3.52	2.87	6.56	8.03	1.75	7.10	3.69
Trace Elements (ppm)																		
Ni				3500	3200	91	240	180	130	1300	1200	1000	910	2600	3700	850	3300	830
Cu				2000	2000	2700	280	180	33	1200	580	6300	2200	20000	12000	910	7000	2500
ppb																		
Os	<3	3	3	0.7	<3	<3	<3	<3										
Ir	0.3	2.6	3.6	<0.3	0.6	0.1	0.1	0.1										
Ru	5	<5	10	<5	<5	<5	<5	<5										
Rh	1	4	6	2	2	1	2	1										
Pt	25	45	15	14	76	<5	5	<5										
Pd	5	5	5	<5	55	<5	<5	<5										
Au	51	44	12	5														
Re	<5	<5	15	5	<5	<5	<5	<5										

Analyses by X-Ray Assay Laboratories, Toronto: S, Ni and Cu by XRF; PGE, Au and Re by neutron activation using Ni-bead preconcentration (*see* Hoffman et al. 1979).

84-2: Occurrence in NW Whitesides Township.
84-14: NW Carscallen Township occurrence (No. 10 in Figure 4).
84-63: Occurrence in NE Enid Township.
84-135: Occurrence in Western Carscallen Township, adjacent to partially assimilated iron formation.
84-175: Whitesides Bean Lake occurrence (No. 11 in Figure 4).
84-171a: NW Carscallen Township occurrence (No. 10 in Figure 4).
86-27: Whitesides Bean Lake occurrence (No. 11 in Figure 4).
86-321 to 329: Western Whitesides Township occurrences (No. 12 in Figure 4).

Discussion

GABBROIC COMPLEX-GRANITOID RELATIONSHIPS IN THE SOUTHERN SUPERIOR PROVINCE

One of the notable features in the Kamiskotia area is the close temporal relationship between voluminous tholeiitic magmatism followed by calc-alkaline magmatism. This phenomenon has been documented by geological and/or geochronological studies across the southern Superior Province: at the Bird River Sill, Manitoba (Trueman and Bannatyne 1982); the Bad Vermilion Complex, Ontario (Ashwal et al. 1985); the Mulcahy Lake and related gabbroic intrusions, Ontario (Morrison et al. 1985); the Sturgeon Lake gabbro, Ontario (Davis and Trowell 1982); Lac des Iles and related intrusions, Ontario (Sutcliffe et al. 1989); the Montcalm Gabbroic Complex, Ontario (Barrie and Naldrett 1989); the Bell River Complex, Quebec (Sharpe 1968); and the Doré Lake Anorthosite, Quebec (Dimroth et al. 1986). It would appear that these relationships are widespread, and the process of nearly coeval, voluminous mafic and felsic magma generation is integral to the development of granitoid-greenstone terranes in the Superior Province.

For the Kakagi Lake–Savant Lake volcanic belt (KSVB) and the Wabigoon diapiric axis in northwestern Ontario, Morrison et al. (1985) proposed that partial melting of a slightly depleted mantle produced tholeiitic magmas, parental to supracrustal gabbroic intrusions, and concurrent partial melting of overlying, young oceanic crust produced calc-alkaline magmas, parental to major granitoid complexes. Both melting events were in response to the same thermal event. They considered a migrating mantle plume as the most plausible heat source. In contrast, Davis et al. (1988) suggested that tholeiitic metavolcanic rocks of the lower KSVB evolved, for the most part, in an ensimatic, oceanic environment, in the absence of older sialic material. They postulated that late calc-alkaline magmatism is the product of an arc-like tectonic setting, related to partial melting above a southward-subducting oceanic slab.

In the Kamiskotia area, trace element studies indicate that KGC parental magmas are compatible with a 34% bulk partial melt of a primitive mantle, whereas granitoid rocks may be derived from partial melting of either a hydrated basaltic eclogite or reasonable lower crustal compositions (Barrie 1990). Older sialic crust was at least partly involved in the calc-alkaline magmatism that produced the regional granitoid complexes. For example, granitoid B has one zircon population that shows inheritance from a crustal component at least 2926 million years old. Further evidence is provided by Sm-Nd isotopic systematics for Kamiskotia area rocks. Low, enriched $\varepsilon_{Nd(t)}$ values of +1.0 to -0.4 have been determined for two less than 2700 million-year-old granitoids and a 2702 million-year-old ferroan gabbro sample in the region, implying the presence of an enriched, older crustal reservoir (Barrie 1990). Elsewhere in the southern Abitibi Subprovince, isotopic studies have provided indirect evidence for a sialic basement. For example, a model 3.0 billion-year-old crustal reservoir has been proposed for late granitoids in the eastern Abitibi Subprovince, based on $^{207}Pb/^{206}Pb$ isotope systematics (Gariepy and Allegre 1985).

CHEMICAL COMPARISON OF THE KGC WITH OTHER SYNVOLCANIC INTRUSIONS OF THE SOUTHERN SUPERIOR PROVINCE

The KGC is one of several large, Neoarchean mafic intrusions that underlie massive sulphide-bearing, bimodal volcanic centres in the southern Superior Province, including the Bad Vermilion, Bell River and Doré Lake complexes. At the Bad Vermilion Complex, the majority of gabbros have flat REE patterns at 2 to 10 times chondrites and positive Eu anomalies, nearly identical to the MZ and lower UZ cumulates (Ashwal et al. 1985). The complex intrudes into, and is overlain by, basalts similar to the Kamiskotia basalts that exhibit similar fractionation trends, and by felsic metavolcanic rocks similar to the distinctive, trace element-enriched Kamiskotia rhyolites (Hart 1984). The complex and related metavolcanic rocks have $\varepsilon_{Nd(t)} = +2.0 \pm 1.4$ (Ashwal et al. 1985), similar to but slightly less depleted than the KGC Nd isotopic signature. Rocks of this region of the Superior Province are generally slightly isotopically enriched with respect to the Abitibi–Wawa Subprovinces (Shirey and Carlson 1988; Barrie and Shirey 1989). Detailed trace element and isotope geochemistry is lacking for the Bell River and Doré Lake complexes. However, by virtue of similar geologic settings and similar geochemistry of overlying bimodal metavolcanic rocks (MacGeehan and MacLean 1980; Ludden et al. 1984), it is probable that they, as is the case for the Bad Vermilion Complex, have petrogenetic histories similar to the KGC.

COMPARISON WITH THE SKAERGAARD INTRUSION AND EASTERN ICELAND VOLCANIC FIELDS

Perhaps the closest modern analogs for the KGC and associated basalts are found in rift-related, tholeiitic magmatism represented by the Skaergaard Intrusion, East Greenland and the bimodal volcanic fields of Eastern Iceland. The petrology and geochemistry of the KGCs MZ and UZ resembles that of the Lower Zone and Middle Zone at Skaergaard, which is renowned for its classic tholeiitic iron-enrichment trend (Wager and Brown 1968). Estimates of the liquid compositions based on mass balance calculations (Wager and Brown 1968; Hunter and Sparks 1987) and nearby dike compositions (Brooks and Nielson

1978) indicate that the Skaergaard magma probably remained below 50% SiO_2 until magnetite precipitation, at the top of the Lower Zone. Silica behaves in a similar manner in the Kamiskotia system. Hunter and Sparks (1987) believed that as the Skaergaard magma continued to fractionate, it produced iron- (and titanium- and P_2O_5-) rich andesitic liquids, parental to the apatite-bearing Upper Zone, and finally rhyolitic liquids, parental to the Sandwich Zone horizon. The major element trends of their model liquids are similar to the Kamiskotia basalt-evolved basalt-andesite-rhyolite trends (Hart 1984; Barrie 1990).

Hunter and Sparks (1987) noted the similarities in major element chemistry between their Skaergaard model liquids and several of the bimodal volcanic fields of Eastern Iceland. They proposed that Iceland volcanic suites were the products of similar, fractionation-dominated systems. The basalt-ferrobasalt-icelandite-rhyolite suite of the Askja 1875 eruption, believed to reflect a fractionation-dominated system (MacDonald et al. 1987), has major and trace element characteristics similar to the Kamiskotia volcanic suite (Hart 1984). Sigurdsson and Sparks (1981) and MacDonald et al. (1987) envisioned a dynamic, compositionally stratified magma chamber beneath the Askja volcanic field. They postulated that prior to the eruption, a ferrobasaltic liquid, which represents 60 to 70% fractionation of parental, magnesian basaltic liquid, was present at the floor of the chamber, progressively overlain by andesitic to rhyolitic liquids. If such a chamber ceased to erupt and crystallized *in situ*, this could represent the KGC's UZ and granophyric cap of intermediate to felsic composition.

The compositions of basalts, iron-titanium basalts and rhyodacites at the 85°W propagating ridge of the Galapagos Spreading Center, are also similar to the Kamiskotia suite. The rocks at 85°W are too far from the Galapagos hot spot to reflect mantle plume characteristics, so their petrology and geochemistry are believed to reflect a variation of mid-ocean ridge magma chamber processes (Schilling et al. 1976; Verma et al. 1983). Mineral compositions closely resemble the compositions in the KGC, and glass compositions follow fractionation trends similar to the Kamiskotia basalts (Byerly 1980; Juster et al. 1989). These fractionation trends have been duplicated in experiments on iron-titanium basalts at one-atmosphere, but under more oxidizing conditions (Ni-NiO buffer) than would be expected by a closed system, implying an interaction with oxidizing surroundings (Juster et al. 1989). At Kamiskotia, fractionation occurred at shallow levels, and may have been influenced by extensive, and potentially oxidizing hydrothermal fluids that formed the contemporaneous volcanogenic Cu-Zn deposits (Barrie and Davis 1990).

COGENESIS OF THE KGC AND KVC AND SIGNIFICANCE WITH RESPECT TO THE FORMATION OF VMS DEPOSITS

That the KGC and the Kamiskotia rhyolite are coeval within geochronological error strengthens geochemical arguments for their cogenetic relationship. The Kamiskotia felsic metavolcanic rocks and the underlying KGC granophyric cap have nearly identical rare earth element abundances, which implies that the rhyolites are eruptive equivalents of the granophyre (Campbell et al. 1981). Both have distinctive high, flat chondrite-normalized patterns with strong negative Eu anomalies, consistent with low pressure fractionation of mafic phases and plagioclase. The rhyolites have been termed "tholeiitic" rhyolites by Campbell et al. (1982), or "Type IIIb" rhyolites by Lesher et al. (1986). Kamiskotia basalts were successfully modeled as fractionation products of a primitive MORB-like basalt, with the residual phases represented in the KGC (Hart 1984). Samarium-neodymium isotope systematics are also compatible with the cogenesis of the KGC and KVC: a seven-point, KGC-KVC whole rock and mineral isochron has an age of 2730±30 Ma, in agreement with the U-Pb age, and all samples have identical $\varepsilon_{Nd(t)}$ values within error (Barrie 1990).

The presence of metavolcanic-hosted massive sulphide deposits within a 2 km thick stratigraphic level in the KVC is consistent with the coeval nature of the KGC and KVC. During crystallization and cooling, the KGC was capable of providing the heat necessary to drive hydrothermal convection cells that would leach metals from a volcanic pile and precipitate them onto the paleoseafloor, given geologically reasonable permeability and temperature constraints (Cathles et al. 1983). Hypabyssal gabbroic intrusions that underlie massive sulphide-bearing "tholeiitic" rhyolites are present elsewhere in the southern Superior Province, namely, 1) the Bad Vermilion Complex overlain by the Gagne Lake deposits, Ontario (Poulsen 1984), 2) the Bell River Complex and Matagami Lake district (MacGeehan and MacLean 1980), 3) numerous gabbro sills in the Noranda district, and 4) the Doré Lake anorthosite overlain by the Patino-Lamoine mine and other deposits (Guha et al. 1988). It seems likely that in these areas, as in the Kamiskotia area, the gabbroic intrusions are synvolcanic, and they provided the heat necessary for massive sulphide-precipitating hydrothermal systems.

KAMISKOTIA–KIDD CREEK RELATIONSHIPS

Pyke (1978, 1982) tentatively correlated the Kidd Creek rhyolite with Kamiskotia rhyolites. He noted their similar geochemistry, the presence of massive sulphide mineralization and their general stratigraphic position below the metasedimentary rocks of the Tisdale Group in the Timmins area, and assigned them to the Upper Deloro Group. In the MERQ–OGS (1983) lithostratigraphic map of the Abitibi Subprovince, both metavolcanic piles are placed at the top of the Cycle III Volcanics, one of four cyclic metavolcanic packages tentatively correlated across the Abitibi Subprovince.

The U-Pb ages reported in Barrie and Davis (1990) here indicate that modification is necessary for the correlations of metavolcanic rocks for the western Abitibi Subprovince. It is apparent that the Kidd Creek and Prosser rhyolites are at least 10 million years older than the KGC, the Kamiskotia rhyolite, and the Reid rhyolite, 11 km to the west-northwest of the Kidd Creek Mine. The Kidd megaagglomeritic flow-banded rhyolite sample and the Kamiskotia flow-banded rhyolite sample both represent proximal volcanic facies and are proximal to mine sites. In contrast, the Prosser and Reid samples are crystal-ash tuffs intercalated with graphitic argillites, typical of distal, subaqueous volcanic facies. They may represent crystal-ash deposits distal to the Kidd and Kamiskotia volcanic centers, respectively. Samples of the more distal deposits have lower zirconium contents (*see* Appendix I) and yielded far fewer zircons. This may reflect crystal sorting during ash fall eruptions, which would be consistent with their distal characteristics, or it may indicate that these eruptions tapped relatively zircon-poor siliceous magmas.

TIME-STRATIGRAPHIC CORRELATION OF VOLCANIC ROCKS IN THE SOUTHERN ABITIBI SUBPROVINCE

Corfu et al. (1989) reported an age for a proximal(?), banded rhyolite from the Stroughton–Roquemaure Group of 2714±2 Ma, and a revised age for a dacitic unit in the Hunter Mine Group to the east of the Ontario–Quebec border of 2713±2 Ma. These samples were taken generally along strike from the Kidd Creek Mine, to the east-southeast 75 km and 110 km, respectively. Thus, there is a consistent decrease in ages over this 110 km trend, from 2717±2 Ma at the minesite to 2713±2 Ma. This may imply that volcanism migrated eastward over a 4 million year period. Furthermore, the geochemistry of the tholeiitic mafic metavolcanic rocks is similar from Kidd Creek to the Hunter Mine Group area (Pyke 1982; Jensen and Pyke 1982), and the distinctive tholeiitic rhyolite geochemistry of the Kidd Creek rhyolite is found farther to the east along strike, in southeast Harker Township (Goodwin, unpublished data). By comparison with the geology and geochemical modeling at Kamiskotia, this would imply that the Kidd Creek–Hunter Mine Group trend may be associated with hypabyssal mafic intrusions that have not been noted in outcrop.

Four U-Pb ages for metavolcanic lithologies and one hypabyssal dunite sill to the east of the Kamiskotia area are coeval to slightly younger than the KGC and Kamiskotia rhyolite, from 2707±1.5 to 2698±4 Ma (Corfu et al. 1989). These include rocks previously included in the Upper Deloro, Tisdale, Skead, Larder Lake and Blake River Groups. The upper Blake River Group metavolcanic rocks are similar to the KVC rocks in several respects: 1) they were deposited during active tectonism, with synvolcanic faulting (Gibson et al. 1989), 2) they are bimodal, 3) the rhyolites have similar, flat REE profiles with negative Eu anomalies (Lesher et al. 1986), 4) they are underlain by a subvolcanic sill, the coeval (both at 2701±2 Ma: Corfu et al. 1989), and cogenetic (Paradis et al. 1988) Flavrian pluton, that has magma mixing textures (Goldie 1978), and 5) they are host to volcanogenic copper-zinc deposits of the Noranda camp. Considering these similarities, the KVC and upper Blake River Group may have erupted in a similar tectonic settings.

LATE TRANSPRESSION ACROSS THE SOUTHERN SUPERIOR PROVINCE

Late north-south compression has been documented by structural and geochronologic studies for areas across the southern and central Superior Province, at major subprovince boundaries (Stott 1985; Corfu and Stott 1986; Stott et al. 1987; Davis et al. 1989) and within greenstone belts (Hubert et al. 1984; Dimroth et al. 1986; Hudleston et al. 1988). The majority of these studies have indicated that transcurrent motion on regional east- or west-northwest-trending shear zones in the Southern Superior Province is dextral. These observations are compatible with a subhorizontal stress regime oriented in a west-northwest sense (Stott et al. 1987). Dextral transcurrent motions along the Quetico–Wawa and Quetico–Wabigoon Subprovince boundaries are tightly bracketed by U-Pb analyses of deformed and undeformed rocks at 2689 to 2684 Ma and 2696 to 2686 Ma, respectively (Corfu and Stott 1986; Davis et al. 1989). The timing and sense of displacement along these subprovince boundaries are virtually identical to that in the Kamiskotia area. The age of the Bristol Township lamprophyre suite is 2687±3 Ma, and is interpreted to have been emplaced after the formation of the DPFZ, but was subsequently deformed within it. Late-stage, predominantly dextral transpression is recorded in the splay of the DPFZ, and interpreted for the Kamiskotia Highway fault in the Kamiskotia area. This implies a synchronous, crustal shortening event across 1200 km of the

southern Superior Province at approximately 2690 to 2685 Ma.

TIMING OF LATE ARCHEAN MAGMATISM IN THE SOUTHERN SUPERIOR PROVINCE

Figure 35 presents a compilation of high precision U-Pb ages for "Kenoran-aged" magmatism in the southern Superior Province, designed to highlight the timing of different rock types. In a sense, this compilation of U-Pb ages supersedes the compilation of Rb-Sr whole rock isochron ages and K-Ar mineral ages used in the original definition of the Kenoran Orogeny, which has a mean age of 2480 Ma (Stockwell et al. 1970). Rb-Sr and K-Ar data most probably reflect cooling histories and/or later thermal events that have effected the southern Superior Province (e.g., Beakhouse et al. 1988; York and Hyodo 1988; Barrie 1990).

All of the divisions are straightforward, with the exception of the division between rocks enriched in LILE and LREE and calc-alkalic intrusive rocks. Rocks enriched in LILE and LREE are represented by alkalic metavolcanic rocks, shoshonitic ("calc-alkalic") lamprophyres, and intermediate to felsic intrusions that are known to have a component of LILE and LREE enrichment and/or alkalic affinity. Several of the intermediate to felsic intrusions are predominantly silica-saturated and have Na_2O+K_2O contents that do not clearly distinguish them as alkalic; however, higher LILE and LREE contents coupled with high Cr, Ni and MgO contents distinguish them from trondhjemite-tonalite or granodiorite-granite series intrusions (e.g., Ottertail Lake pluton, Quetico Subprovince: Shirey and Hanson 1986).

From this compilation, calc-alkalic volcanism appears to have ended abruptly at 2695 to 2700 Ma: the youngest calc-alkalic metavolcanic rocks are found in the southern Abitibi Subprovince (Krist Fragmental tuff: Corfu et al. 1989; upper Blake River Group: Mortensen 1987). From the few U-Pb ages available, tholeiitic and ultramafic magmatism also appear to end at this time. Barrie and Davis (1990) speculated that this may be due to the cessation of the subduction of an oceanic plate at 2695 to 2700 Ma.

The timing of calc-alkalic intrusive activity approximates a Gaussian distribution with a mean (n=58) at 2700 Ma. Gneissic rocks represent amphibolite to granulite grade calc-alkalic intrusions, from the Kapuskasing Structural Zone and related rocks to the southwest. Generally, their ages are younger than 2700 Ma. Corfu (1987) recognized that there may be a progressive younging of the gneisses with depth, and discussed the possibility of magmatic underplating by mantle-derived material (e.g., Bohlen 1987).

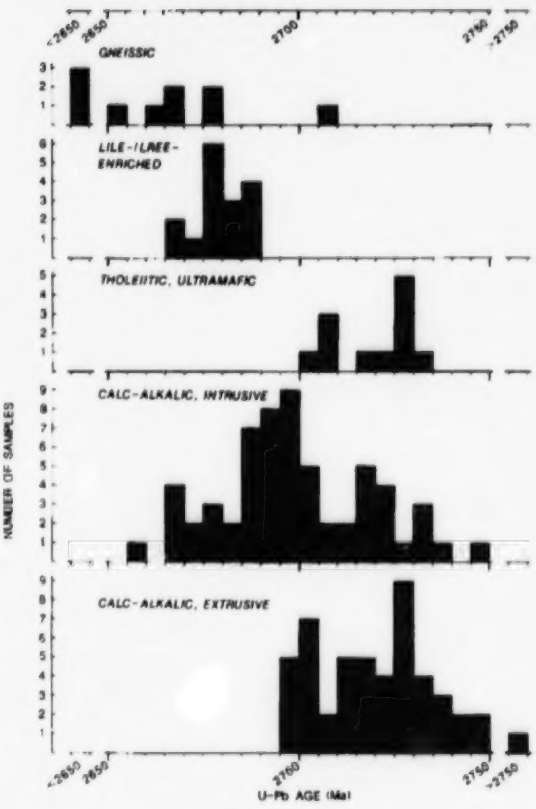

Figure 35. Histogram of high precision, U-Pb ages for the southern Superior Province (excluding well-defined basement terrane older than 2780 Ma, and samples with complex U-Pb data that do not clearly define primary igneous ages). The majority of these ages have 2-sigma errors of ± 2 to 4 Ma. The $^{207}Pb/^{206}Pb$ ages for the detrital sedimentary grains generally have significantly larger errors: *see* references below for details. **Gneissic**: predominantly calc-alkalic intrusive rocks at amphibolite or granulite facies in the Kapuskasing (or related) terrane; **LILE-/LREE-enriched**: intrusive and extrusive rocks, including one alkalic metavolcanic rock, an albitite dike, lamprophyres, and monzodiorite-syenite-granodiorite intrusions with alkalic affinity (e.g., Otto Stock, Kirkland Lake area); **Tholeiitic, Ultramafic**: supracrustal tholeiitic intrusions and related metavolcanic rocks, and one ultramafic dike; **Calc-alkalic, Intrusive**: tonalite-trondhjemite and diorite-granodiorite-granite intrusions, quartz-feldspar porphyries associated with gold mineralization, and sedimentary conglomerate clasts of these compositions; **Calc-alkalic, Extrusive**: rhyolites and dacites; Data *from* Barrie and Davis (1990); Barrie and Shirey (1989), Cattell et al. (1984); Corfu, (1987); Corfu and Grunsky, (1987); Corfu and Stott (1986); Corfu (1993); Davis et al. (1985; 1989); Davis and Edwards (1982, 1986); Davis and Trowell (1982); Frarey and Krogh (1986); Gariepy et al. (1984);Krogh and Turek(1981); Mortensen (1987; and unpublished data); Nunes and Pyke (1981); this study; Turek et al. (1982); and Percival and Krogh (1983).

LATE THERMAL EVENTS IN THE KAMISKOTIA AREA

Thermal events after crystallization have affected rocks in the Kamiskotia area and reset both the Nd and Sr mineral

systematics locally. As mentioned above, a Rb-Sr isochron for the KGC ferroan gabbro whole rock and mineral separates agrees with U-Pb ages for the Hearst–Matachewan dike swarm (Heaman 1989). This ferroan gabbro sample was taken 7 m away from a 6 m thick, vertical Matachewan dike in an area where the dikes are particularly densely spaced at 200 m intervals on average. The Rb-Sr isochron age is interpreted as the age of thermal and/or hydrothermal metamorphism due to the emplacement of the neighboring dike. Delaney (1987) has reviewed heat transfer processes by conduction adjacent to cooling vertical mafic dikes. For cases where the thermal properties of the dike and host rock are identical, such as for Kamiskotia gabbroic rock and diabase dikes, the ambient temperature at 1.2 dike widths would rise approximately 200°C. This would be in addition to the temperature due to the geothermal gradient, and to heating from other Matachewan dikes and sills in the vicinity. The presence of intergranular fluid would allow for slightly more rapid heat transfer in crystalline igneous rocks and would aid Rb and Sr diffusion. Resetting of the K-Ar system in hydrous phases up to 15 m from a 10 m thick dike has been clearly documented (Hanes et al. 1988) and modeled by convection of fluids adjacent to mafic dikes (York and Hyodo 1988). The Sm-Nd system, generally considered more resistant to resetting than the Rb-Sr and K-Ar systems has not been disturbed for this sample. An internal, whole rock-plagioclase-clinopyroxene Sm-Nd regression line for this sample has an age of 2700±30 Ma, in agreement with the KGC–KVC Sm-Nd isochron, and the U-Pb ages for the KGC and KVC rhyolite.

The emplacement of the Hearst–Matachewan dike swarm represents a major magmatic event after the stabilization of the Superior Province. It extends over greater than 250 000 km^2 of the Superior Province, the second largest dike swarm of the Canadian Shield and one of the largest on earth (Fahrig 1987). The studies of Phinney and Morrison (1988) provide evidence for extensive Matachewan-related tholeiitic magma chambers at upper to mid-crustal levels, which may have been capable of resetting the Rb-Sr system regionally. Their experimental petrology on tholeiitic matrices of megacrystic basalts similar to Matachewan dike matrix material indicated that Matachewan plagioclase compositions can be reproduced only at pressures corresponding to depths of about 10 to 12 km. The thermal effects of Hearst–Matachewan magmatism may have been responsible for partially or completely resetting Rb-Sr and K-Ar ages for Archean rocks in a cryptic fashion, with no detectable change in mineral assemblages. For example, Rb-Sr isochron ages for many granitoids across the southern Superior Province are 2400 to 2460 Ma (e.g., Frith and Doig 1975; Birk and McNutt 1981; Clark and Cheung 1980), and Rb-Sr systematics of three alteration zones along the Destor Porcupine and Larder Lake fault zones give regression ages of 2390, 2410 and 2440 Ma (Kerrich et al. 1987).

Younger regression ages for two granitoid rocks in the Nd and Sr systems are older than the emplacement age for the Hearst dike swarm. Particularly noteworthy are the identical ages of 2530 Ma in the Nd and Sr systems for a sample from granitoid C, coeval with U-Pb titanite ages at the base of the Kapuskasing Structural Zone (Krogh et al. 1988), and more than 160 million-years younger than U-Pb zircon and titanite ages from the same sample.

The young Sm-Nd and Rb-Sr ages may reflect thermal events related to the late addition of mantle-derived magmas into the lower crust of the southern Superior Province, after most of the magmatic activity in the Neoarchean. In the southern Abitibi Subprovince, radiogenic isotopic studies have investigated mineralization and alteration associated with mesothermal gold systems (e.g., Wong et al. 1989; Bell et al. 1989) and volcanogenic sulphide deposits (e.g., Maas et al. 1986; Schandl and Davis 1989). These studies have documented posttectonic hydrothermal fluid migration related to late thermal events from 2650 to 2400 Ma (Bell et al. 1989). Crustal underplating and the intrusion into lower and midcrustal levels by mantle-derived magmas is one mechanism that can adequately explain the late addition of heat to this region (Fyon et al. 1989; Barrie 1990). Crustal underplating has been called on to explain anticlockwise P-T paths documented in numerous granulite terranes, and is believed to be characteristic of continental arc environments (Bohlen 1987). For thermal modeling of the nearby Kapuskasing Structural Zone uplift, it is necessary to include regional uplift and continued elevated heat input from the mantle between 2680 and 2500 Ma (Percival et al. 1988). This is consistent with the addition of mantle-derived magmas into the lower crust at 2530 Ma. Therefore, a continental arc environment would account not only for the igneous characteristics of the Abitibi and Wawa subprovinces, but the Kapuskasing Structural Zone metamorphic and cooling histories, as well (Percival et al. 1988).

COMPARISON TO MODERN TECTONIC SETTINGS: SYNTHESIS

Perhaps the closest Phanerozoic analog to the tectonic setting of the KGC, considering its close temporal relationship with regional calc-alkalic plutonism, is found in the continental arc setting of the central Peruvian Andes. The vast Coastal Batholith of Peru exhibits classic exposures of Mesozoic and Cenozoic intrusive rocks that have been exhumed by continued uplift and erosion. The Coastal Batholith intruded into a tectonically thinned, extensional marginal basin (Atherton et al. 1983) underlain by a relatively dense basement, is interpreted to represent mantle or lower crustal material (Couch et al. 1981). A series of large (up to 5 by 40 km), elongate gabbro to diorite intrusions comprise approximately 16% of the Coastal Batholith (McCourt 1981; Regan 1985). Geological relationships and geochronology have shown that the gabbros predate the voluminous calc-alkaline magmatism. In the Arequipa (southern) segment, the early gabbros, at 101 to 106 Ma, were followed by a series of granitic intrusions at 37 to 101 Ma (Moore and Agar 1985; Mukasa 1986). There is abundant textural evidence in the gabbros for syncrystallization deformation, volatile activity, and net veining by granitic magmas to form hybrid rocks during consolidation (Regan 1985). All of these textures are found within the KGC

(Barrie 1990). Atherton et al. (1981) have proposed that the parent magmas for the gabbros were olivine tholeiites, a product of partial melting in a mantle wedge above a subducting slab, leaving behind a garnet-free residuum. The partial melts were modified by olivine and clinopyroxene fractionation prior to emplacement at mid- to upper crustal levels. Generally, calc-alkaline to mildly alkaline granitoid rocks like those of the Coastal Batholith, may have parental magmas that were derived by partial melting of amphibolitic or ecolgitic, subducted oceanic crust, and hydrated peridotitic upper mantle, respectively (Arth and Hanson 1975; Shirey and Hanson 1986). Lead and Sr isotope studies indicate minimal interaction with older crustal material for Coastal Batholith rocks (Barreiro and Clark 1984; Pitcher et al. 1985).

Other extensional tectonic settings are suggested through comparisons of the geochemistry, physical volcanology and mineralization of the KVC. The geochemistry and distinctive mixed magma textures in felsic pyroclastic rocks compare favourably to Askja, Iceland volcanic rocks, representing a hot spot, mid-ocean rift setting (Sigurdsson and Sparks 1981). The presence of copper-zinc volcanogenic massive sulphide deposits at Kamiskotia is commonly regarded to indicate subaqueous rifted settings (Cathles et al. 1983). This analogy would apply for the older, Kidd Creek–Hunter Mine Group metavolcanic trend also. Kamiskotia and Kidd Creek rhyolites are chemically and texturally similar to a number of high silica rhyolite suites from bimodal fields in the extensional, back-arc setting of the Basin and Range (e.g., Crecraft et al. 1981; Bacon et al. 1981).

The trace element and isotopic signatures of the KGC and KVC are consistent with geologic and U-Pb geochronological evidence for their formation in a continental arc-like regime. The bimodal KVC, with its massive sulphide mineralization, is typical of settings generally considered to represent a rifted back-arc or arc tectonic regime (e.g., Cathles et al. 1983). The presence of older crustal rocks nearby (described above) would suggest that rifting must have been within or proximal to an ensialic crust, possibly a continental margin. One notable feature about the geochemistry of the KGC chill margins and basalt is their similarity to MORB trace element signatures. The trace element contents of KGC chill margin rocks are consistent with partial melting of a chemically primitive mantle peridotite at shallow depths, and show little or no contamination by crustal components. Similarly, the Nd isotopic signature for the entire Kamiskotia suite is consistent with a direct derivation from the Abitibi depleted (in an isotopic sense) mantle with little or no interaction from enriched crustal material. In modern continental arc settings such as in the central Peruvian Andes or the Peninsular Ranges Batholith of Baja California, there is isotopic evidence that mantle-derived tholeiitic magmas rose through the lithosphere with little or no interaction from crustal material. Large gabbroic intrusions which represent the earliest intrusive rocks of the Coastal Batholith were emplaced in a tectonically thinned, extensional marginal basin (Atherton et al. 1983). Lead and Sr isotope studies indicate minimal interaction with older crustal material for Coastal Batholith rocks (Barreiro and Clark 1984; Pitcher et al. 1985). Large gabbroic intrusions in the Peninsular Ranges are slightly older and more isotopically depleted than the majority of nearby granitoid plutons (Walawender 1976; Walawender and Smith 1980; DePaolo 1981b).

The granitoid rocks were emplaced during times of extensional tectonics associated with the KGC, and later during a more compressional regime. In this respect the granitoid suite is similar to the Cretaceous Peninsular Ranges Batholith of Baja California, the product of arc magmatism formed during subduction of the Pacific plate under the North American plate. Gromet and Silver (1987) found that tonalites and low-potassium granodiorites exhibit a systematic increase in Ce/Yb from west to east, generally accompanied by an increase in I_{Sr} (initial Sr isotope ratio) values. High level fractionation of major and trace silicate phases cannot explain these trends. They are consistent with partial melting of arc basalt under increasingly high pressures, leaving behind gabbroic or amphibolitic residue at low pressures to the west, and an eclogitic residue to the east (Gromet and Silver 1987). The Kamiskotia granitoids have Ce/Yb ratios most similar to the central and eastern granitoids of the Peninsular Ranges, consistent with their derivation from a basaltic source at high pressures. Enriched Nd isotopic signatures and generally higher Ce/Yb ratios for the central granitoids, which represent a regional granitoid terrane that encompasses the greenstone belts of the southern Superior Province, are consistent with derivation from an older basaltic source at greater depths in this area. Further Nd isotopic studies of the regional granitoids are necessary to test whether there are aerially distinct domains of older, enriched crust in the vicinity of the southern Abitibi Subprovince and elsewhere in the southern Superior Province.

The late, predominantly transpressional regime represents a major change in tectonic style in the Kamiskotia area and across the southern Superior Province. Transpressional tectonics were at least in part responsible for the development of Superior Province-wide structural discontinuities, and were generally coincident with alkaline magmatism (Frarey and Krogh 1986; Corfu and Stott 1986; Corfu et al. 1989; Davis et al. 1989; Wyman and Kerrich 1988; Barrie and Davis 1990). The close spatial association between major fault structures and mantle-derived alkaline rocks in the southern Abitibi Subprovince implies that, at least locally, these faults served as conduits for alkaline magmas that extended to mantle depths (Kerrich et al. 1987; Wyman and Kerrich 1988).

Similar spatial and temporal relationships between mantle-derived alkalic rocks and incipient transpressive regimes occur in Phanerozoic and modern arc settings, associated with a transition between relative plate motions. A rapid transition from subduction and collision-related calc-alkaline magmatism to alkaline magmatism in a transpressive regime has been documented by a structural and geochemical study of dike swarms, accompanied by Rb-Sr geochronology, for a part of the Pan–African belt in Mali (Liegois and Black 1987). Quaternary alkalic volcanic centers in the Colima graben area, Mexico, represent the transition from compressional to transpressional tec-

tonics at the southern end of the San Andreas Fault system (Luhr and Carmichael 1981). Morrison (1980) determined that arc-related shoshonitic rocks are commonly associated with the termination of subduction or the transition between two subduction regimes of different orientation in island arc and continental arc settings. This infers that for the Kamiskotia area and the southern Superior Province, late transpression may have been related to a sudden change in plate motions in an Andean-type continental arc setting (Figure 36a,b).

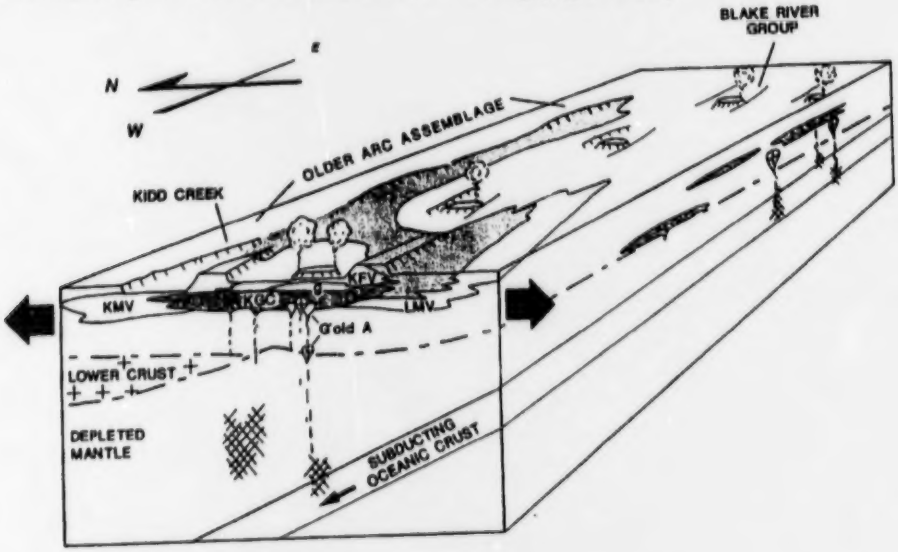

Figure 36a. Tectonic model for the Kamiskotia area and parts of the southwestern Abitibi Subprovince. Generalized block diagram looking east from Kamiskotia area at 2707 Ma to 2698 Ma. Kamiskotia complex represented in continental marginal basin-like extensional setting. KGC-Kamiskotia gabbroic complex; KMV-Kamiskotia mafic metavolcanic rocks of the KVC; KFV Kamiskotia felsic metavolcanic rocks of the KVC; g-Kamiskotia granophyre; LMV-lower mafic metavolcanic rocks of the Lower volcanic suite; shaded-sedimentary rocks; patterned-mafic intrusions; cross pattern-early granitoid intrusions. Dashed line represents division between predominantly supracrustal rocks above and depleted mantle below. Hatchured areas represent areas of partial melting.

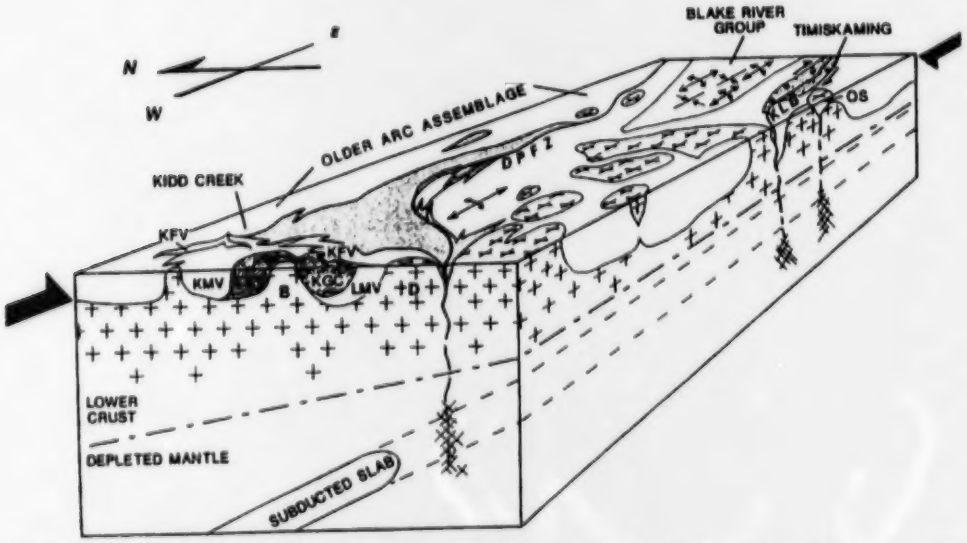

Figure 36b. Same area, at 2690 Ma to 2670 Ma. Symbols same as in Figure 36a. Additionally: B-granitoid B; D-granitoid D, DPFZ-Destor–Porcupine Fault Zone; KLB-Kirkland Lake–Larder Lake Break; OS-Otto Stock (mildly alkalic); Timiskaming-sedimentary rocks and alkalic metavolcanic rocks of the Timiskaming Group; cross pattern- predominantly granitoid intrusions and gneisses; no pattern-predominantly metavolcanic rocks, unsubdivided. After voluminous granitoid emplacement, north-south bulk shortening and subduction, a dextral, transpressive tectonic regime predominates across the region, with development of late ductile shear fabrics along the major fault zones, and wrench-style folding in metavolcanic rocks. *From* Barrie and Davis (1990).

Appendix I: Sample Locations, Petrographic Descriptions and Geochemistry for U–Pb Samples*

SAMPLE	LITHOLOGY	TOWNSHIP	UTM NORTHING	UTM EASTING	DESCRIPTION
KGC	Kamiskotia Gabbroic Complex	Turnbull	5366430	449075	Pegmatitic hornblende quartz gabbro; 69% hornblende, 20% plagioclase, 10% quartz, trace zircon, sphene; no fabric.
KR	Kamiskotia rhyolite	Godfrey	5368630	457900	Flow–banded, quartz– and feldspar–phyric; 85% fine grained quartz–sericite matrix, 7% quartz, 7% potassium feldspar, trace zircon, apatite; weakly developed foliation.
GC	Groundhog River tonalite	Enid	5373290	433390	Medium to coarse grained; 45% plagioclase (An_{30}), 35% quartz, 10% orthoclase, 5% muscovite, 1% epidote, trace zircon, apatite, sphene, hematite; foliated.
GB	Côté Township tonalite	Côté	5378860	438620	Medium to course grained; 50% plagioclase (An_{35}), 35% quartz, 10% hornblende, 1% biotite, 1% chlorite, trace zircon, apatite, sphene, epidote, sericite; slightly foliated.
KCR	Kidd Creek rhyolite	Kidd	5392630	473300	Quartz–phyric crystal lapilli tuff breccia; 95% carbonate–sericite, chlorite and quartz matrix with 30% rhyolite tuff fragments containing 5% fine grained quartz phenocrysts.
PR	Prosser rhyolite	Prosser	5398000	478800	Massive and laminated ash tuff; 97% quartz, sericite, chlorite matrix with epidote–carbonate veinlets, containing 2% fine–grained altered potassium feldspar phenocrysts and 1% quartz phenocrysts.
RR	Reid rhyolite	Reid	5396000	465000	Laminated ash and lapilli tuff; 90% quartz, sericite, epidote, carbonate and sulphide (pyrite, sphalerite) matrix, containing 8% medium–grained altered potassium feldspar phenocrysts, 2% fine–grained quartz phenocrysts, trace zircon, apatite.

* (*from* Barrie and Davis, 1990).

Appendix I. (continued)

Geochemistry

	KGC	KR	GC	GB	KCR**	PR	RR
Major Oxides (wt %)							
SiO_2	46.0	74.4	71.4	73.9	75.1	74.4	75.1
TiO_2	0.09	0.25	0.17	0.35	0.14	0.10	0.12
Al_2O_3	20.9	11.4	15.6	12.5	15.1	11.7	11.1
Fe_2O_3	4.90	2.63	1.80	3.30	3.14	3.97	2.61
MnO	0.10	0.02	0.03	0.06	0.04	0.11	0.06
MgO	8.86	1.27	0.70	0.78	1.58	0.91	0.64
CaO	13.20	1.06	2.82	2.64	0.93	1.39	2.06
Na_2O	0.95	1.18	5.25	4.00	0.81	1.16	2.19
K_2O	0.26	4.73	1.75	1.24	3.12	3.56	3.12
P_2O_5	0.01	0.03	0.06	0.07	0.02	0.02	0.02
LOI	3.93	2.23	0.39	1.00	—	2.31	3.80
TOTAL	99.20	99.20	99.97	99.84	100.0	99.63	100.82
Trace Elements (ppm)							
Zr	14	360	70	183	318	210	170
Y	6	70	16	13	126	120	
Sr	161	10	426	319	73		
Ba	63	570	620	540	290		
Rb	5	90	11	58	109	180	80
La	2.06	46.9	5.88	13.7	63.4		
Ce	4.5	107	10.2	32.7	162		
Nd	2.0	58.0	6.4	15.6	85.0		
Sm	0.6	11.5	2.0	3.1	21.0		
Eu	0.38	1.00	0.28	0.72	2.85		
Tb	0.2			0.3	3.9		
Yb	0.8	7.9	0.3	1.2	14.6		
Lu	0.13	1.18	5.00	0.25	2.20		

Major elements by XRF; trace elements by XRF and INAA at the University of Toronto, except for samples PR and RR, with trace elements analyzed at X-Ray Assay Laboratories, Toronto by a less accurate, fast-count method.

* *Data from Lesher et al. (1986). reported on a volatile-free basis.

Appendix II: Sample Locations by Universal Transverse Mercator Grid Coordinates.*

Table 4. Kamiskotia Gabbroic Complex cumulates

SAMPLE	Northing	Easting	Township
86-260	5366260	446090	Whitesides
84-12	5366260	445950	Whitesides
84-18	5365060	446790	Carscallen
84-19	5365062	446790	Carscallen
86-309	5364150	439170	Whitesides
86-310	5364075	439290	Whitesides
86-311	5363828	439300	Whitesides
84-271a	5362950	439390	Whitesides
84-271b	5362950	439392	Whitesides
84-271c	5362950	439394	Whitesides
86-313	5363680	439415	Whitesides
86-315	5363680	439540	Whitesides
86-317	5363575	439600	Whitesides
86-316	5363680	439600	Whitesides
84-237	5364120	439420	Whitesides
84-226	5364350	440080	Whitesides
84-227	5365570	440770	Whitesides
84-219	5363020	441360	Whitesides
86-295	5363920	441460	Whitesides
86-296	5363950	441630	Whitesides
86-297	5364010	441760	Whitesides
86-298	5363900	441700	Whitesides
86-300	5363850	441750	Whitesides
84-402	5377800	451370	Robb
84-406	5377920	451340	Robb
TH-150	5378060	451400	Robb
TH-172	5377790	452820	Robb
TH-174	5377570	453090	Robb
84-415	5377960	452840	Robb
TH-85	5377480	454400	Robb
TH-37	5377160	455160	Robb
TH-133	5376950	455420	Robb
TH-146	5381120	451400	Robb

Table 5. Gabbro chill samples

SAMPLE	Northing	Easting	Township
87-14	5367890	447120	Turnbull
87-15	5368080	447120	Turnbull
87-18	5370840	447150	Turnbull
84-186	5368160	447180	Turnbull
86-285	5363940	449410	Carscallen

* Table numbers correspond to tables in "Geochemistry" and "Economic Geology".

Appendix II. (continued)

Table 6. Lower volcanic suite

SAMPLE	Northing	Easting	Township
84-48	5378260	432760	Enid
84-72	5374910	435440	Enid
84-86	5381480	436320	Fortune
84-136	5362300	446340	Carscallen
84-217	5361840	442040	Whitesides
84-265	5360320	440410	Whitesides
86-6	5359450	448430	Carscallen
86-7	5360010	447830	Carscallen
86-12	5361520	446500	Carscallen
86-306	5364210	438360	Whitesides
86-307	5364510	438550	Whitesides

Table 7. Granitoid rocks

SAMPLE	Northing	Easting	Township
84-31	5367710	446500	Turnbull
86-267	5367010	446300	Turnbull
86-101	5378860	438620	Côté
84-246	5373320	437170	Massey
84-43	5373290	433390	Enid
86-220	5386300	424450	Fortune
84-174	5378420	437390	Côté
84-130	5355450	447610	Denton
84-266	5359700	438600	Whitesides

Table 8. Bristol Township lamprophyre suite

SAMPLE	Northing	Easting	Township
87-4	5358150	458850	Bristol
87-6	5358157	458810	Bristol
88-2	5358160	458810	Bristol
88-3	5358145	458850	Bristol
88-4	5358095	458875	Bristol
88-5	5358162	458865	Bristol
88-6	5358160	458815	Bristol
89-5	5358575	458085	Bristol
89-8	5358590	459080	Bristol
89-9	5358110	458795	Bristol
89-10	5358115	458800	Bristol
89-13	5358110	458805	Bristol
89-14	5358110	458807	Bristol
89-15	5358160	458865	Bristol

Appendix II. (continued)

Table 9. KGC sulphide occurrence samples

SAMPLE	Northing	Easting	Township
84-2	5366440	440860	Whitesides
84-14	5365980	446410	Carscallen
84-63	5376760	436250	Enid
84-135	5362970	447960	Carscallen
84-175	5361850	442100	Whitesides
86-27	5361850	442100	Whitesides
86-321	5363700	439360	Whitesides
86-322	5363650	439300	Whitesides
86-324	5363880	439400	Whitesides
86-326	5363880	439420	Whitesides
86-327	5363960	439475	Whitesides
86-328	5363960	439475	Whitesides
86-329	5363960	439475	Whitesides

Appendix III – Partition Coefficients and Average Modes used in Mass Balance and Assimilation–Fractional Crystallization Calculations

Partition coefficients

	Ol[1]	Opx[1]	Cpx	Plag[2]	Mt[3]	Ap[4]
La	0.01	0.005 (0.009)	0.08	0.13 (0.28)	0.06	16.0
Ce	0.012	0.008 (0.009)	0.10	0.13 (0.28)	0.06	16.6
Nd	0.012	0.012 (0.02)	0.20	0.10 (0.20)	0.07	21.0
Sm	0.012	0.015 (0.02)	0.25	0.07 (0.17)	0.07	20.7
Eu	0.012	0.015 (0.02)	0.28	0.32 (0.44)	0.07	14.5
Tb	0.02	0.03 (0.03)	0.30	0.04 (0.21)	0.08	21.0
Yb	0.03	0.07 (0.17)	0.30	0.03 (0.30)	0.11	9.4
Lu	0.03	0.07 (0.17)	0.30	0.03 (0.30)	0.12	9.0

K_Ds from experimental work at atmospheric pressure between mineral and basaltic melts. Values in parentheses used for Kamiskotia evolved basalt–UZ cumulate calculations.

[1] McKay and Weill (1977); [2] Average of GSFC 184 (An_{80}) and GSFC 271 (An_{77}); in parentheses: GSFC 204 (An_{50}) all from Schnetzler and Philpotts (1970); [3] Lowest values quoted for andesites (Gill 1981). [4] Arth and Barker (1976).

Average modes of KGC cumulates*

	olivine–bearing cumulates	Lower Zone	Middle Zone	lower Upper Zone	upper Upper Zone
Olivine	39	16	0	0	0
Orthopyroxene	27	12	20	24	28
Clinopyroxene	0	13	24	24	30
Plagioclase	34	60	54	49	46
Magnetite	0	0	1	1	2
Hornblende	0	0	0	0.5	0
Apatite	0	0	0	0.1	0.2
Sulphide	0.5	0.1	0.1	0.2	0.2

* Average modes taken from Figure 13. Hornblende is not a cumulus phase and is not included in the mass balance calculations. Sulphides are not included in mass balance calculations for the REE.

Olivine–bearing cumulates: samples 1 to 4; Lower Zone; samples 5 to 15; Middle Zone: samples 16 to 23; lower Upper Zone: samples 24 to 29; upper Upper Zone: samples 30 to 33.

References

Arth, J. C., and Barker, F., 1976, Rare-earth partitioning between hornblende and dacitic liquid and implications for the genesis of trondhjemitic-tonalitic magmas: Geology v, 4, p. 534-536.

Arth, J.G. and Hanson, G.N. 1975. Geochemistry and origin of the early Precambrian crust of northeastern Minnesota; Geochimica et Cosmochimica Acta, v.39, p.325-362.

Ashwal, L.D., Wooden, J.L., Phinney, W.C. and Morrison, D.A. 1985. Sm-Nd and Rb-Sr isotope systematics of an Archean anorthosite and related rocks from the Superior Province of the Canadian Shield; Earth and Planetary Science Letters, v.74, p.338-346.

Atherton, M.P., McCourt, W.J., Sanderson, L.M. and Taylor, W.P. 1981. The geochemical character of the segmented Peruvian Coastal Batholith and associated volcanics; *in* Origin of Granite Batholiths, Geochemical Evidence, Shiva Publ. Ltd., p.45-64.

Atherton, M.P., Pitcher, W.S. and Warden, V. 1983. The Mesozoic marginal basin of central Peru; Nature, v.305, p.303-306.

Bacon, C.R., Kurasawa, H., Delevaux, M., Kistler, R. and Doe, B. 1984. Lead and strontium isotopic evidence for crustal interaction and compositional zonation in the source regions of Pleistocene basaltic and rhyolitic magmas of the Coso volcanic field, California; Contributions to Mineralogy and Petrology, v.85, p.366-375.

Bacon, C.R., Macdonald, R., Smith, R.L. and Baedecker, P.A. 1981. Pleistocene high-silica rhyolites of the Coso volcanic field, Inyo County, California; Journal of Geophysical Research, v.86, p.10223-10241.

Barlow, R.B. 1988. Calculated second vertical derivative colour image from digital archives of the Ontario Geological Survey, Timmins Area, Districts of Cochrane and Timiskaming; Ontario Geological Survey, Map 81139, Geophysical/Geochemical Series, scale 1:100 000.

Barnes, S.J. 1984. The origin of the fractionation of platinum group elements in Archean komatiites of the Abitibi greenstone belt, northern Ontario, Canada; unpublished PhD thesis, University of Toronto, Toronto, Ontario, 230p.

Barreiro, B.A. and Clark, A.H. 1984. Lead isotopic evidence for evolutionary changes in magma-crust interaction, Central Andes, southern Peru; Earth and Planetary Science Letters, v.69, p.30-42.

Barrie, C.T. 1990. Petrogenesis and tectonic evolution of the Kamiskotia and Montcalm gabbroic complexes and adjacent granitoid greenstone belt terrane, western Abitibi Subprovince, Ontario, Canada; unpublished PhD thesis, University of Toronto, Toronto, Ontario, 317p.

Barrie, C.T. and Davis, D.W. 1990. Timing of magmatism and deformation in the Kamiskotia-Kidd Creek area, western Abitibi Subprovince, Ontario, Canada; Precambrian Research, v.46, p.217-240.

Barrie, C.T. and Naldrett, A.J. 1989. Geology and tectonic setting of the Montcalm gabbroic complex and Ni-Cu deposit, western Abitibi Subprovince, Ontario, Canada; *in* Magmatic Sulphides; *in* The Zimbabwe Volume, Institution of Mining and Metallurgy, London, p.151-164.

Barrie, C.T. and Shirey, S.B. 1989. Geochemistry and Nd-Sr isotope systematics of the Kamiskotia area, western Abitibi Subprovince, Canada: implications for mantle processes during formation of the southern Superior craton; Workshop on the Archean Mantle, Lunar and Planetary Institute, Houston, Texas, p.31-33.

Barrie, C.T. and Shirey, S.B. 1991, Nd and Sr isotope systematics for the Kamiskotia-Montcalm area: implications for the formation of Late Archean crust in the western Abitibi Subprovince, Canada: Canadian Journal of Earth Sciences, v.28. p. 58-76.

Basu, A.R., Goodwin, A.M. and Tatsumoto, M. 1984. Sm-Nd study of Archean alkalic rocks from the Superior Province of the Canadian Shield; Earth and Planetary Science Letters, v.70 p.40-46.

Bateman, R. 1985. Aureole deformation by flattening around a diapir during in situ ballooning: the Cannibal Creek Granite; Journal of Geology, v.93, p.293-310.

Beakhouse, G.P., McNutt, R.H. and Krogh, T.E. 1988. Comparative Rb-Sr and U-Pb zircon geochronology of late- to post-tectonic plutons in the Winnipeg River belt, northwestern Ontario, Canada; Chemical Geology, v.72, p.337-351.

Bell, K., Anglin, C.D. and Franklin, J.M. 1989. Sm-Nd and Rb-Sr isotope systematics of scheelites: possible implications for the age and genesis of vein-hosted gold deposits; Geology, v.17, p.500-504.

Beswick, A. 1982. Some geochemical aspects of alteration, and genetic relations in komatiitic suites; *in* Komatiites, Allen Unwin, London, p.283-308.

Birk, D. and McNutt, R.H. 1981. Geochronology of Wabigoon belt granitoids, northwestern Ontario: Rb/Sr isochrons for seven late-tectonic plutons; Canadian Journal of Earth Sciences, v.18, p.157-175.

Bohlen, S.R. 1987. Pressure-temperature-time paths and a tectonic model for the evolution of granulites; Journal of Geology, v.95, p.617-632.

Bright, E.G. and Hunt, D.S. 1973. Côté Township, District of Cochrane; Ontario Department of Mines, Preliminary Map P.840, scale 1:15 840.

Brooks, C.K. and Nielsen, T.F. 1978. Early stages in the differentiation of the Skaergaard magma as revealed by a closely related suite of dike rocks; Lithos, v.11, p.1-14.

Brugmann, G.E. 1985. Geochemistry of the noble metals and lithophile elements in komatiite flows from Alexo, Canada, and Gorgona, Colombia; unpublished PhD thesis, Johannes Gutenberg-Universitat, Mainz, Federal Republic of Germany, 261p.

Byerly, G. 1980. The nature of differentiation trends in some volcanic rocks from the Galapagos Spreading Center; Journal of Geophysical Research, v.85, p.3797-3810.

Campbell, I.H., Coad, P., Franklin, J.M., Gorton, M.P., Scott, S.D., Sowa, J. and Thurston, P.C. 1982. Rare earth elements in volcanic rocks associated with Cu-Zn massive sulfide mineralization: preliminary report; Canadian Journal of Earth Sciences, v.19, p.619-623.

Campbell, I.H., Franklin, J.M., Gorton, M.P., Hart, T.R. and Scott, S.D. 1981. The role of subvolcanic sills in the generation of massive sulfide deposits; Economic Geology, v.76, p.2248-2253.

Campbell, I.H., Lesher, C.M., Coad, P., Franklin, J.M., Gorton, M.P. and Thurston, P.C. 1984. Rare earth element mobility in alteration pipes below massive sulfide deposits; Chemical Geology, v.45, p.181-202.

Capdevila, R., Goodwin, A.M., Ujike, O. and Gorton, M.P. 1983. Trace-element geochemistry of Archean volcanic rocks and crustal growth in southwestern Abitibi belt, Canada; Geology, v.10, p.418-422.

Cathles, L.M., Guber, A.L., Lenagh, T.C. and Dudas, F.O. 1983. Kuroko-type massive sulphide deposits of Japan: products of an aborted island-arc rift; *in* Economic Geology Monograph 5, The Kuroko and Related Volcanogenic Massive Sulphide Deposits, Economic Geology Publishing Company, p.96-114.

Cattell, A., Krogh, T.E. and Arndt, N.T. 1984. Conflicting Sm-Nd whole rock and U-Pb zircon ages for Archean lavas from Newton Township, Abitibi belt, Ontario; Earth and Planetary Science Letters, v.70, p.280-290.

Christiansen, E.H., Sheridan, M.F. and Burt, D.M. 1986. The geology and geochemistry of Cenozoic topaz rhyolites from the western United States; Geological Society of America, Special Paper 25, 82 p.

Clark, G.S. and Cheung, S.P. 1980. Rubidium-strontium ages from the Oxford Lake-Knee Lake greenstone belt, northern Manitoba; Canadian Journal of Earth Sciences, v.17, p.560-568.

Colvine, A.C., Fyon, J.A., Heather, K.B., Marmont, S., Smith, P.M. and Troop, D.G. 1988. Archean lode gold deposits in Ontario; Ontario Geological Survey, Miscellaneous Paper 139, 136p.

Comba, C.D.A., Binney, W.P., Stewart, R.D., Cunnison, K.M. and Mullen, D.V. 1986. Timmins, Ontario: exceptional exposures of Archean subaerial and shallow subaqueous volcanic rocks, and associated ore deposits; Geological Association of Canada/Mineralogical Association of Canada 1986 Field Trip Guidebook #5, 25p.

Corfu, F. 1987. Inverse age stratification in the Archean crust of the Superior Province: evidence for infra-and subcrustal accretion from high resolution U-Pb zircon and monazite ages; Precambrian Research, v.36, p.259-275.

——1993. The evolution of the southern Abitibi greenstone belt in light of precise U-Pb geochronology: Economic Geology, v.88, p.1323-1341.

Corfu, F. and Grunsky, E.C. 1987. Igneous and tectonic significance of the Batchewana greenstone belt, Superior Province: a U-Pb zircon and titanite study; Journal of Geology, v.95, p.87-105.

Corfu, F., Krogh, T.E., Kwok, Y.Y., Marmont, S. and Jensen, L.S. 1989. U-Pb zircon geochronology in the southwestern Abitibi greenstone belt, Superior Province; Canadian Journal of Earth Sciences, v.26, p.1747-1763.

Corfu, F. and Stott, G.M. 1986. U-Pb ages for late magmatism and regional deformation in the Shebandowan Belt, Superior Province, Canada; Canadian Journal of Earth Sciences, v.23, p.1075-1082.

Couch, R.W., Whitsett, R.M. and Hachu, B. and Briceno-Guarupe, L. 1981. Structures of the continental margin of Peru and Chile; *in* Nazca Plate: Crustal Formation of Andean Convergence, Geological Society of America Memoir 154, p.703-726.

Crecraft, H.R., Nash, W.P. and Evans, S.H. 1981. Late Cenozoic volcanism at Twin Peaks, Utah: geology and petrology; Journal of Geophysical Research, v.86, p.10303-10320.

Daly, R.A., Manger, G.E. and Clark, S.P. 1966. Density of rocks; *in* Handbook of Physical Constants, Geological Society of America Memoir 97, p.19-26.

Davis, D.W. and Edwards, G.R., 1982. Zircon U-Pb ages from the Kakagi Lake area, Wabigoon Subprovince, northwest Ontario; Canadian Journal of Earth Sciences, v.19, p.1235-1245.

—— 1986. Crustal evolution of Archean rocks in the Kakagi Lake area , Wabigoon Subprovince, Ontario, as interpreted from high precision U-Pb geochronology; Canadian Journal of Earth Sciences, v.23, p.182-192

Davis, D.W. Krogh, T.E., Hinzer, J. and Nakamura, E. 1985. Zircon dating of polycyclic volcanism at Sturgeon Lake and implications for base metal mineralization; Economic Geology, v.80, p.1942-1952.

Davis, D.W., Poulsen, K.H. and Kamo, S.L. 1989. New insights into Archean crustal development from geochronology in the Rainy Lake area, Superior Province, Canada; Journal of Geology, v.97, p.379-398.

Davis, D.W., Sutcliffe, R.H. and Trowell, N.F. 1988. Geochronological constraints on the tectonic setting of a late Archean greenstone belt; Precambrian Research, v.39, p.171-191.

Davis, D.W. and Trowell, N.F. 1982. U-Pb zircon ages from the eastern Savant Lake-Crow Lake metavolcanic-metasedimentary belt, northwest Ontario; Canadian Journal of Earth Sciences, v.19, p.868-877.

Delaney, P.T. 1987. Heat transfer during emplacement and cooling of mafic dikes; *in* Mafic Dike Swarms, Geological Association of Canada Special Paper 34, p.31-46.

DePaolo, D.J. 1981a. Trace element and isotopic effects of combined wallrock assimilation and fractional crystallization; Earth and Planetary Science Letters, v.53, p.189-202.

——1981b. A neodymium and strontium isotopic study of the Mesozoic calc-alkaline granitic batholiths of the Sierra Nevada and Peninsular Ranges, California; Journal of Geophysical Research, v.86, p.10470-10488.

——1985. Isotopic studies of processes in mafic magma chambers: the Kiglapait Intrusion, Labrador; Journal of Petrology, v.26, p.925-951.

Dimroth, E., Imreh, L., Goulet, N. and Rocheleau, M. 1983a. Evolution of the south-central part of the Archean Abitibi belt, Quebec. Part II: Tectonic evolution and geomechanical model; Canadian Journal of Earth Sciences, v.20, p.1355-1373.

——1983b. Evolution of the south-central part of the Archean Abitibi belt, Quebec. Part III: Plutonic and metamorphic evolution and geotectonic model; Canadian Journal of Earth Sciences, v.20, p.1374-1388.

Dimroth, E., Imreh, L., Rocheleau, M. and Goulet, N. 1982. Evolution of the south-central part of the Archean Abitibi belt, Quebec. Part I: Stratigraphy and paleogeographic model; Canadian Journal of Earth Sciences, v.19, p.1729-1758.

Dimroth, E., Mueller, W., Heidelberg, R., Brisson, H., Poitras, A. and Rocheleau, M. 1986. Diapirism during regional compression: the structural pattern in the Chibougamau region of the Archean Abitibi belt, Quebec; Geologische Rundschau, v.75, p.715-736.

Dixon, J.M. 1975. Finite strain and progressive deformation in models of diapiric structures; Tectonophysics, v.28, p.89-124.

Doe, B.R., Leeman, W.P., Christiansen, R.L. and Hedge, C.E. 1982. Lead and strontium isotopes and related trace elements and genetic tracers in the upper Cenozoic rhyolite-basalt association of the Yellowstone volcanic field; Journal of Geophysical Research, v.87 4785-4806.

Dupre, B., Chauvel, C. and Arndt, N.T. 1984. Pb and Nd isotopic study of two Archean komatiitic flows from Alexo, Ontario; Geochimica et Cosmochimica Acta, v.48, p.1965-1972.

Eby, G.N. 1975. Abundance and distribution of the rare-earth elements and yttrium in the rocks and minerals of the Oka carbonitite complex, Quebec; Geochimica et Cosmochimica Acta, v.39, p.597-620.

Evensen, N. M., Hamilton, P. J., and O'Nions, R. K., 1978, Rare-earth abundances in chondritic meteorites: Geochimica et Cosmochimica Acta, v. 42, p. 1199-1212.

Fahrig, W.F., 1987. The tectonic settings of continental mafic dike swarms; *in* Mafic Dike Swarms, Geological Association of Canada Special Paper 34 p.331-348.

Ferguson, S.A. 1957a. Bristol Township, District of Cochrane; Ontario Department of Mines, Map 1957-7, scale 1:12 000.

——1957b. Carscallen Township, District of Cochrane; Ontario Department of Mines, Preliminary Map P.23, scale 1:15 840.

Flinn, D. 1965. On the symmetry principle and the deformation ellipsoid; Geological Magazine, v.102, p.36-45.

Frarey, M.J. and Krogh, T.E. 1986. U-Pb zircon ages of late internal plutons of the Abitibi and eastern Wawa subprovince, Ontario and Quebec; *in* Current Research, Geological Survey of Canada, Paper 86-1A, p.43-48.

Frey, F.A., Bryan, W.B. and Thompson, G. 1974. Atlantic ocean floor: geochemistry and petrology of basalts from legs 2 and 3 of the Deep Sea Drilling Project; Journal of Geophysical Research, v.79, p.5507-5527.

Frith, R.A. and Doig, R. 1975. Pre-Kenoran tonalitic gneisses in the Grenville Province; Canadian Journal of Earth Sciences, v.12, p.844-849.

Fyon, J.A., Troop, D.G., Marmont, S., and Macdonald, A.J. 1989. Introduction of gold into Archean crust, Superior Province, Ontario: coupling between mantle-initiated magmatism and lower crustal thermal maturation; *in* Economic Geology Monograph 6, p.479-491.

Gariepy, C. and Allegre, C.J. 1985. The lead isotope geochemistry and geochronology of late-kinematic intrusives from the Abitibi greenstone belt, and the implications for late crustal evolution; Geochimica et Cosmochimica Acta, v.49, p.2371-2383.

Gariepy, C., Ailegre, C.J. and LaJoie, J. 1984. U-Pb systematics in single zircons from the Pontiac sediments, Abitibi greenstone belt; Canadian Journal of Earth Sciences, v.21, p.1296-1304.

Gibson, H.L., Watkinson, D.H. and Comba, C.D.A. 1989. Subaqueous phreatomagmatic explosion breccias at Buttercup Hill, Noranda, Quebec; Canadian Journal of Earth Sciences, v.26, p.1428-1439.

Gill, J., 1981, Orogenic Andesites and Plate Tectonics: Springer-Verlag, New York, 390 p.

Goldie, R. 1978. Magma mixing in the Flavrian pluton, Noranda area, Quebec; Canadian Journal of Earth Sciences, v. 15, p.132–144.

Graham, A.R. 1931. Groundhog–Kamiskotia area, District of Cochrane; Ontario Department of Mines Geological Report, v.40, p.23–36.

Green, D.H. 1970. The origin of basaltic and nephelenitic magmas; Transactions of the Leicester Literature and Philosophical Society, v.64, p.28–54.

Gromet, L.P. and Silver, L.T. 1987. REE variations across the Peninsular Ranges batholith: implications for batholithic petrogenesis and crustal growth in magmatic arcs; Journal of Petrology, v.28, p.75–125.

Grove, T. and Donnelly–Nolan, J.M. 1986. The evolution of young silicic lavas at Medicine Lake volcano, California: Implications for the origin of compositional gaps in calc–alkaline series lavas; Contributions to Mineralogy and Petrology, v.92, p.281–302.

Guha, J., Dube, B., Pilote, P., Chown, E., Archambault, G. and Bouchard, G. 1988. Gold mineralization patterns in relation to the lithologic and tectonic evolution of the Chibougamau mining district, Quebec, Canada; Mineralium Deposita, v.23, p.293–299.

Halliday, A.N., Mahood, G.A., Holden, P., Metz, J.M., Dempster, T.J. and Davidson, J.P., 1989. Evidence for long residence times of rhyolitic magma in the Long Valley magmatic system: the isotopic record in precaldera lavas of Glass Mountain; Earth and Planetary Science Letters, v.94, p. 274–290.

Hanes, J.A., Queen, M. and Archibald, D.A. 1988. $^{40}Ar/^{39}Ar$ geochronology of dikes and their contact aureoles in the Kapuskasing uplift; *in* Project Lithoprobe, Kapuskasing Structural Zone Workshop II, p.165–172.

Hanson, G.N., Goldich, S.S., Arth, J.G. and Yardley, D.H. 1971. Age of the Early Precambrian rocks of the Saganaga Lake–Northern Light Lake area, Ontario–Minnesota; Canadian Journal of Earth Sciences, v.8, p.1110–1124.

Hart, T.R. 1984. The geochemistry and petrogenesis of a metavolcanic and intrusive sequence in the Kamiskotia area; Timmins, Ontario; unpublished MSc thesis, University of Toronto, Toronto, Ontario, 179 p.

Heaman, L.M. 1989. U–Pb dating of mafic dike swarms: what are the options?; abstract *in* International Association of Volcanology and Chemistry of the Earth's Interior, Santa Fe, New Mexico.

Helz, R.T., 1985. Compositions of fine–grained mafic rocks from sills and dikes associated with the Stillwater Complex; Montana Bureau of Mines and Geology Special Publication 92, p.97–118.

Hildreth, W. 1981. Gradients in silicic magma chambers: implications for lithospheric magmatism; Journal of Geophysical Research, v.86, p.10153–10192.

Hoffman, E.L. Naldrett, A.J., Alcock, R.A. and Hancock, R.G.V. 1979. The noble–metal content of ore in the Levack West and Little Stobie Mines, Ontario; Canadian Minerologist, v.17, p.437–451.

Hofmann, A.W. 1988. Chemical differentiation of the Earth: the relationship between mantle, continental crust and oceanic crust; Earth and Planetary Science Letters, v.90, p.297–314.

Hogg, N. 1954. Geology of Godfrey Township, Cochrane District, Ontario Department of Mines Annual Report, v.63, Part 7, 55p.

Hubert, C., Trudel, P. and Gelinas, L. 1984. Archean wrench fault tectonics and structural evolution of the Blake River Group, Abitibi belt, Quebec; Canadian Journal of Earth Sciences, v.21, p.1024–1032.

Hudleston, P.J., Schultz–Ela, D. and Southwick, D.L. 1988. Transpression in an Archean greenstone belt, northern Minnesota; Canadian Journal of Earth Sciences, v.25, p.1060–1068.

Hunter, R.H. and Sparks, R.S.J. 1987. The differentiation of the Skaergaard Intrusion; Contributions to Mineralogy and Petrology, v.95, p.451–461.

Irvine, A.J. 1978. A review of experimental studies of crystal/liquid trace element partitioning; Geochemica et Cosmochima Acta, v.42, p.743–770.

Irvine, T.N. 1982. Terminology for layered intrusions; Journal of Petrology, v.23, p.127–162.

Jackson, S.L., Sutcliffe, R.H., Ludden, J.N., Hubert, C., Green, A.G., Milkereit, B., Mayrand, L., West, G.F. and Verpaelst, P. 1990. Southern Abitibi greenstone belt: Archean crustal structure from seismic–reflection profiles; Geology, v.18, p.1086–1090.

Jacques, A.L. and Green, D.H. 1980. Anhydrous melting of peridotite at 0–15 Kb pressure and the genesis of tholeiitic basalts; Contributions to Mineralogy and Petrology, v.73, p.287–310.

Jambon, A. 1982. Tracer diffusion in granitic melts: experimental results for Na, K, Rb, Cs, Ca, Sr, Ba, Ce, Eu to 1300°C and a model of calculation; Journal of Geophysical Research, v.87, p.10797–10810.

Jensen, L.S. and Pyke, D.R. 1982. Komatiites in the Ontario portion of the Abitibi belt; *in* Komatiites, George Allan and Unwin, London, p.147–157.

Juster, T.C., Grove, T.L. and Perfit, M.R. 1989. Experimental constraints on the generation of Fe–Ti basalts, andesites, and rhyodacites at the Galapagos Spreading Center, 85°W and 95°W; Journal of Geophysical Research, v.94, p.9251–9274.

Kerr, H.L. 1906. Exploration in the Mattagami Valley; *in* Report of the Bureau of Mines, Ontario, p.116–135.

Kerrich, R., Fryer, B.J., King, R.W., Willmore, L.M. and van Hees, E. 1987. Crustal outgassing and LILE enrichment in major lithosphere structures, Archean Abitibi greenstone belt: evidence on the source reservoir from strontium and carbon isotope tracers; Contributions to Mineralogy and Petrology, v.97, p.156–168.

King, R.W. and Kerrich, R. 1987. Fluorapatite fenitization and gold enrichment in sheeted trondhjemites within the Destor–Porcupine fault zone, Taylor Township, Ontario; Canadian Journal of Earth Sciences, v.24, p.479–502.

Krogh, T.E., Heaman, L.M. and Machado, N. 1988. Detailed U–Pb chronology of successive stages of zircon growth at medium and deep levels using parts of single zircon and titanite grains; *in* Project Lithoprobe, Kapuskasing Structural Zone Transect Workshop, 243p..

Krogh, T.E. and Turek, A. 1981. U–Pb zircon ages from the Gamitagama greenstone belt, southern Superior Province. Canadian Journal of Earth Sciences, v.19, p.859–867.

Leahy, E.J. 1968. Whitesides Township, District of Cochrane; Ontario Department of Mines, Preliminary Map P.488, scale 1:15 840.

LeBaron, P. 1985. Summary report on work performed on the Croxall option, Bristol and Thorneloe townships; Noranda Exploration Company Limited, Timmins Resident Geologist's Office, assessment file AFRI# 42A05SE001, 16p.

Lee, C.A. and Sharpe, M.R. 1979. Spheroidal pyroxenite aggregates in the Bushveld Complex: a special case of silicate liquid immiscibility; Earth and Planetary Science Letters, v.44, p.295–310.

Legault, M.H. 1985. The geology and alteration associated with the Genex volcanogenic massive sulphide deposit, Godfrey Township, Timmins, Ontario; unpublished MSc thesis, Carleton University, Ottawa, Ontario, 222 p.

Lesher, C.E. 1986. Effects of silicate liquid composition on mineral–liquid element partitioning from Soret diffusion studies; Journal of Geophysical Research, v.91, p.6123–6141.

Lesher, C.M., Goodwin, A.M., Campbell, I.H. and Gorton, M.P. 1986. Trace–element geochemistry of ore–associated and barren, felsic metavolcanic rocks in the Superior Province, Canada; Canadian Journal of Earth Sciences, v.23, p.222–237.

Liegois, J.P. and Black, R, 1987. Alkaline magmatism subsequent to collision in the Pan–African belt of the Adrar des Iforas (Mali); *in* Alkaline Igneous Rocks, Geological Society Special Publication no. 30, p.381–401.

Lindstrom, D.J. 1976. Experimental study of the partitioning of the transition metals between clinopyroxene and coexisting silicate liquids; unpublished PhD thesis, University of Oregon, Eugene, Oregon, 188p.

Longhi, J., Walker, D. and Hays, J.F. 1978. The distribution of Fe and Mg between olivine and lunar basaltic liquids; Geochimica et Cosmochimica Acta, v.42, p.1545–1558.

Ludden, J.N., Francis, D. and Allard, G.O. 1984. The geochemistry of the volcanic rocks of the Chibougamau region of the Abitibi metavolcanic belt; *in* Chibougamau—Stratigraphy and Mineralization, Canadian Institute of Mining and Metallurgy Special Volume 34, p.20–34.

Ludden, J., Gelinas, C. and Trudel, P. 1982. Archean metavolcanics from the Rouyn–Noranda district, Abitibi greenstone belt, Quebec: 2. mobility of trace elements and petrogenetic constraints; Canadian Journal of Earth Sciences, v.19, p.2276–2287.

Luhr, J.F. and Carmichael, I.S.E. 1981. The Colima volcanic complex, Mexico. Part II: Late Quaternary cinder cones; Contributions to Mineralogy and Petrology, v.76, p.127–147.

Maas, R., McCulloch, M.T., Campbell, I.H. and Coad, P.R. 1986. Sm–Nd and Rb–Sr dating of an Archean massive sulfide deposit: Kidd Creek, Ontario; Geology, v.14, p.585–588.

Macdonald, R., Sparks, R.S.J., Sigurdsson, H., Mattey, D.P., McGarvie, D.W. and Smith, R.L. 1987. The 1875 eruption of Askja volcano, Iceland: combined fractional crystallization and selective contamination in the generation of rhyolitic magma; Mineralogical Magazine, v.51, p.183–202.

MacGeehan, P.J. and MacLean, W.H. 1980. Tholeiitic basalt–rhyolite magmatism and massive sulphide deposits at Matagami, Quebec; Nature, v.283, p.153–157.

Machado, N., Brooks, C. and Hart, S.R. 1986. Determination of initial $^{87}Sr/^{86}Sr$ and $^{143}Nd/^{144}Nd$ in primary minerals from mafic and ultramafic rocks: experimental procedure and implications for the isotopic characteristics of the Archean mantle under the Abitibi greenstone belt, Canada; Geochimica et Cosmochimica Acta, v.50, p 2334–2348.

Malpas, J., Foley, S.F. and King, A.F. 1986. Petrology of the alkaline–ultrapotassic lamprophyres of Aillik Bay, Labrador; Canadian Journal of Earth Sciences, v.23, p.1902–1918.

Marsh, B.D. 1982. On the mechanics of igneous diapirism, stoping and zone melting; American Journal of Science, v.282, p.808–855.

Martin, H. 1987. Petrogenesis of Archean trondhjemites, tonalites and granodiorites from eastern Finland: major and trace element geochemistry; Journal of Petrology, v.28, p.921–953.

McBirney, A.R. 1985. Igneous petrology; Freeman and Cooper, 600p.

McCourt, W.J. 1981. The geochemistry and petrography of the Coastal Batholith of Peru, Lima segment; Journal of the Geological Society of London, v.138, p.407–420.

McIntyre, G.A., Brooks, A.C., Compston, W. and Turek, A. 1966. The statistical assessment of Rb–Sr isochrons; Journal of Geophysical Research, v.71, p.5459–5468.

McKay, G. A., and Weill, D. F., 1977, Petrogenesis of KREEP revisited: Proceedings Eighth Lunar Science Conference, p. 2339–2355.

Menzies, M.A., Rogers, N., Tindle, A. and Hawkesworth, C.J. 1987. Metasomatic and enrichment processes in lithospheric peridotites, an effect of asthenosphere–lithosphere interaction; *in* Mantle Metasomatism, Academic Press, London, p.313–364.

Menzies, M., Seyfried, W. and Blanchard, D. 1979. Experimental evidence of rare earth element immobility in greenstones; Nature, v.282, p.398–399.

MERQ–OGS 1983. Lithostratigraphic map of the Abitibi Subprovince; Ontario Geological Survey/Ministère de l'Énergie et des Ressources, Quebec, scale 1:500 000, Map 2484.

Middleton, R.S. 1969. Jamieson Township, District of Cochrane geophysical series; Ontario Department of Mines, Preliminary Map P.521, scale 1:15 840.

——1970. Robb Township, District of Cochrane geophysical series; Ontario Department of Mines, Preliminary Map P.598, scale 1:15 840.

——1971a. Geophysical series, ground vertical field magnetics, Turnbull Township, District of Cochrane; Ontario Department of Mines, Preliminary Map P.638, scale 1:15 840.

——1971b. Geophysical series, ground vertical field magnetics, Godfrey Township, District of Cochrane; Ontario Department of Mines, Preliminary Map P.639, scale 1:15 840.

——1973a. Robb and Jamieson townships, District of Cochrane; Ontario Department of Mines, Map 2255, scale 1:31 680.

——1973b. Magnetic survey of Robb and Jamieson townships, District of Cochrane; Ontario Department of Mines, Geophysical Report 1, 56p.

——1975. Geology of Turnbull and Godfrey townships, District of Cochrane; Ontario Geological Survey, Open File Report 5118, 267p.

——1976. Turnbull and Godfrey townships, District of Cochrane; Ontario Department of Mines, Map 2330, scale 1:31 680.

Moore, N.D. and Agar, R.A. 1985. Variations along a batholith: the Arequipa segment of the Coastal Batholith of Peru; *in* Magmatism at a Plate Edge, the Peruvian Andes, John Wiley and Sons, New York, p.108–118.

Morrison, D.A., Davis, D.W., Wooden, J.L., Bogard, D.D., Maczuga, D.E., Phinney, W.C. and Ashwal, L.D. 1985. Age of the Mulcahy Lake intrusion, northwest Ontario, and implications for the evolution of greenstone–granite terranes; Earth and Planetary Science Letters, v.73, p.306–316.

Morrison, G.W. 1980. Characteristics and tectonic setting of the shoshonitic rock association; Lithos, v.13, p.97–108.

Mortensen, J.K. 1987. Preliminary U–Pb zircon ages for volcanic and plutonic rocks of the Noranda–Lac Abitibi area, Abitibi Subprovince, Quebec; Geological Survey of Canada, Paper 87–1A, p.581–590.

Moyer, T.C. and Esperanca, S. 1989. Geochemical and isotopic complexities in bimodal magma systems: the Kaiser Spring volcanic field, Arizona; Journal of Geophysical Research, v.94, p.7841–7859.

Mukasa, S.B. 1986. Zircon U–Pb ages of super–units in the Coastal Batholith, Peru: implications for magmatic and tectonic processes; Geological Society of America Bulletin, v.97, p.241–254.

Naldrett, A.J. 1981. Nickel sulfide deposits: classification, composition and genesis; Economic Geology 75th Anniversary Volume, Economic Geology Publishing Company, p.628–686.

Nathan, H.D. and Van Kirk, K. 1978. A model for magmatic crystallization; Journal of Petrology, v.19, p.66–94.

North American Commission on Stratigraphic Nomenclature, 1983. North American stratigraphic code; The American Association of Petroleum Geologists Bulletin, v.67, no.5, p.841–875.

Nunes, P.D. and Pyke, D.R. 1981. Time–stratigraphic correlation of the Kidd Creek orebody with volcanic rocks south of Timmins, Ontario, as inferred from zircon U–Pb ages; Economic Geology, v.76, p.944–951.

O'Driscoll, M. 1988. Rare earths, enter the dragon; Industrial Minerals, v.254, p.21–55.

O'Hara, M.J. 1977. Geochemical evolution during fractional crystallization of a periodically refilled magma chamber; Nature, v.266, p.503–507.

Pallister, J.S. and Knight, R.J. 1981. Rare earth element geochemistry of the Samail ophiolite near Ibra, Oman; Journal of Geophysical Research, v.86, p.2673–2697.

Paradis, S., Ludden, J. and Gelinas, L. 1988. Evidence for contrasting compositional spectra in comagmatic intrusive and extrusive rocks of the late Archean Blake River Group, Abitibi, Quebec; Canadian Journal of Earth Sciences, v.25, p.134–144.

Parks, W.A. 1900. Nivin's base line, Part 1, 1899; *in* Report of the Bureau of Mines, Ontario, p.125–142.

Parsons, I. 1979. The Klokken gabbro–syenite complex, south Greenland: cryptic variation and origin of inversely graded layering; Journal of Petrology, v.20, p.653–694.

Percival, J.A. and Krogh, T.E. 1983. U–Pb zircon geochronology of the Kapuskasing structural zone and vicinity in the Chapleau–Foleyet area, Ontario; Canadian Journal of Earth Sciences, v.20 p.830–843.

Percival, J.A., Krogh, T.E. and Peterman, Z.E. 1988. When did the Kapuskasing Zone come up?; *in* Project Lithoprobe Kapuskasing Structural Zone, Transect Workshop, p.43–48.

Phinney, W.C. and Morrison, D.A. 1988. Constraints on the environment of the Matachewan dike intrusion; abstract *in* International Geological Correlation Program 257 Annual Meeting, Lund, Sweden, p.25.

Pitcher, W.S., Atherton, M.P., Cobbing, E.J. and Beckinsale, R.D. 1985. A model for the Coastal Batholith; *in* Magmatism at a Plate Edge, The Peruvian Andes, Pitcher, John Wylie and Sons, New York, p.340–341.

Platt, R.G., Mitchell, R.H. and Holm, P.M. 1983. Marathon dikes: Rb–Sr and K–Ar geochronology of ultrabasic lamprophyres from the vicinity of McKellar Harbour, northwestern Ontario, Canada; Canadian Journal of Earth Sciences, v.20, p.961–967.

Poulsen, K.H. 1984. The geological setting of mineralization in the Mine Centre–Fort Frances area, District of Rainy River; Ontario Geological Survey, Open File Report 5512, 126p.

Pyke, D.R. 1978. Regional geology of the Timmins–Matachewan area, Districts of Cochrane and Timiskaming; *in* Summary of Field Work, Ontario Geological Survey, Miscellaneous Paper 82, p.73–77.

—— 1982. Geology of the Timmins area, District of Cochrane; Ontario Geological Survey, Report GR 219, 141p.

Pyke, D.R. and Middleton, R.S. 1970. Distribution and characteristics of the sulphide ores of the Timmins area; Ontario Department of Mines, Miscellaneous Paper 41, 24p.

Regan, P.F. 1985. The early basic intrusions; *in* Magmatism at a Plate Edge The Peruvian Andes, John Wiley and Sons, New York, p.72–89.

Rock N. M.S. 1986.The nature and origin of ultramafic lamprophyres: alnoites and allied rocks; Journal of Petrology, v.27, p.155–196.

——1987. The nature and origin of lamprophyres: an overview; *in* Alkaline Igneous Rocks, Geological Society of London Special Publication 30, p.191–226.

Roeder, P.L. 1974. Activity of iron and olivine solubility in basaltic liquids; Earth and Planetary Science Letters, v.23, p.397–410.

Roeder, P.L. and Emslie, R.F. 1970. Olivine–liquid equilibrium; Contributions to Mineralogy and Petrology, v.29, p.275–289.

Ryerson, F.J. and Hess, P.C. 1978. Implications of liquid–liquid distribution coefficients to mineral–liquid partitioning; Geochimica et Cosmochimica Acta, v.44, p.611–624.

Schandl, E.S. and Davis, D.W. 1989. Are sericite/fuchsite and chlorite alterations related to massive sulphide mineralization at the Kidd volcanic centre? Evidence from Pb–Pb and U–Pb systematics of hydrothermal rutile; Geological Association of Canada/Mineralogical Association of Canada Program with Abstracts, v.14, p.A120.

Schilling, J.G., Anderson, R.N. and Vogt, P. 1976. Rare earth, Fe and Ti variations along the Galapagos spreading centre, and their relationship to the Galapagos mantle plume; Nature, v.261, p.108–112.

Schnetzler, C.C. and Philpotts, J.A. 1970. Partition coefficients of rare earth elements between igneous matrix material and rock–forming mineral phenocrysts– II; Geochimica et Cosmochimica Acta, v.34, p.331–340.

Schwerdtner, W.M., Stott, G.M. and Sutcliffe, R.H. 1983. Strain patterns of crescentic granitoid plutons in the Archean greenstone terrain of Ontario; Journal of Structural Geology, v.5, p.419–430.

Schwerdtner, W.M., Sutcliffe, R.H. and Troeng, B. 1978. Patterns of total strain in the crestal region of immature diapirs; Canadian Journal of Earth Sciences, v.15, p.1437–1447.

Sharpe, J.I. 1968. Field relations of the Matagami area; Quebec Department of Natural Resources, Geological Report no.137, 50p.

Sharpe, M.R. 1986. Bushveld Complex – Excursion Guidebook; Institute for Geological Research on the Bushveld Complex, Pretoria, 143p.

Sharpe, M.R. and Hulbert, L. 1985. Ultramafic sills beneath the eastern Bushveld Complex: mobilized suspensions of early lower zone cumulates in a parental magma with boninitic affinities; Economic Geology, v.80, p.849–871.

Shaw, D.M., Cramer, J.J., Higgins, M.D. and Truscott, M.G. 1986. Composition of the Canadian Precambrian Shield and the continental crust of the Earth; *in* The Nature of the Lower Continental Crust, Geological Society Special Publication 24, p.275–282.

Shirey, S.B. 1984. The origin of Archean crust in the Rainy Lake area, Ontario; unpublished PhD thesis, State University of New York at Stonybrook, Stoneybrook, New York, 393p.

Shirey, S.B. and Carlson, R.W. 1988. Pb and Nd isotopic constraints on crustal evolution in the southern Superior Province and inferences for a heterogeneous Archean mantle; abstract *in* Geological Society of America Abstracts with Programs, v.20, p.A137.

Shirey, S.B. and Hanson, G.N. 1986. Mantle heterogeneity and crustal recycling in Archean granite–greenstone belts: Evidence from Nd isotopes and trace elements in the Rainy Lake area, Superior Province, Ontario, Canada; Geochimica et Cosmochimica Acta, v.50, p.2631–2651.

Sigurdsson, H. and Sparks, R.S.J. 1981. Petrology and rhyolitic and mixed–magma ejecta from the 1875 eruption of Askja, Iceland; Journal of Petrology, v.22, p.41–84.

Simmons, E.C., Hanson, G.N. and Lumbers, S.B. 1980. Geochemistry of the Shawmere Anorthosite Complex, Kapuskasing Structural Zone, Ontario; Precambrian Research, v.11, p.43–71.

Smith, P.E., Tatsumoto, M. and Farquhar, R.M. 1987. Zircon Lu–Hf systematics and the evolution of the Archean crust in the southern Superior Province, Canada; Contributions to Mineralogy and Petrology, v.97, p.93–104.

Somerville, R. 1967. Kam–Kotia mine; Canadian Inst. Min. Met. Guide Book for Centennial Field Excursions Northwestern Quebec and Northern Ontario, p.132–134.

Sorensen, S.S. and Grossman, J.N. 1989. Enrichment of trace elements in garnet amphibolites from a paleo–subduction zone: Catalina Schist, southern California; Geochimica et Cosmochimica Acta, v.53, p.3155–3177.

Sparks, R.S.J. 1986. The role of crustal contamination in magma evolution through geological time; Earth and Planetary Science Letters, v.78, p.211–223.

Spulber, S.D. and Rutherford, M.J., 1983. The origin of rhyolite and plagiogranite in oceanic crust: an experimental study; Journal of Petrology, v.24, part 1, p.1–25

Steele, K.F. and Wagner, G.H. 1979. Relationship of the Murfreesboro kimberlite and other igneous rocks of Arkansas, USA; *in* Kimberlites, Diatremes, and Diamonds: their Geology, Petrology and Geochemistry, American Geophysical Union, Washington, p.71–91.

Stockwell, C.H., McGlynn, J.C., Emslie, R.F., Sanford, B.V., Norris, A.W., Donaldson, J.A., Fahrig, W.F. and Currie, K.L. 1970. Geology of the Canadian Shield; *in* Geology and Economic Minerals of Canada, Economic Geology Report Number 1, p.45–80.

Stott, G.M. 1985. A structural analysis of the central part of the Archean Shebandowan greenstone belt and a crescent–shaped granitoid pluton, northwestern Ontario; unpublished PhD thesis, University of Toronto, Toronto, Ontario, 284p.

Stott, G.M., Sanborn–Barrie, M. and Corfu, F. 1987. Major transpression events recorded across Archean Subprovince boundaries in northwestern Ontario; abstract *in* Yellowknife '87, Geological Association of Canada, Summer Field Meeting, Program with Abstracts, p.26.

Sutcliffe, R.H. 1988. Geology of the Fletcher Lake area, District of Thunder Bay; Ontario Geological Survey, Report 251, 64p.

Sutcliffe, R.H., Sweeney, J.M. and Edgar, A.D. 1989. The Lac des Iles Complex, Ontario: Petrology and platinum group element mineralization in an Archean mafic intrusion; Canadian Journal of Earth Sciences, v.26, p.1408–1427.

Taylor, S.R. and McLennan, S.M. 1985. The continental crust: its composition and evolution; Blackwell Scientific Publications, Oxford Press, 312p.

Thurston, P.C. and Fryer, B.J. 1983. The geochemistry of repetitive cyclical volcanism from basalt through rhyolite in the Uchi–Confederation greenstone belt, Canada; Contributions to Mineralogy and Petrology, v.83, p.204–226.

Treiman, A.H. 1982. The Oka Carbonatite Complex, Quebec: aspects of carbonatite petrogenesis; unpublished PhD thesis, University of Michigan, Ann Arbor, Michigan, 168p.

Trueman, D.L. and Bannatyne, B.B. 1982. Chromite reserves and the geology of the Bird River Sill, Manitoba; Manitoba Minerals Resource Division, Open File Report number 1, 73p.

Turek, A., Smith, P.E. and Van Schmus, W.R. 1982. Rb–Sr and U–Pb ages of volcanism and granite emplacement in the Michipicoten belt – Wawa, Ontario; Canadian Journal of Earth Sciences, v.19, p.1608–1626.

Verma, S.P., Schilling, J.G. and Waggoner, D.G. 1983. Neodymium isotopic evidence for Galapagos hotspot–spreading centre system evolution; Nature, v.306, p.654–657.

Wager, L.R. 1960. The major element variation of the layered series of the Skaergaard intrusion and a re–estimation of the average composition of the hidden layered series and of the successive residual magmas; Journal of Petrology, v.1, p.364–398.

Wager, L.R. and Brown, G.M. 1968. Layered igneous rocks; Oliver and Boyd, Edinburgh, 588p.

Walawender, M.J. 1976. Petrology and emplacement of the Los Piños pluton, southern California; Canadian Journal of Earth Sciences, v.13, p.1288–1320.

Walawender, M.J. and Smith, T.E. 1980. Geochemical and petrologic evolution of the basic plutons of the Peninsular Ranges Batholith, southern California; Journal of Geology, v.88, p.233–242.

Walker, D., Shibata, T. and DeLong, S.E. 1979. Abyssal tholeiites from the Oceanographer Fracture Zone; Contributions to Mineralogy and Petrology, v.70, p.111–125.

Watson, E.B. 1976. Two liquid partition coefficients: experimental data and geochemical implications; Contributions to Mineralogy and Petrology, v.56, p.119–134.

——1982. Basalt contamination by continental crust: some experiments and models; Contributions to Mineralogy and Petrology, v.80, p.73–87.

Weibe, R.A. 1987. Evidence for stratification of basic, silicic and hybrid magmas in the Newark Island layered intrusion, Nain, Labrador; Geology, v.15, p.349–352.

Weibe, R.A. and Wild, T. 1983. Fractional crystallization and magma mixing in the Tigalak layered intrusion, the Nain Anorthosite Complex, Labrador; Contributions to Mineralogy and Petrology, v.84, p.327–344.

Whitford, D.J., and Arndt, N.T., 1978, Rare earth element abundances in a thick, layered komatiite lava flow from Ontario, Canada: Earth and Planetary Science Letters, v. 41, p. 188–196.

Windley, B.F. 1976. Archean anorthosites: a review with the Fiskenasset Complex, west Greenland as a model for interpretation; Geological Society of South Africa Special Publication 3, p.319–322.

Wolfe, W.J. 1970. Distribution of copper, nickel, cobalt, and sulfur in mafic intrusive rocks of the Kamiskotia–Whitesides area, District of Cochrane; Ontario Department of Mines, Miscellaneous Paper 44, 28p.

——1971. Kamiskotia–Whitesides area, District of Cochrane; Ontario Department of Mines, Preliminary Map P.633, scale 1:31 680.

Wong, L., Davis, D.W., Hanes, J.A. and Robert, F. 1989. An integrated U–Pb and Ar–Ar geochronological study of the Archean Sigma gold deposit, Val D'Or, Quebec; abstract *in* Geological Association of Canada/Mineralogical Association of Canada Program with Abstracts, v.14, p. A45.

Wood, D.A. 1978. Major and trace element variations in the Tertiary lavas of eastern Iceland and their significance with respect to the Iceland geochemical anomaly; Journal of Petrology, v.19, p.393–436.

Wyman, D.A. and Kerrich, R. 1988. Alkaline magmatism, major structures, and gold deposits: implications for greenstone belt gold metallogeny; Economic Geology, v.83, p.454–461.

York, D. and Hyodo, H. 1988. Argon kinetics at a dike contact: $^{40}Ar/^{39}Ar$ laser step–heating study; abstract *in* EOS Transactions, American Geophysical Union, v.69, p.518.

Metric Conversion Table

Conversion from SI to Imperial			Conversion from Imperial to SI		
SI Unit	*Multiplied by*	*Gives*	*Imperial Unit*	*Multiplied by*	*Gives*
		LENGTH			
1 mm	0.039 37	inches	1 inch	**25.4**	mm
1 cm	0.393 70	inches	1 inch	**2.54**	cm
1 m	3.280 84	feet	1 foot	**0.304 8**	m
1 m	0.049 709	chains	1 chain	20.116 8	m
1 km	0.621 371	miles (statute)	1 mile (statute)	**1.609 344**	km
		AREA			
1 cm^2	0.155 0	square inches	1 square inch	**6.451 6**	cm^2
1 m^2	10.763 9	square feet	1 square foot	**0.092 903 04**	m^2
1 km^2	0.386 10	square miles	1 square mile	2.589 988	km^2
1 ha	2.471 054	acres	1 acre	0.404 685 6	ha
		VOLUME			
1 cm^3	0.061 023	cubic inches	1 cubic inch	**16.387 064**	cm^3
1 m^3	35.314 7	cubic feet	1 cubic foot	0.028 316 85	m^3
1 m^3	1.307 951	cubic yards	1 cubic yard	0.764 554 86	m^3
		CAPACITY			
1 L	1.759 755	pints	1 pint	0.568 261	L
1 L	0.879 877	quarts	1 quart	1.136 522	L
1 L	0.219 969	gallons	1 gallon	**4.546 090**	L
		MASS			
1 g	0.035 273 962	ounces (avdp)	1 ounce (avdp)	28.349 523	g
1 g	0.032 150 747	ounces (troy)	1 ounce (troy)	**31.103 476 8**	g
1 kg	2.204 622 6	pounds (avdp)	1 pound (avdp)	**0.453 592 37**	kg
1 kg	0.001 102 3	tons (short)	1 ton (short)	**907.184 74**	kg
1 t	1.102 311 3	tons (short)	1 ton (short)	**0.907 184 74**	t
1 kg	0.000 984 21	tons (long)	1 ton (long)	**1016.046 908 8**	kg
1 t	0.984 206 5	tons (long)	1 ton (long)	**1.016 046 90**	t
		CONCENTRATION			
1 g/t	0.029 166 6	ounce (troy)/ ton (short)	1 ounce (troy)/ ton (short)	34.285 714 2	g/t
1 g/t	0.583 333 33	pennyweights/ ton (short)	1 pennyweight/ ton (short)	1.714 285 7	g/t

OTHER USEFUL CONVERSION FACTORS

	Multiplied by	
1 ounce (troy) per ton (short)	31.103 477	grams per ton (short)
1 gram per ton (short)	0.032 151	ounces (troy) per ton (short)
1 ounce (troy) per ton (short)	20.0	pennyweights per ton (short)
1 pennyweight per ton (short)	0.05	ounces (troy) per ton (short)

Note: Conversion factors which are in bold type are exact. The conversion factors have been taken from or have been derived from factors given in the Metric Practice Guide for the Canadian Mining and Metallurgical Industries, published by the Mining Association of Canada in co-operation with the Coal Association of Canada.

MAPS NOT FILMED

CARTES NON REPRODUITES

micromedia
a division of IHS Canada

20 Victoria Street
Toronto, Ontario M5C 2N8
Tel.: (416) 362-5211
Toll Free: 1-800-387-2689
Fax: (416) 362-6161
Email: info@micromedia.on.ca